

SOIL PATHOGEN FATE AND TRANSPORT: BIOPORES FACILITATING
ESCHERICHIA COLI TRANSPORT

By

JORGE ALBERTO GUZMAN

Bachelor of Science in Civil Engineering
Universidad Industrial de Santander
Bucaramanga, Colombia
1989

Master in Computer Science
Universidad Industrial de Santander
Bucaramanga, Colombia
1994

Master of Science in Hydrology and Water Resources
UNESCO-IHE Institute for Water Education
Delft, The Netherlands
2003

Submitted to the Faculty of the
Graduate College of the
Oklahoma State University
in partial fulfillment of
the requirements for
the Degree of
DOCTOR OF PHILOSOPHY
December, 2010

SOIL PATHOGEN FATE AND TRANSPORT: BIOPORES FACILITATING
ESCHERICHIA COLI TRANSPORT

Dissertation Approved:

Dr. Garey A. Fox

Dissertation Adviser

Dr. Glenn O. Brown

Dr. Daniel E. Storm

Dr. Chad J. Penn

Outside Committee Member

Dr. Mark Payton

Dean of the Graduate College

ACKNOWLEDGMENTS

I deeply express my gratitude to my committee Dr. Garey A. Fox, Dr. Chad J. Penn, Dr. Glenn O. Brown, and Dr. Daniel E. Storm for their support, valuable comments and exemplifying academic life. I profoundly admire Garey for his work and devotion in making science a daily experience, his scientific curiosity, impeccable organization, and his commitment to teach through practice cannot be surpassed by the best benevolent dictator. I am in debt to Chad who initiated me in the wonderful and complex world of soil chemistry, made his laboratory an unforgettable experience, and guided me from scratch. I have my respect for Glenn who was always cooperative and hasty to help and discuss any porous media issues, and finally, I am deeply grateful to Daniel who made field work a memorable and enjoyable experience with his new tools.

I also want to express my appreciation to the faculty and staff of Biosystems and Agricultural Engineering Department at Oklahoma State University for their support through the research activities. I deeply express my gratitude to Mr. Wayne Kiner for his invaluable ideas during our laboratory setups and equipment development.

I would like to give my gratitude to my wife Maria L for her support and lovely scientific discussions. To my parents Emma and Alejandro, who didn't understand what I was doing but were always receptive and interested in my results and Amanda Fox for her priceless editorial advices. To my friends who shared or sacrificed part of his/her life to make this research possible.

Furthermore, I acknowledge the financial assistance of a 2007-2010 United States Department of Agriculture (USDA), Cooperative State Research, Extension, and Education Service (CSREES) National Research Initiative Grant, Award No. 2007-35102-18242.

Jorge A. Guzmán
Oklahoma State University
Fall 2010

ABSTRACT

Fecal bacteria being transported by surface runoff and infiltration from fields treated with manure as fertilizer may result in contamination of adjacent water bodies. During infiltration, the presence of macropores and biopores allows manure effluent constituents and microorganisms to rapidly bypass a portion of the soil matrix, reaching deeper soils and perhaps interconnecting to subsurface drainage systems. This research investigated the significance of biopores in facilitating fecal bacteria transport to deeper soils and subsurface drainage systems and incorporated fecal bacteria fate and transport routines and a biopore concept in the Root Zone Water Quality Model (RZWQM). A laboratory study was conducted using artificial biopores in a 28 cm by 50 cm wide and 95 cm long soil column to investigate biopores facilitating fecal bacteria transport to subsurface drainage systems in two contrasting soils. Soil sorption of fecal bacteria relative to constituents in swine effluent was investigated using batch experiments with natural and artificial soils treated with liquid swine manure at different concentrations. For field conditions, transport of fecal bacteria in surface runoff and the effect of the time lag between poultry litter application and the occurrence of a 2-yr and 5-yr rainfall event were investigated on a series of 2 m by 2 m pasturelands plots. Finally, routines were incorporated in RZWQM to simulate fecal bacteria fate and transport through the soil matrix, macropores, and surface runoff. Also, an open surface connected biopore concept was developed to simulate rapid flow and fecal bacteria transport bypassing a portion of the soil matrix and interconnecting to subsurface drainage systems.

Biopores provided a mechanism for rapid flow bypassing a portion of the soil profile and transporting fecal bacteria to deeper soils and tile drainage systems. The transport process was as a function of the soil type, the layer thickness above or below the biopore, and the presence of macropores from soil structure. Manure effluents primarily consisted of sessile fecal bacteria and effluent constituents that increased the soil bulk solution pH when in contact with soils and provided exchangeable ions that may promote soil dispersion, decreasing soil sorption of fecal bacteria. A predictive equation was developed to determine the parameters of a nonlinear equation that described soil sorption of *E. coli* as a function of clay content, total carbon and amorphous Al and Fe. Event mean concentrations (EMC) of fecal bacteria in surface runoff from poultry litter amended plots were observed to decrease between 0 hr and 24 hr and then increase 120 hr following manure application. Also, fecal bacteria from sources independent of the immediate poultry litter application significantly contributed to the total *E. coli* EMCs. The updated RZWQM predicted rapid flow and fate and transport of fecal bacteria in the soil matrix, macropores, biopores, subsurface drains, and surface runoff. The biopore concept represented the observed rapid flow and fecal bacteria transport at the subsurface drain during the soil column experiments. However, the modified RZWQM poorly represented flow in the drain during the recession part of the hydrograph and surface runoff. This research contributed to the understanding of fate and transport of fecal bacteria in soils in the presence of biopores and will be useful in assessing further mitigation and regulatory strategies relative to fecal bacteria contamination of soil and water.

INTRODUCTION

Following manure application, rapid transport of fecal bacteria in runoff and infiltration may result in fecal bacteria contamination of deeper soils and adjacent water bodies. Fecal microorganisms are a group of virus, bacteria and protozoa commonly not pathogenic. Investigations for fecal soil and water contamination, and fate and transport are typically conducted using indicator organisms such as *Escherichia coli* and *Enterococcus faecalis*. In most cases, indicator organisms exhibit negative growth rates in soil and water following manure application but detection is still possible after several weeks in some cases.

Macropores and biopores play an important role in facilitating fecal bacteria transport to deeper soils and to drainage systems, and help explain the rapid fecal bacteria breakthrough concentrations observed in subsurface drain pipes following manure application, under rainfall or irrigation events. Macropores from soil structure are not sufficient to explain the rapid fecal bacteria transport to drainage systems but rather serve as a complementary flow pathway and transport mechanism in the presence of biopores. Macropores and mesopores found in the soil layer thickness between the end of the biopore and drain pipe or between the surface and the biopore allow open surface connected and buried surface disconnected biopores to interconnect to subsurface drains.

Manure effluent constituents possess the capability to impact the soil bulk solution pH and provide solute concentrations that may result in different fecal bacteria

sorption mechanisms as a function of the effluent concentrations, soil properties, and sessile or planktonic fecal bacteria population. This effect may further impact fecal bacteria transport through macropores and biopores, and deeper soils interconnecting drainage systems. Available fecal bacteria on soils following litter application may exhibit varied die-off rates as a function of environmental variables and lag time between manure application and the occurrence of rainfall or irrigation events. This condition may play an important role in further defining the fecal bacteria population available for mixing and transport in runoff and through macropores and biopores.

Extensive experimentation and modeling on soil fate and transport of fecal bacteria have been conducted at the field and laboratory scale. In the laboratory, the use of mono-strain fecal indicator organisms suspended in inert solutions has been a common practice with disturbed and undisturbed soils. At the field scale, a more comprehensive approach has been used, but more research is still needed due to the physical, chemical and biological complexity of the processes involved. On the other hand, modeling of soil fecal bacteria transport is frequently conducted with the idea of physical equilibrium occurring in a representative elementary volume (REV) using the Richards' equation and Green-Ampt method to describe flow in combination with the advection-dispersion equation. However, the presence of soil macropores and biopores in natural soils may invalidate the REV concept when vertical flow and contaminants move rapidly in the unsaturated soil profile without allowing horizontal equilibrium of water pressure and solute/contaminant concentrations. In the last decade a large effort has been in place on understanding and modeling this phenomenon using continuum, multi-continuum and network approaches.

The fate of fecal bacteria in soils is controlled by the bacteria strain characteristics, external variables (e.g., physical and chemical) and the microbial community. In the intestinal tract of warm-blooded animals, fecal bacteria exhibit stable populations with favorable environmental conditions and nutrient availability. After excretion, fecal bacteria are under stress by environmental and nutritional conditions and the competitive well-adapted microbial communities (e.g., virus, bacteria, protozoa, and nematodes) present in soils. Also, manure constituents found in aged manures (e.g., organic compounds, solutes, and microbial byproducts) can potentially modify soil properties when placed in contact with soils and result in diverse soil-bacteria or soil bacteria-substrate attachment mechanisms.

Soil fecal bacteria transport in the presence of macropores is mainly driven by advective processes occurring at the surface and in the subsurface. During rainfall or irrigation events, available fecal bacteria in top soils are transported through the surface, soil matrix, macropores and biopores with different flow regimes. In the absence of macropores and biopores, the soil matrix potentially immobilizes and inactivates fecal bacteria (e.g., planktonic and sessile) being transported during infiltration as a function of the pore size opening and sorptive properties. The occurrence of rapid vertical flow through biopores allows fecal bacteria to bypass a portion of the soil matrix, reaching deeper soils and perhaps interconnect with drainage systems. Although some fecal microorganisms possess motility, diffusion is most likely not an important fecal transport mechanism due to the fact that most of the fecal bacteria from manure effluents are in sessile form rather than free cells, and the preference of bacteria to be surface bonded. However, in those cases in which fecal bacteria colonize soils and establish mature

biofilms, release of fecal bacteria from biofilms in search of readily available nutrients can mimic diffusive transport mechanisms. Also, diffusion and dispersion of colloids carrying fecal bacteria can be present as a transport mechanism in some cases.

This research investigated the significance of biopores in facilitating fecal bacteria transport to deeper soils and subsurface drainage systems and incorporated fecal bacteria fate and transport routines and a biopore concept in the Root Zone Water Quality Model (RZWQM). Four interrelated chapters form this dissertation:

- Chapter 1 investigates the significance of open surface connected (OSC) and buried surface disconnected (BSD) biopores on *E. coli* transport to subsurface drainage systems. Experiments were conducted on a soil column (28 x 50 x 85 cm) packed with two contrasting soils types (e.g., loamy sand and sandy loam) and OSC or BSD biopores placed at different depths. Also, the sandy loam soil was packed in two ways to mimic the presence of soil structure.
- Chapter 2 investigates soil sorption of *E. coli* in a series of soils treated with liquid swine manure at different concentrations and the effect of the effluent constituents in soil sorption of fecal bacteria. Batch experiments were conducted using 6 g of soil mixed with 6 mL of swine manure effluent at five dilution ratios. Soil properties were used to develop a predictive equation to determine the parameters of the nonlinear equation describing *E. coli* sorption.
- Chapter 3 investigates surface runoff transport of *E. coli* on pasturelands plots treated with poultry litter and the effect of time lag between application

and the occurrence of a rainfall event. Experiments were conducted on a series of 2 by 2 m plots subjected to an artificial 2-yr or 5-yr return period storm event in Haskell, OK, and 0-hr, 24-hr, and 120-hr time lag following litter application.

- Chapter 4 incorporates routines in RZWQM to simulate fecal bacteria fate and transport through the soil matrix, macropores, and surface runoff. Also, an open surface connected (OSC) biopore concept was developed to simulate rapid flow and fecal bacteria transport bypassing a portion of the soil matrix and interconnecting to subsurface drainage systems.

The incorporation of fecal bacteria fate and transport routines and a biopore concept in RZWQM provided a tool to simulate physical non-equilibrium flow in the vadose zone. In combination with the macropore model available in RZWQM, the implemented biopore concept improved flow and fecal bacteria transport simulations at the subsurface drain, in runoff, and through the soil profile and therefore may be useful when assessing fecal bacteria contamination of soil and water and mitigation and regulatory strategies.

TABLE OF CONTENTS

ACKNOWLEDGMENTS	III
ABSTRACT.....	V
INTRODUCTION	VII
TABLE OF CONTENTS	XII
LIST OF TABLES	XVI
LIST OF FIGURES.....	XIX
CHAPTER 1.....	1
<i>ESCHERICHIA COLI</i> TRANSPORT FROM SURFACE-APPLIED MANURE TO SUBSURFACE DRAINS THROUGH ARTIFICIAL BIOPORES	
	1
1.1. ABSTRACT.....	1
1.2. INTRODUCTION	2
1.3. MATERIAL AND METHODS.....	5
1.4. RESULTS AND DISCUSSION	12
1.4.1. Soil Property Characterization	12
1.4.2. Water and Manure Suspension Flow	14
1.4.3. <i>Escherichia coli</i> Transport: Soil Type and Packing.....	16
1.4.4. <i>Escherichia coli</i> Transport: Open-Surface Connected versus Buried Surface Disconnected Biopores.	18

1.5. SUMMARY AND CONCLUSIONS	23
CHAPTER 2.....	25
SORPTION OF <i>ESCHERICHIA COLI</i> IN AGRICULTURAL SOILS INFLUENCED BY SWINE MANURE CONSTITUENTS	25
2.1. ABSTRACT.....	25
2.2. INTRODUCTION	26
2.3. MATERIAL AND METHODOLOGY	28
2.3.1. Soil Samples	28
2.3.2. <i>Escherichia coli</i> Source	32
2.3.3. Quantification of <i>E. coli</i> Sorption	33
2.3.4. Effluent Bacteria Growth: Microcalorimeter	34
2.3.5. SAR, <i>E. coli</i> Quantification, and Nonlinear <i>E. coli</i> Sorption.....	35
2.4. RESULTS AND DISCUSSION	37
2.4.1. Sessile <i>E. coli</i> and Effluent Solute Concentrations	37
2.4.2. Influence of Clay, Total Carbon, and Dispersion on <i>E. coli</i> Sorption	41
2.4.3. Predictive Equations for Sorption of <i>E. coli</i>	43
2.5. SUMMARY AND CONCLUSSIONS	46
CHAPTER 3.....	48
SURFACE RUNOFF TRANSPORT OF <i>ESCHERICHIA COLI</i> AFTER POULTRY LITTER APPLICATION ON PASTURELAND.....	48
3.1. ABSTRACT.....	48
3.2. INTRODUCTION	49

3.3. MATERIAL AND METHODS	52
3.3.1. Experimental Area.....	54
3.3.2. Rainfall Simulator	56
3.3.3. Plot Instrumentation	56
3.3.4. <i>Escherichia coli</i> Concentration	57
3.3.5. Data Processing	57
3.4. RESULTS AND DISCUSSION	58
3.4.1. Hydrological Response	58
3.4.2. <i>Escherichia coli</i> Event Mean Concentrations	60
3.4.3. <i>Escherichia coli</i> Surface Runoff Concentrations	62
3.5. SUMMARY AND CONCLUSIONS	65
CHAPTER 4.....	68
IMPLEMENTATION AND VALIDATION OF BIOPORE AND FECAL BACTERIA FATE AND	
TRANSPORT ROUTINES INTO THE ROOT ZONE WATER QUALITY MODEL (RZWQM).....	68
4.1. ABSTRACT.....	68
4.2. INTRODUCTION	69
4.3 MATERIALS AND METHODS.....	71
4.3.1 Fecal Bacteria Fate and Transport Modeling	72
4.3.2 Biopore Flow and Transport	74
4.3.3 Sources of Fecal Bacteria	76
4.3.4 Model Calibration and Validation.....	76

4.4 RESULTS AND DISCUSSION	78
4.4.1 Hydrological Response	78
4.4.2. Transport of Fecal Bacteria	85
4.5 SUMMARY AND CONCLUSIONS	87
CHAPTER 5.....	90
SUMMARY AND CONCLUSIONS OF DISSERTATION.....	90
5.1 SPECIFIC CONCLUSIONS	90
5.2 FUTURE RESEARCH	93
REFERENCES	95

LIST OF TABLES

Table 1.1. Properties of the loamy sand (LS) and sandy loam (SL) soils used in the soil column experiments.....	6
Table 1.2. Main experimental variables for the open-surface connected (OSC) and buried surface disconnected (BSD) biopore soil column experiments with loamy sand (LS) and sandy loam (SL) soils. The SL soil was packed using either a wet grinding (WG) or dry grinding (DG) technique.	7
Table 1.3. Drainage (Drain) and biopore (BP) breakthrough time (minutes) after manure flush and final water flush for open-surface connected (OSC) and buried surface disconnected (BSD) biopores in loamy sand (LS) and sandy loam (SL) soils. The SL soil was packed using either a wet grinding (WG) or dry grinding (DG) technique.....	15
Table 1.4. Cumulative matrix (Drain) and biopore (BP) discharge in the open-surface connected (OSC) and buried surface disconnected (BSD) biopore experiments with loamy sand (LS) and sandy loam (SL) soils. The SL soil was packed using either a wet grinding (WG) or dry grinding (DG) technique. Cumulative discharge measured 24 h after flush initialization.....	18
Table 1.5.. Macropore length, <i>E. coli</i> initial concentration (C_o), and maximum <i>E. coli</i> recovery from the matrix and macropore flow for the open-surface connected (OSC) and buried surface disconnected (BSD) biopore experiments with loamy sand (LS) and sandy loam (SL) soils. The SL soil was packed using either a wet grinding (WG) or dry grinding (DG) technique.	23
Table 2.1. Soil properties of the natural soils used in the sorption experiments.....	29
Table 2.2. Soil properties of the artificial soils used in the sorption experiments.....	31

Table 2.3. Composition of the swine effluent utilized in the study.	33
Table 3.1. Characteristics of the rainfall events, plot slope, and surface runoff for the experiments. Note that all surface runoff times are non-dimensionalized by the duration of the rainfall event, t_d	54
Table 3.2. <i>E. coli</i> event mean concentration (EMC, MPN/100 mL) and ANOVA test results (95% confidence limits, CL) for significant differences in the EMC averages as a function of the time lag. P-values lower than 0.050 indicated a significant difference in the average EMCs.	60
Table 4.1 Soil macropores and biopore properties for the soil column and plot experiments after calibration. Note that SC is the soil column, MP is macropore radius, FDEP is the fraction of dead end pores, ELWT is the effective lateral wetting thickness, and K_{eff} is the effective biopore infiltration constant.	80
Table 4.2 Soil hydraulic properties for the soil column and plot experiments after calibration. Note that h_b is the bubbling pressure, λ is the pore size distribution index, N is the exponent for the $k(h)$ curve, K_{sat} is the saturated hydraulic conductivity, θ_r is the residual water content, θ_s is the saturation water content, and K_{sat-d} is the lateral saturated hydraulic conductivity to the drain.	80
Table 4.3 Soil textural properties for the soil column and plot experiments after calibration, where BD is the soil bulk density and ϕ is the soil porosity.	81
Table 4.4 Subsurface drainage soil column calibration and validation results, where MC_{obs} and MC_{sim} are the mass curve values for the observed and simulated drainage runoff; NSI is the Nash-Sutcliffe efficiency index; MC_{err} is the mass curve error; f_{avg} is the average infiltration rate; REC is the rainfall <i>E. coli</i> concentration; Man is the manure flush; and DI is the distilled water flush.	82
Table 4.5 Surface runoff plot experiments calibration and validation results, where MC_{obs} and MC_{sim} are the mass curve for observed and simulated surface runoff, NSI is the Nash-Sutcliffe efficiency index, MC_{err} is the mass curve error, $Losses_{avg}$ is the average infiltration, interception and evaporation volume, and PREC is the proportional rainfall <i>E. coli</i> concentration.	83

Table 4.6 Transport parameters for the soil column and plot experiment simulations, where K_{str} is the straining coefficient, D_{tchm} is the detachment coefficient, LP is the liquid phase, SP is the solid phase, and Top is the soil top layer.....	85
Table 4.7 Fecal transport event mean concentrations (EMC) for the soil column experiments, where NEMC is the normalized event mean concentration (EMC_{sim}/EMC_{obs}), NBP refers to the simulations with no biopore routine included, and REC is the rainfall <i>E. coli</i> concentration.....	86
Table 4.8 Fecal transport event mean concentrations (EMC) for the plot experiments, where REC is the rainfall <i>E. coli</i> concentration.	87

LIST OF FIGURES

Figure 1.1. Potential biopores in relationship to a subsurface drain. OSC: open surface connected; BSD: buried surface disconnected; and BD: buried disconnected; a: soil layer thickness between the center of the drainage pipe to the bottom of the biopores; b: soil layer thickness between the soil surface and the top of the biopores; c: initial saturated soil layer thickness equal to 10 cm for all experiments; d: distance from the center of the drain pipe to the vertical center of the biopores equal to zero for all experiments; L: length of the biopores; Φ : drain pipe diameter equal to 5 cm for all experiments.	8
Figure 1.2. Descriptive setup of the soil column and instruments used in all experiments.....	9
Figure 1.3. Hydraulic (i.e., soil moisture) characteristic curve for the loamy sand (LS) and sandy loam (SL) soil and its two preparation techniques (WG, wet soil; DG, dry soil) and fit to the van Genuchten (1980) model (VG). Data represent the means for six cores extracted from two SL columns. Data for the LS are reported by Chu-Agor et al. (2008) for the same bulk density as used in these experiments.....	13
Figure 1.4. <i>Escherichia coli</i> concentrations from the drain (C) relative to the inflow <i>E. coli</i> concentration (C_o) for open-surface connected (OSC) biopore experiments (i.e., 55 and 65 cm biopores lengths) as a function of the number of pore volumes (i.e., product of flow rate, Q, and time, t, divided by the volume of pore space, V_{ps} , of the soil column) of inflow water (a) during manure flush and (b) during the final water application. Experiments correspond to numbers 1, 2, and 5 in Tables 2 to 5.	20
Figure 1.5. <i>Escherichia coli</i> concentrations from the drain (C) relative to the inflow <i>E. coli</i> concentration (C_o) for buried surface disconnected (BSD) biopore experiments (i.e., 55 and 20 cm macropore lengths) as a function of the number of pore volumes (i.e., product of flow rate, Q, and time, t, divided by the volume of pore space, V_{ps} , of the soil column) of inflow water. Figures (a) and (b) are during the manure flush and final water application for the 55-cm BSD biopores,	

respectively (i.e., Exp. 3, 6, and 8 in Tables 2–5). Figures (c) and (d) are during the manure flush and final water application for 20-cm BSD biopores, respectively (i.e., Exp. 4 in Tables 2–5 with Exp. 7 having no observed <i>E. coli</i> from the matrix or biopore). DR = drain flow, BP = biopore flow, LS = loamy sand, SL = sandy loam, WG = wet soil preparation and DG = dried soil preparation.....	22
Figure 2.1. Particle size distribution of organic compounds in swine effluents associated with the percentage of <i>E. coli</i> population finer than a certain mesh size from micro-sieving experiments. Filled circles represent data from nylon mesh and hollow circles from metal disks.	37
Figure 2.2. Major ions sorbed (q_{SP}) by the natural soils and in the swine effluent (C_{man} ; dash line on Figures 2.2c to 2.2h), pH, sodium absorption ratio (SAR), electrical conductivity (EC) and equilibrated <i>E. coli</i> concentrations. Dash lines in Figure 2.2a are the average EC per dilution ratio (i.e., mL of liquid swine manure to mL of distilled water). Dash lines in Figure 2.2c to 2.2h are the solute concentration in the swine effluent before mixing with soils and circles are the sorbed solute concentrations after mixing.	40
Figure 2.3. Sorption of <i>E. coli</i> from swine effluents for the artificial soils with clay contents of (a) 5%, (b) 10%, and (c) 20%. Sorbed <i>E. coli</i> concentrations for the natural soils with clay contents in the range of (d) 0% to 10%, (e) 10% to 20%, and (f) 20% to 30%. See Tables 2.1 and 2.2 for identification and soil property information. Dashed lines and regression equations correspond to the artificial soils with 5%, 10% and 20% kaolinite clay content and no total carbon added. Note that all data points are the average of triplicate experiments.....	42
Figure 2.4. Estimated nonlinear parameters (A and B) from the predictive equations developed in this research: (a) predicted versus observed nonlinear A parameter for the natural soils; (b) relationship between the nonlinear equation parameters (A versus B) for the natural soils. Soils after reduction in total carbon and artificial soils are in the figure for comparison. See Tables 2.1 and 2.2 for identification and soil property information.	44
Figure 2.5. Comparison of <i>E. coli</i> sorbed (q_{SP}) versus solution (C_{LP}) concentrations observed during the experiments and estimated by the proposed predictive equations (i.e., “Estimated”). <i>E. coli</i> sorption predicted by the Ling et al. (2002) relationship based on only percent clay content is also shown. See Table 2.1 for identification and soil property information.	46

Figure 3.1. (a) Aerial image of the Oklahoma State University Eastern Research Station in Haskell, Oklahoma, including the study area location of the plots and the rainfall simulator used for the 2-year and 5-year rainfall intensities, and (b) illustration of vegetation, rain gauge, and borders of one of the plots and the outflow flume and flow collection device at the downslope end of the plot.	53
Figure 3.2. Meteorological conditions during the experimental 5 d period: (a) air temperature at 1.5 m (TAIR-1.5 m) and relative humidity (RELH), and (b) wind speed at 10 m (WVEC-10 m) and solar radiation (SRAD).....	55
Figure 3.3. Smoothed hydrograph response from each plot for (a) T = 2-year and (b) T = 5-year rainfall intensity relative to the time lag (TL) between litter application and rainfall. Only 2-year storm intensities were simulated in the control plots.	59
Figure 3.4. <i>E. coli</i> concentration for the 2-year and 5-year storm intensity and time lags: (a) <i>E. coli</i> concentration and average runoff from the 2-year storm intensity, and (b) <i>E. coli</i> concentration and average runoff from the 5-year storm intensity. Only 2-year storm intensities were simulated in the control plots. Filled square symbols correspond to the minimum concentration (e.g., water samples in which <i>E. coli</i> concentrations were over the range of quantification). TL = time lag (h) and t_d is the rainfall event duration time.	61
Figure 3.5. <i>Escherichia coli</i> concentration in poultry litter samples collected outside the treated plots as a function of time lag.	65
Figure 4.1. Conceptual diagram of the main RZWQM hydrological processes and the new biopore concept. Where XpF is the express fraction concept (Fox et al., 2004) and GWT is the ground water table.....	72
Figure 4.2 Subsurface drain flow and mass curves for the soil column experiments.....	84
Figure 4.3 Surface runoff and mass curve for the plot experiments.	84
Figure 4.4 Observed and simulated fecal bacteria concentrations and mass curves for the soil column experiments. Triangle legends represent observed concentrations over the detection range.	88

Figure 4.5 Observed and simulated fecal bacteria concentrations and mass curves for the plot experiments.....	89
--	----

CHAPTER 1

Escherichia coli Transport from Surface-Applied Manure to Subsurface Drains Through Artificial Biopores¹

1.1. ABSTRACT

Bacteria transport in soils primarily occurs through soil mesopores and macropores. Field research has demonstrated that biopores and subsurface drains can be hydraulically connected. This research was conducted to investigate the importance of surface connected and disconnected (buried) biopores on *Escherichia coli* (*E. coli*) transport when biopores are located near subsurface drains. A soil column (28 by 50 by 95 cm) was packed with loamy sand and sandy loam soils to bulk densities of 1.6 and 1.4 Mg m⁻³, respectively, and containing an artificial biopore located directly above a subsurface drain. The sandy loam soil was packed using two different methods: moist soil sieved to 4.0 mm and air-dried soil manually crushed and then sieved to 2.8 mm. A 1-cm constant head was induced on the soil surface in three flushes: (i) water, (ii) diluted liquid swine (*Sus scrofa*) manure 48 h later, and (iii) water 48 h after the manure. *Escherichia coli* transport to the drain was observed with either open surface connected or buried biopores. In surface connected biopores, *E. coli* transport to the drain was a function of

¹ Published in *Journal of Environmental Quality*, 2009.

Guzman, J.A., G.A. Fox, R. Malone, and R. Kanwar. 2009. *Escherichia coli* transport from surface applied manure to subsurface drains through artificial biopores. J. Environ. Qual. 38: 2412–2421.

the soil type and the layer thickness between the end of the biopore and drain. Buried biopores contributed flow and *E. coli* to the drain in the less sorptive soil (loamy sand) and the sorptive soil (sandy loam) containing a wide (i.e., with mesopores) pore space distribution prevalent due to the moist soil packing technique. Biopores provide a mechanism for rapidly transporting *E. coli* into subsurface drains during flow events.

1.2. INTRODUCTION

Animal excretions, slurry, and liquid manure on soil can easily be diluted and transported into the soil by irrigation or rainfall events. Bacteria can be carried by surface runoff, infiltration, and macropore flow to adjacent soils, deeper soils, or drainage systems. Survival of *E. coli* in soils has been reported to range between 60 and 103 d before falling below detectable levels. Pathogenic bacteria can be transported through the soil in the form of suspended cells or they can attach to colloids, organic matter compounds, and mineral particles. (Stoddard et al., 1998; Sørensen et al., 1999; Wang, 2003).

Normally, the soil matrix acts as an effective pathogenic control during water infiltration and percolation (Darnault et al., 2004; Pachepsky et al., 2006). The natural soil filtration capacity is a function of bacterium properties, microbial community interaction, sorption processes and porous media characteristics such as texture, organic matter content, temperature, pH, solution ionic strength, and pore space distribution (Fontes et al., 1991; Pachepsky et al., 2006). Normally, these processes are simplified when attempting to analyze fate and transport pathways due to the complexity, specificity, lack of knowledge, and/or insufficient data about specific processes.

Macropores can allow bacteria and pathogens to bypass the soil's natural filter capacity and increase the risk of surface water and groundwater contamination (Reddy et

al., 1981; Mawdsley et al., 1996a, 1996b; Guan and Holley, 2003; McGechan and Vinten, 2003; Darnault et al., 2004). Micropores, mesopores, and macropores are defined as pores spaces with equivalent diameters of 5 to 30 μm , 30 to 75 μm , and larger than 75 μm , respectively (SSSA, 2008). With macropores, wetting fronts propagate to significant depths by bypassing matrix pore space. Soil macropores (e.g., pore spaces formed as part of the soil structure) can transport air, water, colloids, organic matter, and microorganisms rapidly from the surface or upper soil (vertically and horizontally) to deeper soil and drainage systems (Lobry de Bruyn and Conacher, 1994; McMahon and Christy, 2000).

Macropores may be subdivided into two major groups based on physical characteristics and origin: natural fractures and cylindrical biopores. Natural fractures originate from soil expansion and contraction or from geological processes. Biopores, on the other hand, are created by tunneling insects, small animals, nematodes, and decaying roots (McMahon and Christy, 2000). Biological (biopores) and mechanical fragmentation (tillage) are common in cultivated lands. Hubert et al. (2007) found that no tillage practices promote biological fragmentation, and biological fragmentation reformed following mechanical fragmentation in soils under annual tillage practices.

Several studies have attempted to investigate the influence of preferential flow pathways on soil pathogen transport (Fontes et al., 1991; Jiang et al., 2007; Garbrecht et al., 2009). For example, Fontes et al. (1991) investigated bacterial transport in homogeneous and heterogeneous sand soil columns (14 cm length). For heterogeneous columns, the preferential path was created by inserting a glass pipe in the center of the column, packing the column with fine sand, filling the glass pipe with coarse sand, and

finally removing the pipe. A double peak was observed in the breakthrough curves as a result of flow velocity differences between the preferential flow path and fine sand. They found that the grain size was the most important variable controlling bacterial transport followed by ionic strength and cell size. On the other hand, Jiang et al. (2007), using homogeneous sand columns, concluded that the length of a column (14 cm length) has no effect on the *E. coli* peak concentration. They found that bacteria were mainly retained in the top 10 cm of soil and that grain size had a significant effect on the bacterial transport and retention.

A significant component of pathogen movement to streams commonly identified but not explicitly considered is pathogen movement to subsurface tile drainage systems (Dorner et al., 2006). However, few, if any, studies to date have investigated soil bacteria transport in relation to biopores located in the vicinity of subsurface drains. Figure 1.1 represents a vertical soil cross-section and conceptual diagram of potential biopore interconnectivity with a subsurface drain. Open-surface connected (OSC), buried surface disconnected (BSD), and buried disconnected biopores are typically found in the vadose zone between the soil surface and the subsurface drain (Akay et al., 2008).

Shipitalo and Gibbs (2000) investigated biopores directly connected to artificial drainage systems by a deep burrowing Anecic earthworm species. The interconnectivity was demonstrated in the field using a smoke test, filling the earthworm's channels with resin, and by measuring the biopore flow using infiltrometers. They later excavated the soil to expose the earthworm channel. Akay and Fox (2007) and Akay et al. (2008) investigated the importance of biopores and drainage system interconnectivity in the movement of water using a soil column (28 cm by 50 cm cross-section and 95 cm long)

by placing an artificial biopores both directly above and shifted away from the drainage pipe without unpacking or disturbing the soil column between experiments. They found that OSC macropores were a highly efficient preferential flow path reducing the breakthrough times to the subsurface drainage outlet as a function of the macropore depth penetration. Simulated BSD macropores diverted as much as 40% of the matrix flow when directly connected to the subsurface drains and after buildup of soil pore-water pressure. Other studies have pointed out the importance of macropore and artificial drainage interconnectivity in the transport of nutrients and pesticides (Villholth et al., 1998; Fox et al., 2004, 2007).

The objective of this research was to investigate the significance of OSC and BSD biopores on *E. coli* transport to subsurface drainage systems. Laboratory experiments of *E. coli* transport through OSC and BSD biopores were performed using the soil column developed by Akay and Fox (2007) with two soils containing different soil organic matter contents and hydraulic conductivities.

1.3. MATERIAL AND METHODS

Transport of *E. coli* in soil was measured using a soil column (28 by 50 by 95 cm) developed by Akay and Fox (2007). Two types of soil were used in the experiments: Dougherty loamy sand (LS; loamy, mixed, active, thermic Arenic Haplustalfs) and Floyd sandy loam (SL; fine-loamy, mixed, superactive, mesic aquic Pachic Hapludolls), selected due to the contrasting particle size distribution, soil organic matter content, and saturated hydraulic conductivity (Table 1.1). Soil organic matter content was estimated from total carbon (TruSpec Carbon and Nitrogen Analyzer, LECO Corp., St. Joseph, MI)

using a 1.724 ratio. Saturated hydraulic conductivity was measured using a falling head permeameter (Amoozegar and Wilson, 1999).

Table 1.1. Properties of the loamy sand (LS) and sandy loam (SL) soils used in the soil column experiments.

Soil type	SP [†]	Bulk density Mg m ⁻³	Specific gravity	Sand	Silt —%—	Clay	SOM [‡] g kg ⁻¹	θ_s^{\S} cm ³ cm ⁻³	θ_r^{\P} cm ³ cm ⁻³	$K_s^{\#}$ m s ⁻¹	$n^{\dagger\dagger}$	$\alpha^{\dagger\dagger}$ pF ⁻¹
LS	—	1.6	2.67	84.5	13.4	2.1	3	0.40	0.01	1.20×10^{-5}	3.20	0.40
SL	WG	1.4	2.30	63.6	32.3	4.1	39	0.39	0.21	—	3.59	0.87
SL	DG	1.4	2.30	63.6	32.3	4.1	39	0.39	0.26	1.94×10^{-6}	4.73	0.89

[†] SP, soil preparation technique (WG: wet grinding; DG: dry grinding). [‡] SOM, soil organic matter content measured from total carbon (TruSpec Carbon and Nitrogen Analyzer, LECO Corp., St. Joseph, MI) using a 1.724 ratio. [§] θ_s , saturated volumetric water content. [¶] θ_r , residual volumetric water content. [#] K_s , saturated hydraulic conductivity measured by falling head permeameter test. ^{††} n , α , van Genuchten model parameters, where pF is defined as $-\log(h)$ and h is the pore water pressure in cm.

Eight experiments were conducted: four with LS and four with SL (Table 1.2).

During the experiments, soil pressure potential was measured at 12 different points at three different depths (20, 50, and 80 cm from the bottom of the column) using pencil-size tensiometers, connected to pressure transducers and a data logger (CR10X, Campbell Scientific, Logan, UT), similar to Akay and Fox (2007).

An artificial biopore built by rolling a metallic mesh around a 6-mm diam. wooden dowel and covered with a plastic mesh was used to simulate OSC biopores with lengths of 55 and 65 cm and BSD biopores with lengths of 20 and 55 cm. All biopores were placed directly above the drain in the center of the soil column (Figure 1.1 and 1.2). A 5-cm diam. perforated tube was placed 6 cm (center of the pipe) from the bottom of the soil column to simulate a zero-pressure head boundary condition, assumed to represent an artificial drain. A 1-cm constant head on top of the column was maintained using a

Mariotte infiltrometer. Inflow at the top of the soil column and the outflow from the drain and the biopore were measured every 10 s using weighing scales (Figure 1.2).

Table 1.2. Main experimental variables for the open-surface connected (OSC) and buried surface disconnected (BSD) biopore soil column experiments with loamy sand (LS) and sandy loam (SL) soils. The SL soil was packed using either a wet grinding (WG) or dry grinding (DG) technique.

	Type	Soil	Soil column dimensions			BD [‡]	Soil preparation	<i>E. coli</i> C _o [§]	<i>E. coli</i> recovery	BP [¶]
			L [†]	a [†]	b [†]					
			cm	cm	cm	Mg m ⁻³		MPN [#] /100 mL	BTT ^{††}	
1	OSC	LS	65	10	0	1.6		11,517	+	NA ^{‡‡}
2	OSC	LS	55	20	0	1.6		15,362	+	NA
3 ^{§§}	BSD	LS	55	0	17.5	1.6		7140	+	Yes
4 ^{§§}	BSD	LS	20	0	52.5	1.6		4130	+	Yes
5	OSC	SL	55	20	0	1.4	WG	8355	+	NA
6 ^{¶¶}	BSD	SL	55	0	17.5	1.4	WG	5771	+	Yes
7 ^{¶¶}	BSD	SL	20	0	52.5	1.4	DG	15,000	–	No
8 ^{¶¶}	BSD	SL	55	0	17.5	1.4	DG	16,780	+	Yes

† Dimensions: a = soil layer thickness between the center of the drainage pipe to the bottom of the biopores; b: soil layer thickness between the surface and the top of the biopores; L: length of the biopores; see Figure 1.1 for more details. ‡ BD = Bulk density. § C_o = Initial *E. coli* concentration in the liquid swine manure. ¶ BP = Biopore. # MPN = Most Probable Number. †† BTT: Breakthrough time. ‡‡ NA = No measurement directly from the biopores because of experimental setup. §§ Rhodamine WT, 50 µg L⁻¹ added in the final water flush. ¶¶ CaCl₂, 0.01 M concentration added in the initial water flush; 1 g of Peptone per L of diluted liquid swine manure was added in the manure flush.

Each experiment consisted of four stages: (i) packing, (ii) an initial water flush (186–257 mm), (iii) a manure flush (107 mm), and (iv) a final water flush (107 mm). The LS and SL soils were packed at 1.6 and 1.4 Mg m⁻³ bulk density, respectively, for a total length of 85 cm. The LS soil was replaced with new soil after each experiment. For this same LS soil and bulk density, Chu-Agor et al. (2008) reported parameters for the soil moisture (i.e., hydraulic) characteristic curve, derived using the pressure plate extractor method on multiple samples as described by Dane and Hopmans (2002). The SL soil

from the Northeast Iowa State University research farm in Nashua was unpacked and reused. The SL was prepared before packing using two processes: (i) moist soil (WG, moisture content 10–20%) forced to pass a 4-mm sieve opening, and (ii) air dried soil, manually crushed by hammering, sieved using a no. 7 sieve, and then moistened to attain a moisture content of <10% before packing. It was hypothesized that the WG packing resulted in a greater distribution of soil pore spaces compared to the DG packing due to the differences in soil structure.

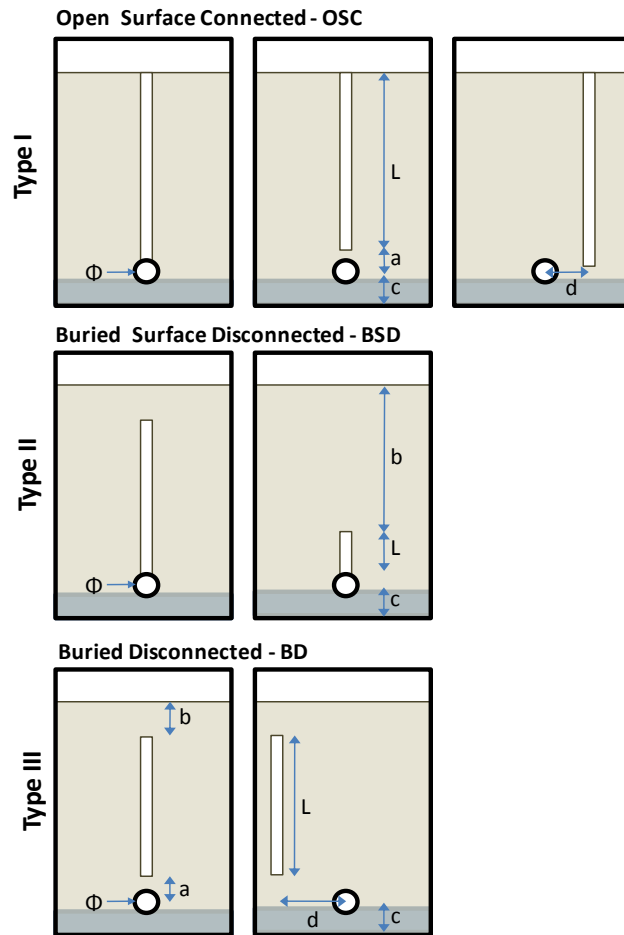


Figure 1.1. Potential biopores in relationship to a subsurface drain. OSC: open surface connected; BSD: buried surface disconnected; and BD: buried disconnected; a: soil layer thickness between the center of the drainage pipe to the bottom of the biopores; b: soil layer thickness between the

soil surface and the top of the biopores; c: initial saturated soil layer thickness equal to 10 cm for all experiments; d: distance from the center of the drain pipe to the vertical center of the biopores equal to zero for all experiments; L: length of the biopores; Φ : drain pipe diameter equal to 5 cm for all experiments.

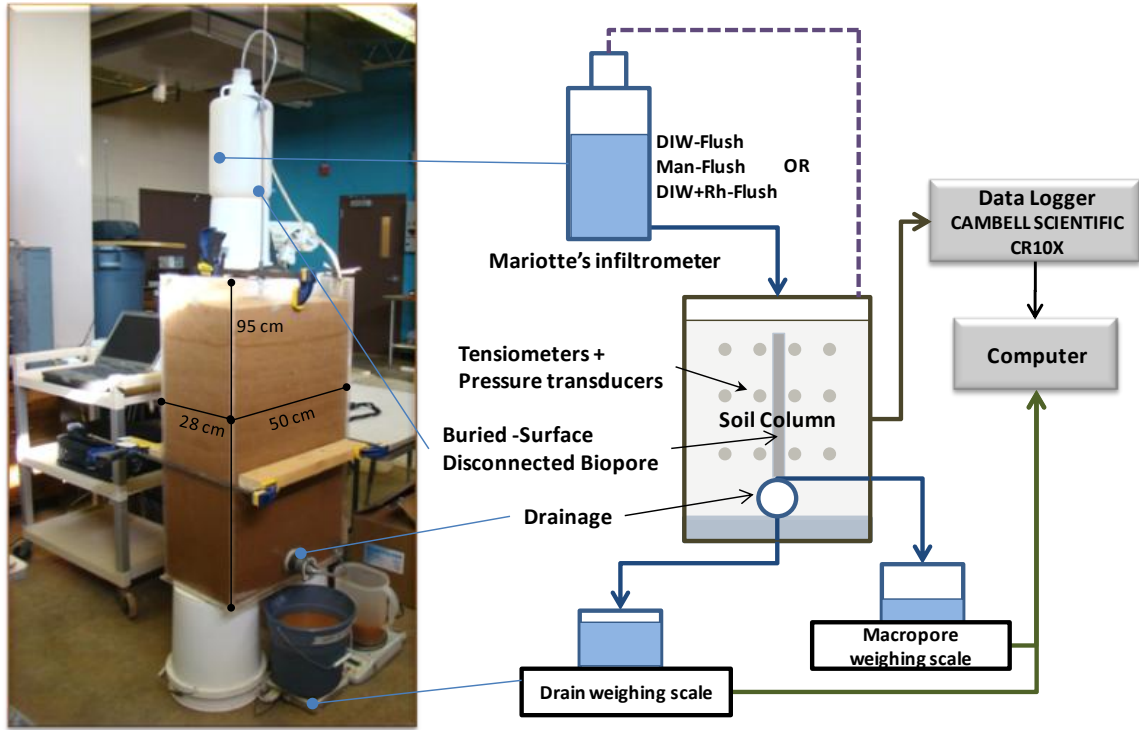


Figure 1.2. Descriptive setup of the soil column and instruments used in all experiments.

During the unpacking of two experiments (i.e., SL-WG and SL-DG, BSD, 55-cm), six soil core samples from each soil preparation were taken at different depths to define the hydraulic characteristic curve. Data from the pressure cell using the 12 SL core samples (WG and DG soil preparation techniques) were grouped and averaged according to the different pressures applied. The final data were plotted and fit with the van Genuchten (1980) model. The fit model was used to compare the LS vs. SL soils and DG

vs. WG packing techniques in terms of their soil moisture characteristic curves and to explain activation of the artificial biopore.

After packing and instrument setup, the initial water flush followed immediately. The manure flush and the final flush followed 48 and 96 h later, respectively. During the initial flush, only matrix flow was allowed by clogging the biopore with a wooden dowel. The initial flush in all experiments provided a hydrostatic, initial moisture content profile, allowed initial consolidation of the soil, established the saturated zone, and verified that there was no initial biopore flow. Water samples were taken in the drain after the initial flush to verify that *E. coli* was not present. Before the manure flush, the wooden dowel was pulled out to the desired biopore length. Diluted liquid swine manure was applied at the top of the soil column with different concentrations (Table 1.2). The liquid swine manure used in all experiments was collected in a 5-d composite sample from the Swine Research and Educational Center at Oklahoma State University and stored at 4°C.

Before each experiment, a manure dilution using distilled water was prepared to assure a proper *E. coli* concentration to minimize dilution during sample analysis and to mimic the effect of rainfall or irrigation in the field. During the manure flush in the SL experiments, 1 g of peptone (Special Peptone L0072, Oxoid, Lenexa, KS) per L of diluted liquid manure was used to reduce bacteria die-off in the Mariotte bottle due to the long infiltration time. The peptone concentration used (1 g per L) is typically recommended to provide or equilibrate a media at a steady bacteria concentration (e.g., growth equivalent to die-off). *Escherichia coli* samples were collected periodically from the Mariotte bottle and water at the top of the soil column and demonstrated that *E. coli* concentrations remained approximately stable during the experiments. Preliminary

experiments indicated that the *E. coli* from diluted liquid swine manure required 8 to 10 h (e.g., lag time) to begin using nutrients from sources other than the manure media.

Distilled as opposed to tap water was used in the initial flush to avoid chlorine residuals in the soil solution that might affect the bacteria population and transport. However, the use of distilled water most likely decreased the bulk soil solution ionic strength as water infiltrated due to the ionic interchange between the soil minerals and the displaced wetting front. This decrease in solution ionic strength may have promoted soil dispersion and progressive clogging of pore spaces as a result of the soil mineral double layer expanding. During preliminary experiments, soil dispersion and clogging was observed when the SL soil was used. To minimize soil dispersion in the SL soil, CaCl_2 (0.01 mol L^{-1} concentration) was added during the initial flush. The authors considered that the addition of CaCl_2 at this concentration allowed equilibrating the soil solution ionic strength to avoid soil dispersion and clogging and only marginally affected the fate and transport results.

Distilled water was used for the final flush of experiments with LS soil while tap water was used for SL soil. The use of tap water for SL was to further minimize soil dispersion and clogging of the soil column. In the LS soil, dispersion was not a problem. Rhodamine WT ($50 \text{ } \mu\text{g L}^{-1}$ concentration) was used in some experiments during the final flush to investigate flow conditions and verify no additional preferential flow along the soil column walls. Rhodamine WT is considered a conservative tracer and therefore minimally adsorbed to soil particles during the soil column experiments. Rhodamine WT was not expected to be used by the bacteria in significant quantities to affect fate and

transport in the time frame of the experiments. The final flush in all cases acted as a replicated experiment of the hydrologic response of the system.

Water samples and flow rates from the drain and the macropore were collected after each flushing for *E. coli* and total Coliform quantification. *Escherichia coli* was used as an indicator organism of fecal contamination and total Coliform for environmental bacterial activity. The semi-automated Quanti-Tray Method (IDEXX, Westbrook, ME), which provides counts from 0.0 to 2419.6 per 100 mL, was used to quantify the *E. coli* and total Coliform concentration by the most probable number (MPN) technique. Initial *E. coli* and total Coliform concentration were estimated as the average concentration between the beginning and end of the manure flush taken from the Mariotte bottle. Discharge and *E. coli* breakthrough time were defined as the point in time in which the constant cumulative discharge gradient changed or *E. coli* was continuously detected, respectively. After each experiment, the soil column was unpacked, disinfected and packed again with soil.

1.4. RESULTS AND DISCUSSION

1.4.1. Soil Property Characterization

A uniform soil pore space distribution was observed after packing the LS soil. Packing the SL soil to the designated bulk density generated an approximately equivalent average pore size between the DG and WG processes. However, the distribution of the pore spaces around this average (i.e., more homogeneous soil pore sizes in the DG and more widely varying in the WG) was hypothesized to be different and qualitatively observed during the experiments. During the SL soil preparation using the WG process, formation of soil aggregates were observed after forcing the soil to pass the sieve mesh.

Soil macropore formation within the soil aggregates was observed to be distributed irregularly along the soil column. On the other hand, the DG process resulted in a uniform pore size distribution with no soil aggregate development and no observable large pore spaces.

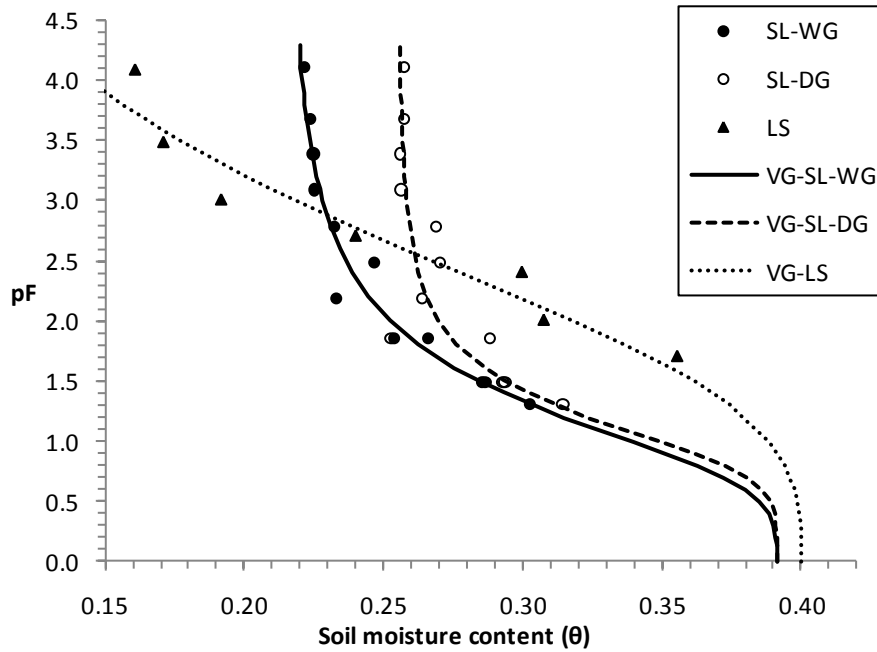


Figure 1.3. Hydraulic (i.e., soil moisture) characteristic curve for the loamy sand (LS) and sandy loam (SL) soil and its two preparation techniques (WG, wet soil; DG, dry soil) and fit to the van Genuchten (1980) model (VG). Data represent the means for six cores extracted from two SL columns. Data for the LS are reported by Chu-Agor et al. (2008) for the same bulk density as used in these experiments.

After the manure flush, some small cracks formed at the surface during the soil column depletion period. These cracks were also observed during the pressure cell experiments in most of the DG samples. Data from the pressure cell and van Genuchten (1980) model confirmed the previous observation (Table 1.1 and Figure 1.3). Parameters of the model indicated a difference in the macropore activation pressure for the two SL

soil preparations primarily in the air-entry pressure value. Estimates from the model based on six replicated samples implied an air-entry pressure difference in the range of 0.3 to 2.3 cm higher in the DG as well as the development of higher water suction values as moisture content decreased (Figure 1.3).

1.4.2. Water and Manure Suspension Flow

For a specific soil type and packing, discharge breakthrough time was inversely proportional to the biopore length in the OSC and BSD experiments. The only exception was for the LS, OSC, 55-cm experiment during the final flush, probably a result of additional preferential flow between the soil and the soil column walls. In general, the breakthrough time in the biopore occurred later than in the drain with the time difference decreasing as a function of the biopore length (Table 1.3). During the manure flush, the discharge breakthrough time for the SL, OSC, 55-cm experiment (i.e., WG soil preparation) was detected earlier than expected, especially in comparison with the LS OSC experiments. This early discharge breakthrough time was probably the result of the soil macropore formation around the soil aggregates.

Reduction in the cumulative matrix flow, measured 24 h after flush initialization, was observed between the manure and final flush (Table 1.4). This phenomenon was a function of the biopore length and soil type, with a stronger effect in the SL soil. It was hypothesized that soil dispersion was the result of distilled water utilization that might change the soil solution ionic strength and promote soil dispersion followed by clogging. Therefore, CaCl_2 (0.01mol L^{-1}) was used during the initial water flush to equilibrate the soil solution ionic strength. However, results indicate that the reduction in flow discharge was a complex combination of soil swelling and dispersion, soil minerals-organic matter

aggregation, and bacteria straining. In the SL soil, the larger proportion of small pore spaces and the higher soil organic matter and clay content was hypothesized to promote sorption of colloids, straining of fine particles in suspension, and straining of bacteria, all of which favored the clogging process.

Table 1.3. Drainage (Drain) and biopore (BP) breakthrough time (minutes) after manure flush and final water flush for open-surface connected (OSC) and buried surface disconnected (BSD) biopores in loamy sand (LS) and sandy loam (SL) soils. The SL soil was packed using either a wet grinding (WG) or dry grinding (DG) technique.

Experiment			Manure-Flush				Final-Flush			
	Type-length (cm)	Soil type	Discharge		<i>E. Coli</i>		Discharge		<i>E. Coli</i>	
			Drain	BP	Drain	BP	Drain	BP	Drain	BP
1	OSC-65	LS	3	NA†	17.5	NA	3.3	NA	4.5	NA
2	OSC-55	LS	7.7	NA	18	NA	2.7	NA	3	NA
3	BSD-55	LS	24.5	25.9	37.0‡	26.1	24.7	25.1	25.5	25.4
4	BSD-20	LS	34.7	47.4	70.0§	50	33.8	52.1	106¶	53.8
5	OSC-55	SL-WG	1.2	NA	60	NA	≈ 4.0	NA	4	NA
6	BSD-55	SL-WG	11.5	≈ 132	170.0#	132	234.5	No Flow	No BTT††	No Flow
7	BSD-20	SL-DG	≈ 30	No Flow	No BTT	No Flow	NA	No Flow	No BTT	No Flow
8	BSD-55	SL-DG	6	60.2	No BTT	No BTT	13	20.2	No BTT	No BTT

† NA = no measurement directly from the biopore because of experimental setup. ‡ *Escherichia coli* was initially detected at 25.4 min followed by no continuous detection until 37 min. § *Escherichia coli* was initially detected at 57 min followed by no continuous detection until 70 min. ¶ *Escherichia coli* was initially detected at 9 min followed by no continuous detection until 106 min. # *Escherichia coli* was not detected continuously; data in the table correspond to the first detection. †† BTT = Breakthrough time.

In the biopore flow, a reduction in the cumulative discharge after 24 h for the SL soil and an increasing discharge for the LS soil were observed (Table 1.4). In the SL soil, this was hypothesized to be the result of pore space clogging as previously discussed. In the LS soil, the biopore discharge increase can be explained by expansion of the biopore

effective radius due to internal erosion along the biopore wall (observed qualitatively based on turbidity in the outflow water) and/or the reduction in the soil matrix suction around the biopore after the manure flush (Table 1.3). In general, during the unpacking of the soil column, it was observed that the soil in contact with the biopore wall was saturated in most of its length 48 h after final flush initialization. The occurrence of this condition after the manure flush in combination with a lower air-entry pressure (higher pF value) in the LS favored macropore discharge during the final flush.

In all BSD experiments, discharge from the biopore and into the macropore weighing scale occurred suddenly. This condition was studied by Akay and Fox (2007) and occurred at the moment in which the matrix suction decreased along the biopore as the water pressure increased near the drain. Comparison between the SL-DG and SL-WG BSD, 55-cm experiments indicated the importance of pore size in the biopore activation due to changes in the soil structure. The SL-DG contained uniform pore spaces and maintained higher pore water suction than SL-WG around the soil in contact with the biopore wall after depletion. This condition reduced the capacity of water to move into the biopore while at the same time moved water from the walls of the biopore into the soil matrix as the wetting front progressed downward. These effects are also applicable when comparing total biopore discharge in the LS and SL soils (Table 1.3).

1.4.3. Escherichia coli Transport: Soil Type and Packing

Water samples taken during the initial flush indicated no initial *E. coli* concentration capable of desorbing into the matrix flow. However, total Coliform was always detected in the drain at concentrations greater than 500 MPN/100 mL. During the manure flush, with the exception of the SL-DG experiments where no activation of the

biopore occurred, *E. coli* and discharge breakthrough time indicated that *E. coli* moved slower than water in the soil matrix, as represented by the drain discharge in Table 3. On the other hand, in the biopore, *E. coli* was always detected at approximately the same time as the discharge (Table 1.3). The difference between the discharge and *E. coli* breakthrough time in the biopore and matrix was hypothesized to be the result of *E. coli* resistance to be transported through pore spaces by using a combination of motile capabilities and adhesion (Hill et al., 2007). In the soil solution, the sorptive properties of the soil, primarily determined by fine particles (i.e., clay and silt) and organic matter content, established the *E. coli* concentration available for transport. Then, *E. coli* in planktonic forms in the soil solution, attached to colloids in suspension, or weakly attached could be transported as water moved through soil pore spaces.

The presence of a larger proportion of small pore spaces (e.g., micropores and small mesopores) in the soil promoted straining (physical and biological) and induced large hydraulic energy losses. Energy losses were translated as a reduction in the pore space velocity distribution and allowed *E. coli* to resist transport (adhesion and/or auto-propulsion) in the direction of flow. In cases where the soil contained a larger proportion of soil macropores, flow and shear stress forces can more effectively mobilize available bacteria in solution, bacteria that are weakly attached, or colloids and aggregates previously colonized by bacteria. In fact, Smith et al. (1985) made similar observations in reporting that the transport of bacteria through sieved or mixed soil columns was negligible when compared to more structured soils.

Table 1.4. Cumulative matrix (Drain) and biopore (BP) discharge in the open-surface connected (OSC) and buried surface disconnected (BSD) biopore experiments with loamy sand (LS) and sandy loam (SL) soils. The SL soil was packed using either a wet grinding (WG) or dry grinding (DG) technique. Cumulative discharge measured 24 h after flush initialization.

Type	Soil type	Flush	Flush	Drain	BP	Drain		BP			
			mL	mL	mL	% of Flush	% Change	% of Flush	% Change	% of Drain	% Change
1	OSC-65	LS	Manure	15,000	14,601	NA [†]	97.3		NA	NA	NA
			Final flush	15,000	13,311	NA	88.7	-8.6	NA	NA	NA
2	OSC-55	LS	Manure	15,000	14,962	NA	99.7		NA	NA	NA
			Final flush	15,000	13,500	NA	90	-9.7	NA	NA	NA
3	BSD-55	LS	Manure	15,000	10,688	3,387	71.3		22.6		31.7
			Final flush	15,000	8930	3,659	59.5	-11.7	24.4	1.8	41
4	BSD-20	LS	Manure	15,000	12,567	934	83.8		6.2		7.4
			Final flush	15,000	10,600	1,261	70.7	-13.1	8.4	2.2	11.9
5	OSC-55	SL-WG	Manure	15,000	11,623	NA	77.5		NA		NA
			Final flush	15,000	DL	NA	DL	DL [‡]	NA	NA	NA
6	BSD-55	SL-WG	Manure	15,000	6,435	1,235	42.9		8.2		19.2
			Final flush	15,000	1,028	0	6.9	-36.0	0	-8.2	0
7	BSD-20	SL-DG	Manure	15,000	10,000	0	66.7		0		0
			Final flush	15,000	1,264	0	8.4	-58.2	0	0	0
8	BSD-55	SL-DG	Manure	15,000	10,506	564	70		3.8		5.4
			Final flush	15,000	6,676	110	44.5	-25.5	0.7	-3	1.6

[†] NA = no measurement directly from the biopore because of experimental setup. [‡] DL = No data available because data were lost due to datalogger failure.

1.4.4. *Escherichia coli* Transport: Open-Surface Connected versus Buried

Surface Disconnected Biopores.

In the OSC experiments, *E. coli* transport to the drain was mainly a function of the soil layer thickness between the end of the biopore and the drain and the *E. coli* concentration along the biopore wall (Figure 1.1 and Table 1.2). The latter was a function

of the energy head in the biopore. The OSC biopores allowed rapid *E. coli* transport from the surface to deeper soil layers at the end of the biopore, followed by slower wetting front movement through the remaining soil profile (i.e., 10 or 20 cm depending of the biopore length) before reaching the drainage pipe. These conditions were verified by the soil tensiometer data. This 10 to 20 cm soil buffer layer in the LS was not important in the *E. coli* breakthrough time. However, changing the soil texture as indicated in the SL experiment (WG, OSC, 55-cm) resulted in an extended *E. coli* breakthrough time. Soil type and organic matter content impacted the straining (physical and biological) and sorption mechanisms as well as allowed *E. coli* to resist being transported when soil pore water shear forces were low (Table 1.3 and Figure 1.4).

Transport of *E. coli* in BSD biopores was subjected to two different processes: the soil-biopore interaction as the wetting front moved downward and the soil water suction relaxation along the biopore wall that allowed water movement into the biopore. In the first case, small water fluxes from the soil solution moved into the biopore as the wetting front moved downward, with a possibility of *E. coli* transport if soil pore space allowed bacteria movement. As water moving into the biopore wall entered in contact with soil containing higher pore water suction, water moved back into the soil matrix. *E. coli* stayed in the soil solution, attached to the soil surrounding the biopore, or moved back into the biopore when the wetting front from matrix flow reached the surrounding soil. In the second case, *E. coli* was transported from the soil solution or detached by stress forces when biopore fluxes created shear forces that exceeded *E. coli* attachment forces. These conditions can explain the large *E. coli* recovery concentration at the beginning of the biopore discharge in Figure 1.5.

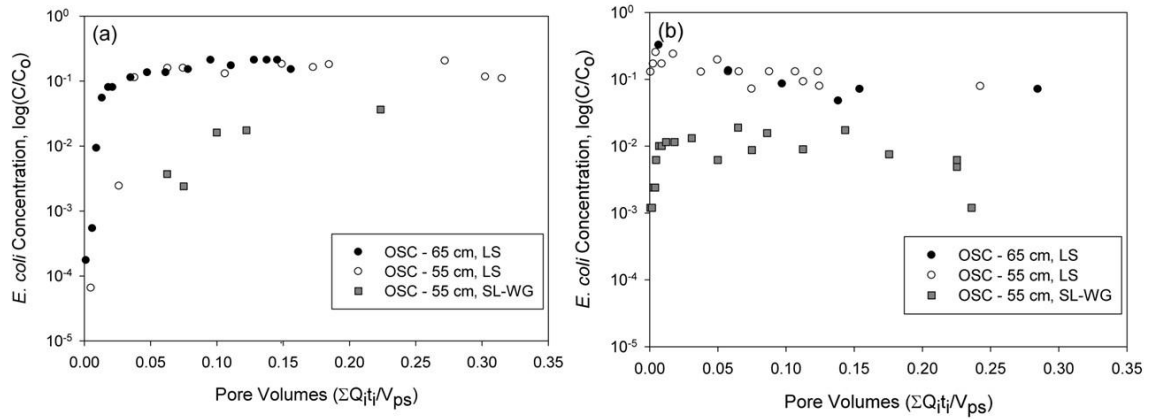


Figure 1.4. *Escherichia coli* concentrations from the drain (C) relative to the inflow *E. coli* concentration (C_0) for open-surface connected (OSC) biopore experiments (i.e., 55 and 65 cm biopores lengths) as a function of the number of pore volumes (i.e., product of flow rate, Q , and time, t , divided by the volume of pore space, V_{ps} , of the soil column) of inflow water (a) during manure flush and (b) during the final water application. Experiments correspond to numbers 1, 2, and 5 in Tables 2 to 5.

During the final flush for most experiments, *E. coli* and discharge breakthrough time in the drain and biopore occurred at approximately the same time (Table 1.3). This demonstrated that *E. coli* was previously established in the soil solution or weakly attached when water fluxes started moving into the biopore. The manure flush provided the initial *E. coli* concentration at different depths through soil matrix and/or biopore domains, followed by an *E. coli* regrowth period. During the final flush, *E. coli* were flushed out from the soil closest to the drain and/or biopore wall, providing the initial *E. coli* concentration observed in the breakthrough curve. The *E. coli* concentrated then peaked and decreased over time in most cases (Figure 1.4b, 1. 5c-d). These results have implications in terms of the impact of pathogenic bacteria transport to subsurface drainage from storm events beyond those immediately following manure applications.

The OSC and BSD biopores may provide a mechanism for transporting bacteria to more favorable survival and growth conditions and therefore may contribute *E. coli* in subsequent drain flow events.

For all LS experiments, *E. coli* was always detected in the drain flow for the OSC and BSD biopores with the highest recovery concentrations during the final flush (Table 1.5). Note that in the case of OSC biopore experiments, *E. coli* recovery and discharge cannot be measured at the biopore due to the experimental setup. The LS soil possessed larger pore spaces and less sorptive properties than the SL soil. Therefore, *E. coli* moved easily through the soil macropores and eventually through mesopores during the manure and final flush. During the final flush, *E. coli* regrowth and lower straining conditions explained the highest concentration recovery in Table 1.5. On the other hand, in the SL soil, the highest *E. coli* recovery occurred during the manure flush indicating the importance of transport restriction due to smaller pore spaces that can easily promote straining. This hypothesis was also associated with the observed flow reduction between the manure and final flush described previously.

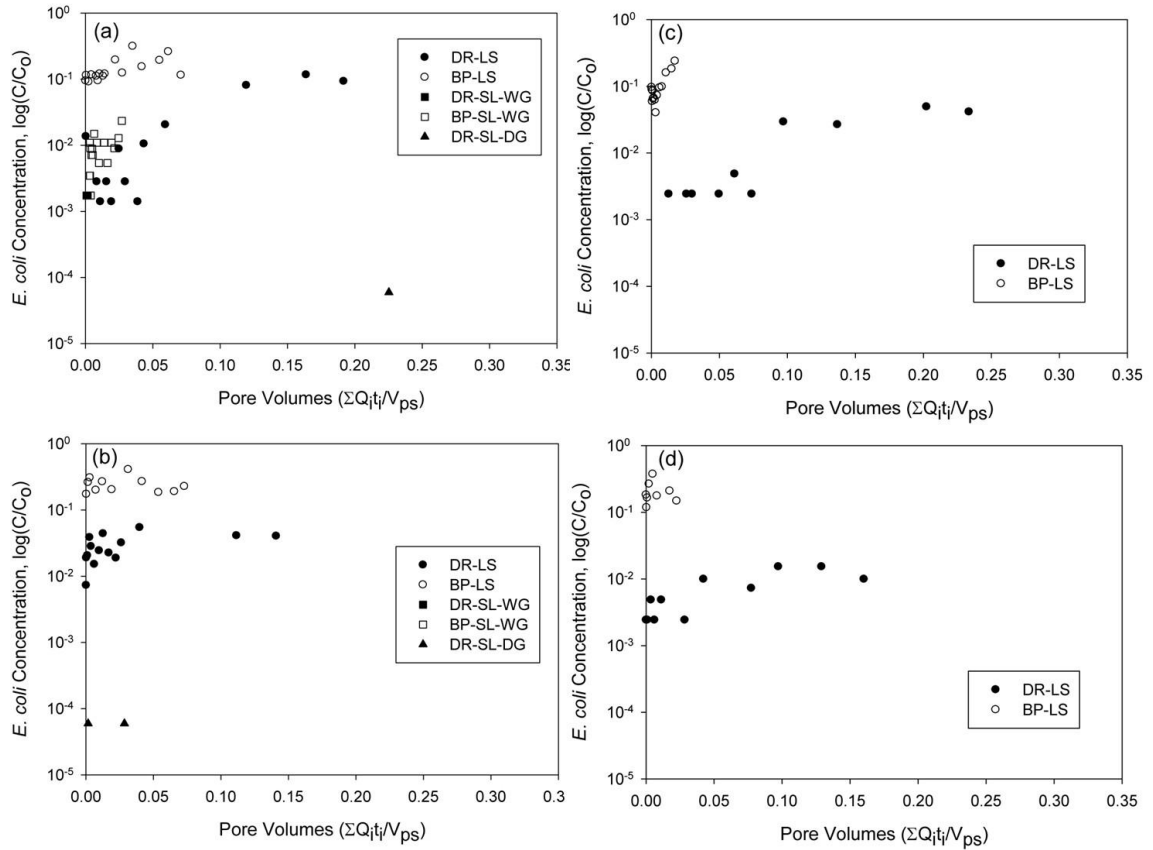


Figure 1.5. *Escherichia coli* concentrations from the drain (C) relative to the inflow *E. coli* concentration (C_0) for buried surface disconnected (BSD) biopore experiments (i.e., 55 and 20 cm macropore lengths) as a function of the number of pore volumes (i.e., product of flow rate, Q , and time, t , divided by the volume of pore space, V_{ps} , of the soil column) of inflow water. Figures (a) and (b) are during the manure flush and final water application for the 55-cm BSD biopores, respectively (i.e., Exp. 3, 6, and 8 in Tables 2–5). Figures (c) and (d) are during the manure flush and final water application for 20-cm BSD biopores, respectively (i.e., Exp. 4 in Tables 2–5 with Exp. 7 having no observed *E. coli* from the matrix or biopore). DR = drain flow, BP = biopore flow, LS = loamy sand, SL = sandy loam, WG = wet soil preparation and DG = dried soil preparation.

Table 1.5.. Macropore length, *E. coli* initial concentration (C_0), and maximum *E. coli* recovery from the matrix and macropore flow for the open-surface connected (OSC) and buried surface disconnected (BSD) biopore experiments with loamy sand (LS) and sandy loam (SL) soils. The SL soil was packed using either a wet grinding (WG) or dry grinding (DG) technique.

Type	Soil Type	Macropore	<i>E. coli</i> C ₀	Matrix flow		Macropore flow		
		Length (cm)	(MPN/100mL)	Man-Flush	Final-Flush	Man-Flush	Final-Flush	
1	OSC	LS	65	11,500	0.21Co [†]	0.32Co	NA [‡]	NA
2	OSC	LS	55	15,400	0.20Co	0.25Co	NA	NA
3	BSD	LS	55	7140	0.12Co	0.05Co	0.32Co	0.41Co
4	BSD	LS	20	4130	0.05Co	0.01Co	0.24Co	0.37Co
5	OSC	SL-WG	55	8355	0.04Co	0.02Co	NA	NA
6	BSD	SL-WG	55	5771	0.002Co	0	0.023Co	No Flow
7	BSD	SL-DG	20	15,000	0	0	No Flow	No Flow
8	BSD	SL-DG	55	16,780	6x10 ⁻⁵ C ₀	6x10 ⁻⁵ C ₀	0	0

[†] *E. coli* exceeded the upper limit of the test procedure (i.e., 2419.6 MPN/100 mL) for two samples. [‡] NA = not measured because of experimental setup (no measurement directly from the biopores).

1.5. SUMMARY AND CONCLUSIONS

Results from this study indicated the efficiency of *E. coli* transport to drainage systems under the presence of interconnected open-surface or buried biopores. Soil macropores and large mesopores play an important role in allowing the movement of pathogens to deeper soils after irrigation or rainfall events. Soils with small soil pore spaces (e.g., micropore and small mesopores) and sorptive properties can filter *E. coli* in most of the cases due to the development of physical and biological straining as well as adsorption. Additionally, low velocities in the soil pore spaces may allow *E. coli* to resist being transported by its auto-propulsion and adhesion capabilities. On the other hand, soils with large pore spaces such as large mesopores and soil macropores favored *E. coli*

transport. The development of shear forces under these conditions may promote transport and detachment of bacteria or colloids colonized by bacteria during wetting front displacement.

Biopores that are directly connected to subsurface drainage systems can provide a direct conduit for *E. coli* transport from the soil surface into tile drainage that may impact drain flow *E. coli* concentrations in immediate and subsequent storm or irrigation events following manure applications. In these experiments, it was clear that biopore activation occurred later than discharge in the drain. In the biopore, *E. coli* and flow were simultaneously detected. In the open-surface connected biopore, *E. coli* transport to the drain was mainly a function of the soil type and/or soil layer thickness between the end of the macropore and the drain. In the LS soil, the thickness of the layer was not important in regard to the *E. coli* peak concentration in the drain; however, in the SL soil, *E. coli* transport to the drain was clearly limited by the soil properties. This study indicated that sorption of *E. coli* to soil determined residual *E. coli* concentrations in the soil solution or attached to soil particles and colloids in solution after manure application. For these reasons, adsorption and adhesion mechanisms of pathogenic bacteria should be further investigated. Buried surface disconnected biopores can be an effective *E. coli* pathway through soils when they are in contact with other soil macropores or large mesopores. However, under the presence of small and homogeneous soil pore spaces, the soil filter capacity will limit the transport of *E. coli* to the biopore and then to the interconnected drainage system.

CHAPTER 2

Sorption of *Escherichia coli* in Agricultural Soils

Influenced by Swine Manure Constituents

2.1. ABSTRACT

Sorption of fecal bacteria in soils has been typically investigated using cultured bacteria suspended in distilled water and found to be proportionally related to the percentage of clay content. Under field conditions, increased concentrations of fecal bacteria are associated with increased application rates of animal waste, containing a variety of waste constituents that can interact with soils. Also, under nutritional depleted environments found in aged manures commonly used as fertilizers, fecal bacteria is mainly found bonded to particles and colloids surfaces (i.e., sessile form as micro colonies and/or biofilms) rather than as a free cells in suspension (i.e., planktonic form). The objective of this research was to investigate the influence of manure constituents and the predominance of sessile bacteria on fecal bacteria sorption/attachment. *Escherichia coli* sorption was investigated using a series of artificial and natural soils treated with swine effluent at varying dilution ratios (i.e., manure effluent concentration). Fecal bacteria in swine effluents consisted primarily of sessile (i.e., attached) bacteria (90%) compared to free cells in suspension (10%). Removal of sessile *E. coli* from solution by sorption/attachment and/or flocculation/precipitation appeared to be controlled by processes occurring in the substrate (i.e., surfaces to which the bacteria attached). For

soils up to 30% clay content and 3.0% total carbon content, nonlinear equations characterized the sorption of *E. coli* from multi-constituent manure effluent in the artificial and natural soils with the equation parameters predicted by the amorphous aluminum and iron content, percent clay, and percent organic carbon. Also, dispersion resulting from alkalinity buildup due to adding effluent to the soils decreased observed sorption of *E. coli*, especially at higher effluent ratios. These influential factors (i.e., manure effluent concentration, sessile bacteria, and soil dispersion under high effluent concentrations) should be considered when modeling fecal bacteria transport in the environment.

2.2. INTRODUCTION

Following manure application in agricultural lands, soil sorption of fecal bacteria is influenced by the soil's physical-chemical properties, animal waste effluent characteristics and bacteria properties (Foppen et al., 2005; Pachepsky et al., 2006; Torkzaban et al., 2008; Kim and Walker, 2009; Guzman et al., 2009, 2010). Under nutritional depleted environments (e.g., aged manures commonly used as fertilizers), fecal bacteria is mainly found bonded to particles and colloids surfaces (i.e., sessile form as micro colonies and/or biofilms) rather than as a free cells in suspension (i.e., planktonic form) (Dunne, 2002; Winfield and Groisman, 2003). Bacteria attachment and adhesion are terms frequently used to describe sorption of *E. coli* (e.g., reversible or irreversible) that may not necessary imply bacteria immobilization under flow conditions. Soil sorption of fecal bacteria following manure applications are complex and difficult to identify and quantify due to the multiple mechanisms and interactions that can occur at the surface/bulk solution interface of the organic and inorganic compounds (Brown et al.,

2000; ter Laak, 2005). Parallel to this, animal wastes contribute loads of organic compounds and solutes to soils when applied as fertilizers, along with a diverse microbial population (Choudhary et al., 1996; Leung and Topp, 2001), thereby promoting changes in the soil properties and the microbial community following application (Gerzabek et al., 1997; Haynes and Naidu, 1998; Eghball et al., 2004).

Soil sorption of fecal bacteria has been typically investigated using planktonic mono-strain cultured bacteria in batch, soil column or microfluid devices and described by linear or nonlinear relationships (e.g., Ling et al., 2002; Mankin et al., 2007; Bolster et al., 2009) or the Derjaguin-Landau-Verwey-Overbeek (DLVO) theory (e.g., Redman et al., 2004; Torkzaban et al., 2008). However, most investigations become limited in applicability with complex soil/bulk solution interactions found in soils treated with animal waste. Previous investigations are typically limited to sediments and particles typically not representative of highly reactive soil minerals (e.g., mostly variably charged) and organic matter (i.e., permanently charged) commonly found in agricultural lands.

Few studies had been conducted to investigate sorption of fecal bacteria on soils treated with manure fertilizers. As an example, experiments conducted on batch experiments using loam and clay loam top soils were conducted to evaluate the effect of bovine manure colloids on *E. coli* attachment (Guber et al., 2005), and to compare the attachment of fecal Coliforms to the same two soil types and its soil fractions (Guber et al., 2007). In both series of experiments, cultured bacteria (e.g., fecal Coliforms or *E. coli*) insulated from bovine manure was used after placed in suspension. Other studies on sorption of fecal bacteria have been conducted on loess clay loam soil (clay, silt, sand and

organic matter content of 29%, 45%, 26% and 0.8%, respectively) treated with waste effluents (Gantzer et al., 2001; Kouznetsov et al., 2004). Nonlinear relationships were reported describing sorption of fecal Coliform in soils. Ling et al. (2002) proposed a linear relationship between the *E. coli* distribution coefficient of the Freundlich model, K_d , and the natural logarithm of the clay content based on two different soils (14% and 35% clay content with 0.84% and 0.54% organic matter content). Moreover, Mankin et al. (2007) conducted similar experiments and reported Freundlich isotherms describing *E. coli* sorption to sand and silt loam soils but concluded that linear isotherms better fit low initial *E. coli* concentrations.

This research hypothesizes that manure constituents and the predominance of sessile fecal bacteria found in animal waste result in unique sorption/attachment observations when compared to previous sorption studies utilizing suspended mono-strain free cells. Therefore, the objectives of this study were to (i) investigate sorption of *E. coli* in a range of soils after liquid swine manure application, (ii) determine the potential for using nonlinear equations to describe this sorption, and (iii) utilize soil properties for estimating the nonlinear parameters. The development of such predictive equations will be useful in estimating *E. coli* sorption in liquid swine manure-amended soils for improved modeling of *E. coli* sorption after manure application.

2.3. MATERIAL AND METHODOLOGY

2.3.1. Soil Samples

Natural soils and artificial soils (e.g., natural soils and natural soils after organic matter removal) were used in *E. coli* sorption experiments performed at room temperature (e.g., $23 \pm 0.5^\circ\text{C}$), as shown in Tables 2.1 and 2.2. Benchmark Oklahoma soils

(e.g., natural soils) were provided by the Soil, Water and Forage Analytical Laboratory (SWFAL) at Oklahoma State University, and Iowa soil collected from the Iowa State Research Farm in Nashua, IA (Table 2.1). Soils were air dried, grinded, and sieved to pass a 2 mm opening. Soil particle size distribution was estimated by wet sieve and hydrometer method (Gee and Or, 2002). Soil pH was measured in natural and artificial soils using 1:1 soil to distilled water dilution (Thomas, 1996).

Table 2.1. Soil properties of the natural soils used in the sorption experiments.

ID	Natural Soils		Soil pH	Clay %	TN [†] %	TC [¶] %
	Name	Classification				
PR	Pratt	Sandy, mixed mesic Lamellic Haplustalfs	6.3	7	0.04	0.36
DO	Dougherty	Loamy, mixed, active, thermic Arenic Haplustalfs	5.2	8	0.06	0.48
DA	Darnell	Loamy, siliceous, active, thermic, shallow Udic Haplustepts	5.4	11	0.06	0.57
BE	Bernow	Fine-loamy, siliceous, active, thermic Glossic Paleudalfs	4.3	11	0.13	1.30
CO	Cobb	Fine-loamy, mixed, active, thermic Typic Haplustalfs	5.5	16	0.06	0.40
CA	Camasaw	Typic Hapludults	5.7	21	0.12	2.83
EA	Easpur	Fine-loamy, mixed, superactive, thermic Fluventic Haplustolls	5.9	22	0.09	0.96
SA	Sallisaw	Fine-loamy, siliceous, superactive, thermic Typic Paleudalfs	5.5	22	0.15	1.26
PA	Parsons	Fine, mixed, active, thermic Mollic Albaqualfs	6.5	30	0.12	1.41
SL [§]	Floyd sandy loam	Fine-loamy, mixed, superactive, mesic Aquic Pachic Hapludolls	6.0	4.1	0.21	2.07
LS	Loamy sand	Arenic Haplustalfs	7.4	2.1	0.01	0.15

[†] TN = total nitrogen

[¶] TC = total carbon

[§] = Soil from Iowa, all other soils from Oklahoma

Artificial soil samples were prepared by mixing Silurian sand (U.S. Silica Company, Berkeley Springs, WV) and well crystalline kaolinite clay (KGa-1b, The Source Clay Repository, Purdue University, West Lafayette, IN) at three different

kaolinite clay and total carbon contents (Table 2.2). In the cases in which total carbon was considered, sphagnum peat moss (Premier Horticulture, Inc., Quakertown, PA) was used. Before mixing, the peat moss was oven dried at 65°C for 24 hr and sieved to pass a #200 sieve (i.e. 74 µm opening) in order to mimic clay particle sizes. Two natural soils were treated to reduce the total carbon content (e.g., loamy sand - LS, and sandy loam - SL) following the procedures described in Kunze (1965): 120 g of soil was placed in a glass container and sodium acetate (NaOAc) was added to achieve a 1:1 soil to NaOAc volume ratio. An initial 30 mL of hydrogen peroxide reagent (30% concentration) was added and the mixture was allowed to stand overnight. The following day the suspension was stirred and heated in order to remove excess H₂O₂ while small H₂O₂ aliquots were added until the soil lost its black color. With the completion of the organic matter decomposition, the pH was increased to 8 using Na₂CO₃ and then the solution was boiled for 10 minutes. After the solution cooled, a 1 N NaCl wash followed at an equivalent volume. The solution was allowed to stand for one day or until a clear supernatant was observed. The supernatant was then discharged and the remaining soil was washed with distilled water twice and then allowed to stand. Once a clear supernatant was observed, the supernatant was poured out and the soil was oven dried at 65°C.

Artificial soils were used to assess and quantify the effect of soil minerals and total carbon on prevailing mechanisms occurring on the soil/bulk solution that might impact attachment of *E. coli* to soils from manure effluents. For all soils and peat (e.g., sieved fraction), total carbon and total nitrogen content were estimated using a TruSpec Carbon and Nitrogen Analyzer (LECO Corp., St. Joseph, MI).

Table 2.2. Soil properties of the artificial soils used in the sorption experiments.

ID	Artificial Soils	Soil pH	Clay %	TN [†] %	TC [¶] %
C5P2	Silurian sand, kaolinite and peat moss	4.4	5	0.03	0.75
C10P2	Silurian sand, kaolinite and peat moss	4.5	10	0.03	0.75
C20P2	Silurian sand, kaolinite and peat moss	4.3	20	0.03	0.75
C5P4	Silurian sand, kaolinite and peat moss	-	5	0.06	1.51
C10P4	Silurian sand, kaolinite and peat moss	-	10	0.06	1.51
C20P4	Silurian sand, kaolinite and peat moss	-	20	0.06	1.51
C5P8	Silurian sand, kaolinite and peat moss	-	5	0.11	3.02
C10P8	Silurian sand, kaolinite and peat moss	-	10	0.11	3.02
C20P8	Silurian sand, kaolinite and peat moss	-	20	0.11	3.02
C5	Silurian sand and kaolinite	5.4	5	0.02	0.00
C10	Silurian sand and kaolinite	5.3	10	0.01	0.00
C20	Silurian sand and kaolinite	5	20	0.01	0.00
SS	Silurian sand	-	0	0.00	0.00
SSPt	Silurian sand and peat moss	4.5	0	0.03	0.75
SL-TCR	Natural soil; Total carbon reduced	9.1	4.1	0.00	0.64
LS-TCR	Natural soil; Total carbon reduced	8.4	2.1	0.08	0.15

[†] TN = total nitrogen

[¶] TC = total carbon

All soil samples for *E. coli* quantification were prepared in triplicate by placing 6.0 g of air dried soil (e.g., room temperature) in a 50-mL plastic centrifuge tubes and then mixing with a 6.0 mL effluent (e.g., approximately 10°C) prepared by diluting liquid swine manure in distilled water at five different dilution ratios (e.g., 1:5, 2:4, 3:3, 5:1, and 6:0 mL of liquid swine manure to mL of distilled water). A total of 15 samples per soil type were prepared (Tables 2.1 and 2.2). Even though soil samples were prepared from disturbed soils, the experiments were intended to mimic the upper 1 to 2 cm of soil in contact with swine effluent under field conditions. Once effluents move through the soil matrix, reduction in solute concentration and organic compounds due to sorption, ion exchange, and filtering may result in different sorption conditions which fall outside the scope of this paper.

2.3.2. *Escherichia coli* Source

Liquid swine manure from the Swine Research and Educational Center at Oklahoma State University was collected in a 5 d composite sample and stored at 4°C in a closed plastic container for one year. Storage of the swine effluent mimicked anaerobic conditions typically found in manure pits before manure application. Before the experiments, the stored manure was mixed with fresh liquid swine manure aliquots in order to increase the *E. coli* concentration to a desired concentration (e.g., approximately 20,000 most probable number (MPN)/mL) and mimic the mixing cycle found in manure pits (e.g., aged manure mixed with fresh manure).

Major ions were measured in the final effluent mixture using ICP-AES and elemental digestion analysis (EPA 3051 method) for the liquid and solid component, respectively (Table 2.3). Solids were separated after 90 minutes of centrifugation at 400 G using 40 mL of liquid swine manure. The percentage of solids and liquid was estimated by weight after pouring the supernatant and evaporating the remained liquid at 65°C. The particle size distribution of the swine manure colloids and their associated *E. coli* concentrations were determined by filtration using a series of 1.27-cm diameter and 0.16-cm thickness stainless steel disks (Applied Porous Technologies, Inc., Tariffville, CT) with 53, 40, 20 and 10 µm openings and a set of Nylon mesh (BioDesign Inc. of New York, Carmel, NY) with 50, 35, 20 15 and 8 µm openings. Samples for *E. coli* enumeration were taken before and after each successive filtration stage in triplicate experiments.

Table 2.3. Composition of the swine effluent utilized in the study.

	Source	%	Na	Ca	Mg	K	S	B	P	Fe	Zn	Cu	Mn	Al	Ni	pH
Liquid	AS [†] (mg L ⁻¹)	99	400.5	159.3	44.6	922.7	817.7	1.2	136.9	2	0.7	0.4	0.4	0.1	-	7.5
	NS [‡] (mg L ⁻¹)		394.2	158.7	15.2	1029.2	345.6	1.2	55.8	1.2	0.2	0	0	0.1	-	7.5
Solid	(mg kg ⁻¹)	1	0.6	1.5	0.7	0.9	0.6	-	1.6	1580	1808	366.6	304.6	-	9	-

[†] Swine effluent used in the artificial soils (AS)

[‡] Swine effluent used in the natural soils (NS)

2.3.3. Quantification of *E. coli* Sorption

After soil sample preparation, *E. coli* sorption was quantified as follow. First, treated soils were re-suspended using a vortex (Genie 2, G-560, Scientific Industries, Inc., Bohemia, NY) for 2 to 3 seconds and then allowed to stand for a 5-minute equilibration time to minimize bacterial activity. This equilibration time was equivalent to that used by Ling et al. (2002) and similar to other reported sorption studies with fecal bacteria (Huysman and Verstraete, 1993). Second, treated soils were centrifuged for 3 minutes at 48G to decant clay particles from *E. coli* (e.g., differential centrifugation) as described in Ling et al. (2002). Note that the complete methodology proposed in Ling et al. (2002) was not followed as it implied a second treatment with a saline solution quantifying the so called “strong adsorption”. Tests conducted to quantify *E. coli* removal by centrifugation in swine effluents (no soil was added) rather than sorption indicated that less than 5% of the *E. coli* population was removed by gravitational forces during the 3 minute centrifugation time. This percentage was not considered significant in the computations. The equilibration time was short enough to minimize microbial activity that may affect the initial fecal bacteria population (e.g., inactivation, bacteria growth, competition and predation), but long enough for the main ion exchange processes to

occur during the mixing process. Note that effluents were used with its entire biological and chemical loads proportional to the dilution ratio.

Subsamples from the supernatant were quantified for *E. coli* concentrations (MPN/mL) using IDEXX Colilert reagent and Quanti-Tray 2000 (IDEXX, Westbrook, ME), a U.S. EPA approved method for *E. coli* quantification. Note that *E. coli* enumeration using Quanti-Tray 2000 is based on fluorescence under UV light (Garbrecht et al., 2009; Guzman et al., 2009, 2010). Electrical conductivity and soil pH were measured after centrifugation (e.g., triplicate samples) per each dilution ratio and refrigerated for additional solution analysis of major ions (e.g., Na, K, Ca, Mg, S, P, B, Fe, Zn, Cu, Mn, and Al) using Inductively Coupled Plasma Atomic Emission (ICP-AES). This research assumed that the experimental process did not lead to cell lysis due to the collision between *E. coli* and the soil particles. Sutura and Mehrjardi (1975) concluded from blood cells experiments (e.g., 6-8 μm size) under turbulent flow that shear stress above 2,500 to 3,000 dynes/cm² may result in cell lysis. This shear stress was equivalent to cells centrifuged an approximately 400 to 480 G.

2.3.4. Effluent Bacteria Growth: Microcalorimeter

Time lag to the exponential bacteria growth phase was investigated using an isothermal titration microcalorimeter (ITC, CSC 4200, Calorimetry Science Corporation) in triplicate experiments. Silurian sand (SS) and sandy loam (SL) soils were sterilized by placing 1 g of dried soil in an oven at 100°C for 24 hours. Soil (e.g., 500 mg) was placed in the microcalorimeter cell with 97 μL of distilled water. The wet soil was left to stand for five minutes in the microcalorimeter equilibration compartment to allow temperature equilibration before placing the cell in the calorimeter chamber. Once the cell was in

place, a 3-minute time lag was allowed to equilibrate the temperature disturbance from positioning the cell. The sample was then inoculated with 97 μL manure effluent.

Temperature in the ITC was set at 35°C for all experiments (e.g., favorable *E. coli* growth temperature) and data from the cell (e.g., microwatts, μW) were recorded every 4 s and then converted to $\mu\text{cal}/\text{mg}$.

2.3.5. SAR, *E. coli* Quantification, and Nonlinear *E. coli* Sorption

Sodium absorption ratio, SAR, was computed based in the ion concentration from each poured effluent dilution:

$$SAR = \frac{[Na^+]}{\sqrt{[Ca^{2+}] + [Mg^{2+}]}} \quad (2.1)$$

where $[Na^+]$, $[Ca^{2+}]$ and $[Mg^{2+}]$ are the soil solution ion concentration in mmol L^{-1} . Also, electrical conductivity (EC) and soil pH were measured from effluent dilutions after mixing with soils.

Sorbed *E. coli* was computed and expressed per g of dry soil as the difference in *E. coli* population in the initial effluent volume (e.g., 6 mL) and the estimated *E. coli* population in the supernatant after centrifugation:

$$q_{SP} = \frac{V(C_o - C_{LP})}{M_{soil}} \quad (2.2)$$

where q_{SP} is the sorbed *E. coli* concentration (MPN/g soil), V is the effluent volume (mL), C_o and C_{LP} are the initial and supernatant *E. coli* concentrations (MPN/100 mL), and M_{soil} is the mass of soil (g). Data from the triplicate experiments were averaged and then fit to the following nonlinear equation:

$$q_{SP} = A \cdot C_{LP}^B \quad (2.3)$$

where A and B are empirical parameters. This equation is mathematically equivalent to the Freundlich isotherm equation. Note that q_{SP} represented sorption of *E. coli* in the solid phase in MPN g⁻¹ and C_{LP} the concentration of *E. coli* in solution after centrifugation in MPN mL⁻¹. The coefficient of determination R^2 between the observed and predicted data was used to quantify the strength of the fit.

A linear model was derived to estimate the measured A parameter based on soil properties. The natural soils were divided in two groups based on the percent clay content in order to estimate the A parameter: (1) an equation based on percent of total carbon (%TC) for soils with percent clay contents less than 11% due to the fact that increased clay content in this range resulted in increased *E. coli* sorption, and (2) an equation for soils with percent clay contents between 11% and 30% based on %TC and amorphous Al and Fe mineral content extracted with acid ammonium oxalate reagent (McKeague and Day, 1966). Finally, relationships between the A and B parameter were derived.

Estimated mean error (EME) between observed (C_{obs}) and estimated (C_{est}) *E. coli* from nonlinear equations were computed for the natural soils using all dilution ratios:

$$EME = \frac{1}{n} \sqrt{\sum (C_{obs} - C_{est})^2} \quad (2.4)$$

where n is number of observations from triplicate samples, and C_{obs} and C_{est} are the sorbed *E. coli* concentrations from the nonlinear and the predictive equation in MPN g⁻¹, respectively.

2.4. RESULTS AND DISCUSSION

2.4.1. Sessile *E. coli* and Effluent Solute Concentrations

Assuming an *E. coli* size in the range of 0.8 to 3 μm (e.g., vertical dash lines in Figure 2.1), the estimated planktonic *E. coli* in the effluent was less than 10% of the detectable *E. coli* after filtering swine manure using a series of porous metal disks and nylon mesh (e.g., estimated from the regression line; Figure 2.1). Approximately 40% of the total *E. coli* population was able to pass a 10 μm pore space opening. Therefore, removal of sessile *E. coli* from solution by sorption and/or flocculation/precipitation was potentially controlled by processes occurring in the substrate (i.e., organic compounds in which the bacteria are attached or aggregate).

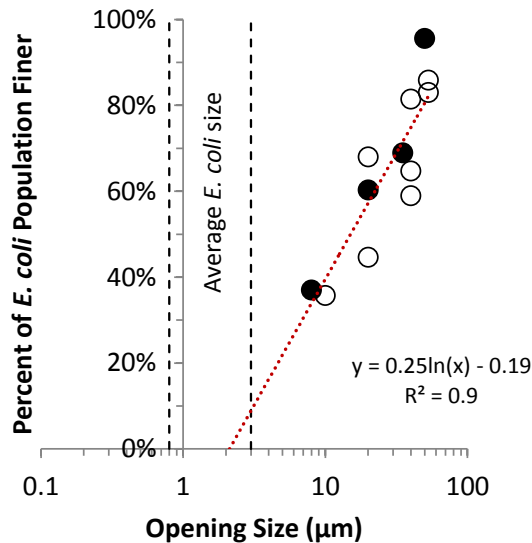


Figure 2.1. Particle size distribution of organic compounds in swine effluents associated with the percentage of *E. coli* population finer than a certain mesh size from micro-sieving experiments. Filled circles represent data from nylon mesh and hollow circles from metal disks.

Note that free cell fecal bacteria (e.g., estimated as a 10%) were the potential bacteria population subject to surface bonding (e.g., reversible or irreversible) while most

of the sessile fecal bacteria were hypothesized to be under irreversible attachment. Reversible bonding may occur quickly as bacteria contact surfaces (e.g., fractions of a second). Irreversible bonding is a secondary stage requiring bacteria to develop exopolysaccharides polymers (e.g., hours to days) as a function of nutritional needs and a stage of biofilm formation (Dunne, 2002). A bacterium to surface bonding differs from sorption of solutes even though both cases have been modeled with DLVO theory. A fecal bacterium has nutritional needs and the capability to modify surfaces, bond soil constituents and change the bulk solution equilibrium through enzymatic action, protein release and by modifying its electrical charge.

The liquid swine manure was rich in organic compounds (e.g., aggregates and colloids) and solutes (see Table 2.3) that upon contact with soils increased the pH and ionic strength of the soils' bulk solution (Figure 2.2a). Note that EC and ionic strength are commonly linearly correlated. Following centrifugation, pH in the bulk solution increased to greater than the initial effluent pH (e.g., 7.5) in most cases. This observation indicated that effluent constituents played an important role in raising the pH in the bulk solution as a function of the soil-effluent mixing ratio and soil pH buffer capacity. However, for the artificial soils, the bulk solution pH did not exceed the initial swine effluent pH, perhaps due to the high pH buffer capacity of peat. Also, note in Figure 2.2a the pH variability in the natural soils for dilution ratios below or equal to 2:4 (e.g., swine effluent to distilled water) compared to dilution ratios above 2:4.

Changes (e.g., increase and decrease) in soil pH following manure application have been reported from laboratory and field experiments as a temporary condition which would be important in immediate sorption of bacteria to soils. Changes in the bulk

solution pH were explained from CO₂ degasification (Husted et al., 1991; Safley et al., 1992) as the swine effluent was initially shaken and increased in temperature during centrifugation:



Essentially, a loss of CO₂ from the system (i.e., degassing) forced the equilibrium in equation (2.5) to shift toward the reactants (left side), which resulted in a consumption of solution protons thereby increasing pH. As an example, recently Lovanh et al. (2010) documented greenhouse gas fluxes (e.g., methane, carbon dioxide, nitrous oxide and ammonia) in fields following manure application. Note that CO₂ and HCO₃⁻ are microbial byproducts in swine effluents. Also, HCO₃⁻ is found in the pig mucosal duodenum secretions (Odes et al, 1995).

Moreover, ion exchange of Mg²⁺ associated with carbonates on clay minerals (Figure 2.2f) and Na⁺, K⁺ and Ca²⁺ in organic compounds from the effluent solution (Figure 2.2c, 2.2d and 2.2e) may have contributed to the increase in pH. Other variables may play a role in pH changes, such as oxidation of volatile fatty acid and ammonia concentrations, which have been reported to buffer swine effluent pH (e.g., 6.3 to 7.5) under anaerobic conditions but favor increases in pH as ammonia volatilization occurred (Georgacaki et al., 1982; Paul and Beauchamp, 1989).

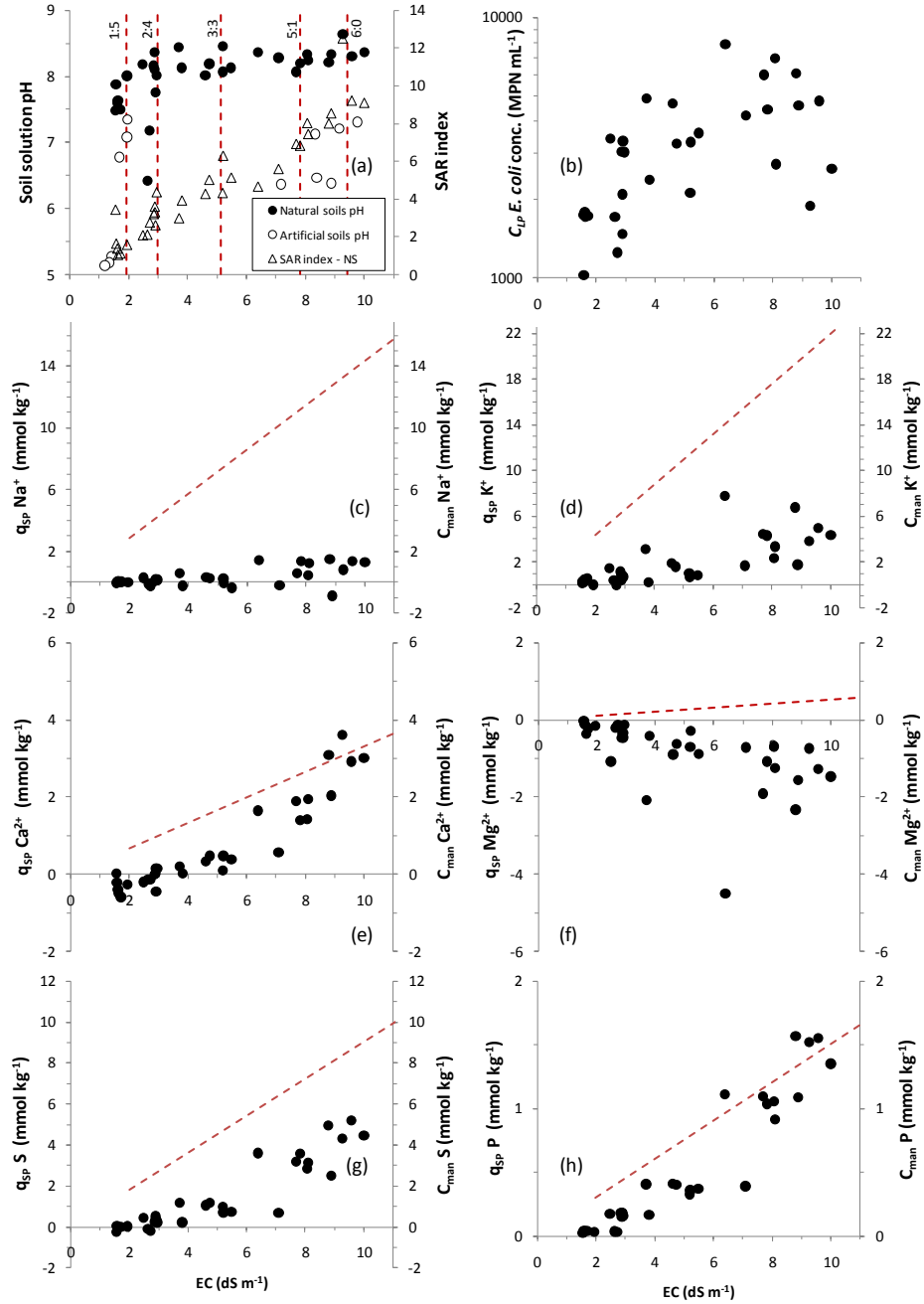


Figure 2.2. Major ions sorbed (q_{SP}) by the natural soils and in the swine effluent (C_{man} ; dash line on Figures 2.2c to 2.2h), pH, sodium absorption ratio (SAR), electrical conductivity (EC) and equilibrated *E. coli* concentrations. Dash lines in Figure 2.2a are the average EC per dilution ratio (i.e., mL of liquid swine manure to mL of distilled water). Dash lines in Figure 2.2c to 2.2h are the solute concentration in the swine effluent before mixing and circles are the sorbed solute concentrations after mixing.

2.4.2. Influence of Clay, Total Carbon, and Dispersion on *E. coli* Sorption

As expected, for the artificial and natural soils, higher clay content increased *E. coli* sorption (Figure 2.3). The magnitude of the additional sorption decreased as the percent clay content increased to 10%. Increases in total carbon contents in artificial soils increased sorption of *E. coli* (Figure 2.3a). In some soils (e.g., C5P8, CA, EA, PA and SA soils in Figure 2.3), a sharp decrease in sorption was observed at the maximum effluent concentration (Figure 2.3a, 2.3e and 2.3f). Note that EC was an indicator of effluent application rates (Figure 2.2a). Soil dispersion (Gupta et al., 1984) and the presence of sessile *E. coli* were hypothesized to explain these results. Note that for the natural soils this phenomenon occurred for those soils with high clay contents. Also, in Figure 2.2a and 2.2e note the change in sorption after the reduction in total carbon treatment in the loamy sand and sandy loam soils. These observations indicate the importance of soil mineralogy and total carbon (e.g. soil organic matter) on sorption of fecal bacteria from manure effluents that are potentially changing the bulk solution pH.

The sodium adsorption ratio (SAR) in the natural soils (Figures 2.2c and 2.2d) indicated that exchangeable Na^+ and K^+ (e.g., dispersing ions) might be contributing to soil dispersion. In addition, increased pH and desorption of Mg^{2+} from soils (e.g., flocculating ion as shown in Figure 2.2f) further favored dispersion as the effluent concentration increased. Note that pH increased to an average of 8.2 as soils were treated with swine effluents (Figure 2.2a; initial pH in swine effluent was 7.5). Dispersion of the clay minerals occurred as the dilution ratio decreased and was visibly present in all soils to some degree. Soil dispersion decreased sorption of *E. coli* due to the fact that clay and organic compounds possessing *E. coli* remained in suspension after centrifugation.

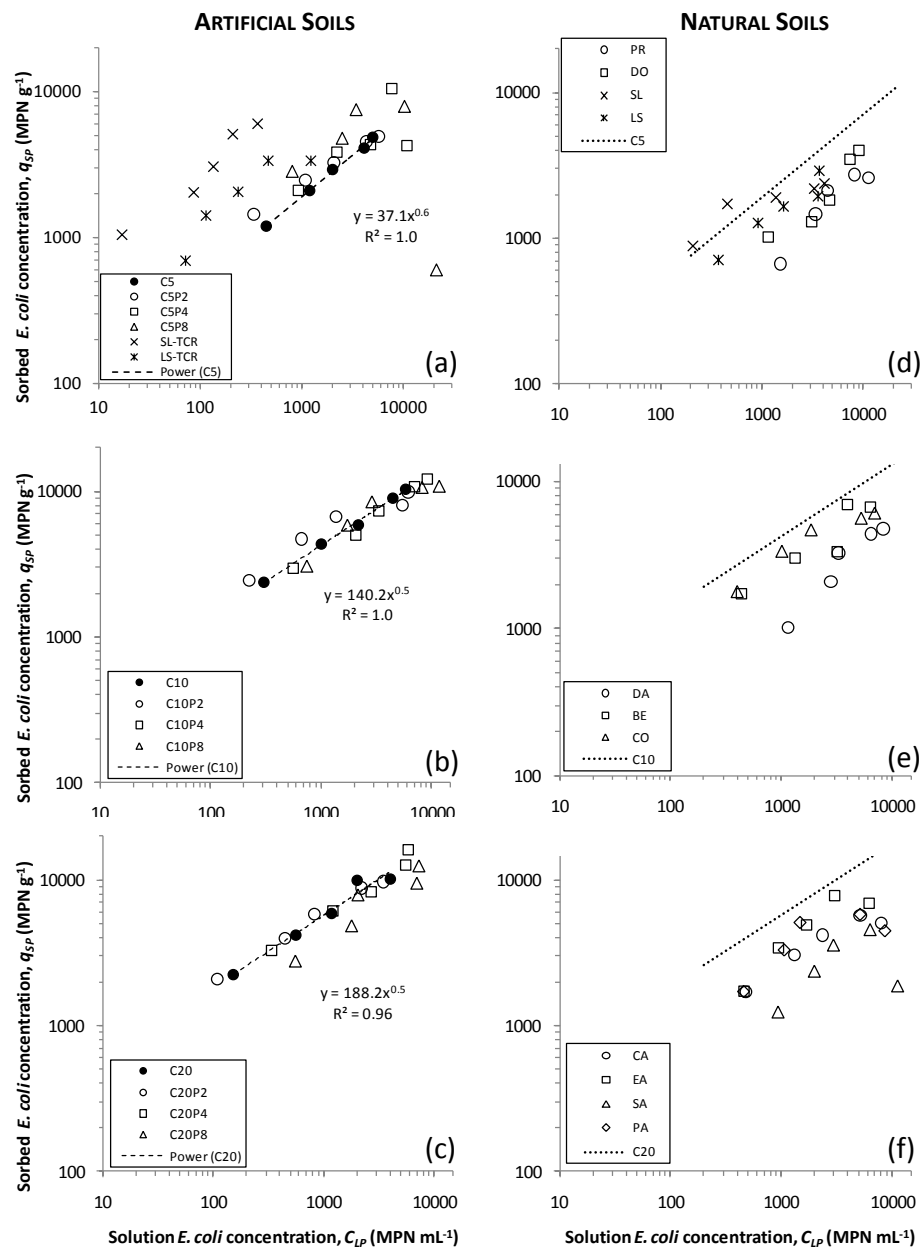


Figure 2.3. Sorption of *E. coli* from swine effluents for the artificial soils with clay contents of (a) 5%, (b) 10%, and (c) 20%. Sorbed *E. coli* concentrations for the natural soils with clay contents in the range of (d) 0% to 10%, (e) 10% to 20%, and (f) 20% to 30%. See Tables 2.1 and 2.2 for identification and soil property information. Dashed lines and regression equations correspond to the artificial soils with 5%, 10% and 20% kaolinite clay content and no total carbon added. Note that all data points are the average of triplicate experiments.

Bacteria growth investigated with calorimetric experiments indicated a time lag of 5 to 10 hr following soil inoculation before bacteria activity was detectable. Note that sorption experiments were completed in less than 20 minutes. It was also hypothesized that dispersion of the effluent organic compounds increased detection of *E. coli* in solution as particles carrying attached *E. coli* were physically split apart. However, further investigation is needed on this hypothesis.

2.4.3. Predictive Equations for Sorption of *E. coli*

In both artificial and natural soils, nonlinear equations described sorption of *E. coli* at different percent clay and total carbon contents. However, the nonlinear equation could not model the sharp decrease in sorption observed in some soils (e.g., CA, EA and SA soils; Figure 2.3). Note that these equations and their parameters are unique in that they characterize different soil and manure application suspensions. For soils with percent clay contents less than or equal to 11%, the *A* parameter was proportional to the %TC:

$$A = 39.0(\%TC)^{2.4} \quad (2.6)$$

For soils with percent clay contents larger than 11% but lower than 30%, the *A* parameter depended on amorphous Al and Fe mineral concentration (mmol kg^{-1}), percent clay content (%clay), and %TC:

$$A = 8.9Al_{\text{mmol kg}^{-1}} + 5.8Fe_{\text{mmol kg}^{-1}} + 0.8(\%clay) - 153.5(\%TC) \quad (2.7)$$

The *B* parameter was related to *A* (Figure 2.4):

$$B = -0.1\ln(A) + 0.9 \quad (2.8)$$

Note that artificial soils were not included in the regression as artificial soil compositions were limited to assess the effect of total carbon and soil minerals on sorption of *E. coli*.

The dependence of the predictive equations for *A* on the percent clay content was expected. Soil colloids smaller than 2 µm are responsible for most of the soil charge in which organic substances and amorphous Al and Fe coating clay mineral surfaces modify the electrochemical properties of the clay surfaces' (Zhuang and Yu, 2002). On the other hand, the *B* parameter inversely represents the potential reduction in sorption of *E. coli*.

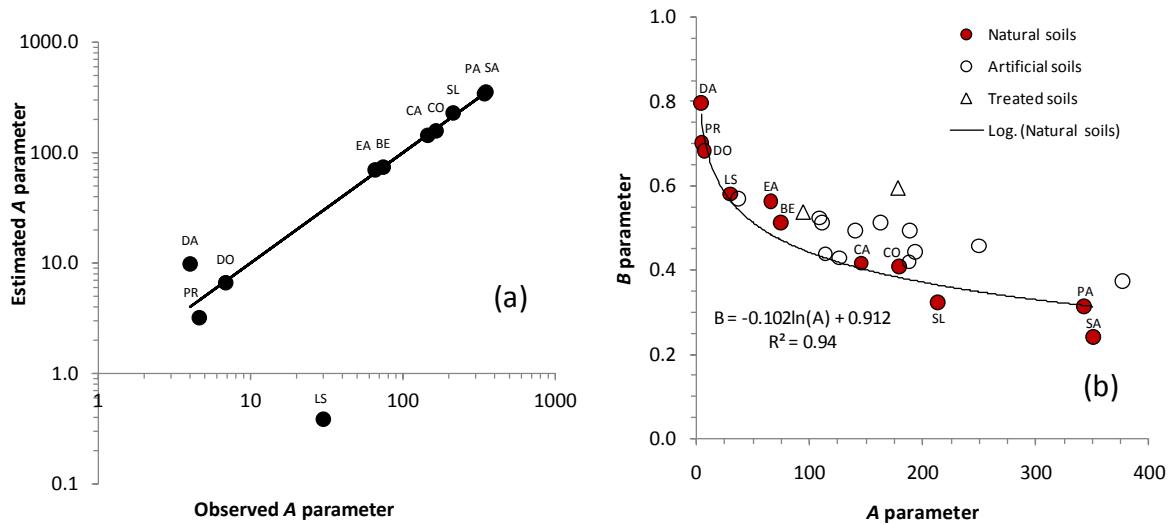


Figure 2.4. Estimated nonlinear parameters (*A* and *B*) from the predictive equations developed in this research: (a) predicted versus observed nonlinear *A* parameter for the natural soils; (b) relationship between the nonlinear equation parameters (*A* versus *B*) for the natural soils. Soils after reduction in total carbon and artificial soils are in the figure for comparison. See Tables 2.1 and 2.2 for identification and soil property information.

For the natural soils, the coefficient of determination for the estimated *A* and *B* parameter were $R^2=0.97$ and 0.94, respectively (Figure 2.4). The mean error between the estimated and the observed sorbed *E. coli* using equations (6), (7) and (8) was 1,326

MPN g⁻¹. The mean error when fitting the experimental data with individual nonlinear equations for each experimental condition was 740 MPN g⁻¹. The mean error of the estimated *A* values was found to be 6.48 and the *B* parameter was 0.09. Residuals from the estimated sorption of *E. coli* were normally distributed and proportional to the increase in the *E. coli* concentration in solution. This increase in error deviation was at least partially the result of the most probable number method used to quantify *E. coli* concentrations (Gronewold and Wolpert, 2008).

A comparison between sorption of *E. coli* using a previously reported equation by Ling et al. (2002) and experimental data indicated that predictions based on the percent clay content alone overestimated sorption of *E. coli* from swine effluent applications (Figure 2.5). The overestimation was commonly at least one order of magnitude for soils with 0% to 11% clay content and more than one order of magnitude for soils with clay content greater than 11%. Note that Ling et al. (2002) carried out the experiments using planktonic fecal bacteria suspended in inert solutions. Therefore, the proposed predictive equations in this research will be valuable in estimating *E. coli* sorption from manure application in agricultural lands.

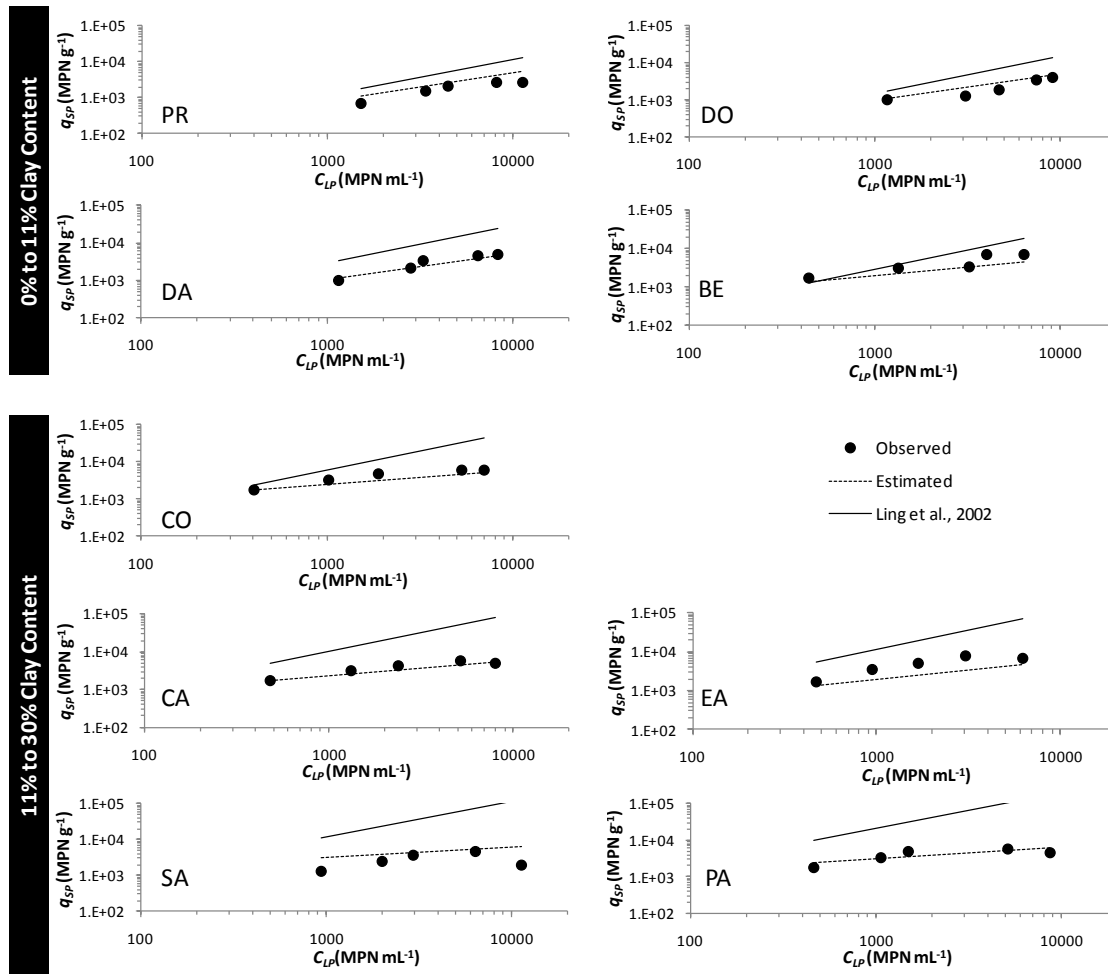


Figure 2.5. Comparison of *E. coli* sorbed (q_{sp}) versus solution (C_{LP}) concentrations observed during the experiments and estimated by the proposed predictive equations (i.e., “Estimated”). *E. coli* sorption predicted by the Ling et al. (2002) relationship based on only percent clay content is also shown. See Table 2.1 for identification and soil property information.

2.5. SUMMARY AND CONCLUSIONS

Swine effluents are rich in solutes and organic colloids and upon contact with soils result in differential sorption mechanisms for *E. coli*. The dominant sessile *E. coli* population in the effluent resulted in different sorption mechanisms, as sorption of sessile *E. coli* was primarily controlled by sorption of the bacteria substrate rather than the bacterium itself. Also, buildup in alkalinity of the bulk solution and ion exchange of

solutes such Na^+ , K^+ , Ca^{2+} and Mg^{2+} may decrease sorption of *E. coli* in presence of organic matter as a result of soil dispersion. Degassing of CO_2 from the swine effluent when aerated via shaking or with increased temperature and ion exchange explained the increase in pH observed in the sorption experiments. Even though complex sorption mechanisms occurred when multiple constituent liquid swine manure was applied to soils, sorption of *E. coli* was adequately represented by a non-linear equation, valid except in cases of soil dispersion. Note that these equations and their parameters are unique in that they characterize different soil and manure application suspensions, rather than typical isotherms characterizing sorption for a constant bulk solution condition.

CHAPTER 3

Surface Runoff Transport of *Escherichia coli* after Poultry Litter Application on Pastureland²

3.1. ABSTRACT

Escherichia coli transported in surface runoff from dissolution of applied poultry litter is a major variable in assessing fecal contamination of streams. However, the relative magnitude of the *E. coli* concentration from a specific poultry litter application and relative to the time lag between litter application and rainfall are not completely understood. This research investigated *E. coli* transport in runoff on fourteen 2 m × 2 m pastureland plots. Poultry litter was manually applied (4,942 kg ha⁻¹) in twelve plots followed by artificial rainfall with intensities equivalent to 2-year and 5-year storm events. Rainfall was applied in duplicate plots immediately after poultry litter application and 24 and 120 h after litter application. Experiments were also conducted on two control plots without poultry litter application. Surface runoff was collected using a flume installed in a trench. *E. coli* was quantified from sampled runoff and used as an indicator of fecal contamination by the most probable number (MPN) technique. No significant differences were observed in average event mean concentrations (EMCs) relative to storm intensity. Statistically significant differences were observed in average EMCs

² Published in *Transaction of ASABE*, 2010

Guzman, J.A., G.A. Fox, and J.B. Payne. 2010. Surface runoff transport of *Escherichia coli* after poultry litter application on pastureland. *Transactions of the ASABE* 53(3): 779-786.

relative to time lag between litter application and rainfall. A nonlinear relationship was observed between average *E. coli* EMC and time lag, with the EMC decreasing between 0 h (1.6×10^5 MPN/100 mL) and 24 h (1.3×10^4 MPN/100 mL) and then increasing at 120 h (4.3×10^4 MPN/100 mL). *E. coli* were always detected in the control plots (average EMC of 6.8×10^3 MPN/100 mL), indicating the presence and transport of fecal bacteria from sources independent of the immediate poultry litter application. Even though poultry litter application may increase *E. coli* concentrations in runoff, other sources of fecal contamination serve as a significant component of the total *E. coli* EMC, especially as the time lag between litter application and rainfall events increases.

3.2. INTRODUCTION

The U.S. poultry industry has provided a plentiful and affordable source of protein for consumers while generating economic revenue. However, modern livestock industries, including poultry production, are frequently unprofitable unless a significant economy of scale can be achieved (Bossman, 2005). To achieve this economical scale, large numbers of birds are generally reared in confinement, resulting in a large amount of animal waste, in the form of poultry litter, produced in a limited geographic area. Poultry litter consists of manure, bedding material, and other components such as feathers and soil (Kelley et al., 1994). Wood shavings, sawdust, and soybean, peanut, or rice hulls are all common manure carriers added to the poultry house floor and utilized for raising four to eight flocks on a single placement prior to complete cleanout. After removal from the poultry house, litter is generally land-applied as a fertilizer source to pastures and cropland. Litter is recognized as an excellent source of the plant nutrients N, P, and K, but it can also contain pathogenic microorganisms such as *Salmonella*, *Campylobacter*,

and fecal indicator bacteria such as enterococci and *Escherichia coli* (de Rezende et al., 2001; Santos et al., 2005; Jenkins et al., 2006).

Surface and subsurface waters can result in fecal bacteria contamination as a function of runoff transport, litter properties, and rainfall events following litter application. *E. coli* can survive for extended periods of time in feces, soil, and water (Stoddard et al., 1998; Sørensen et al., 1999; Wang, 2003) and often serve as indicator organisms of fecal contamination (U.S. EPA, 1986, 2004; Foppen and Schijven, 2006). However, the interaction between land-applied poultry litter and *E. coli* concentration transported by surface runoff is still not well understood. Jenkins et al. (2006) reported that litter can impact *E. coli* concentrations in runoff from cropland when runoff occurs three weeks following litter application; in addition, they concluded that litter application did not appear to impact background concentrations when runoff events occurred seven months after application. In a second study involving poultry litter and commercial fertilizer applications to conventional-till and no-till corn plots subjected to simulated rainfall, Jenkins et al. (2008) concluded that no significant differences were determined between tillage treatments in runoff concentrations of *E. coli*. Litter application appeared to have little potential of pathogen contamination of surface waters. Recently, Sistani et al. (2009) compared the effect of litter application (e.g., surface-broadcast and subsurface banding) on surface runoff transporting *E. coli* following a rainfall event applied on the same plot during three consecutive weeks. The authors concluded that surface-broadcast litter treatment had a significantly greater *E. coli* contribution during all events as compared to subsurface litter application.

Litter application might contribute fecal bacteria to soils in sessile form (e.g., micro-colonies and biofilms) rather than planktonic form. During rainfall events, sessile *E. coli* can be transported in runoff and contribute to surface and subsurface concentration (Reddy et al., 1981; Shipitalo and Gibbs, 2000; Pachepsky et al., 2006). In soil habitats, *E. coli* populations typically exhibit a negative growth rate, balanced by the arrival of new organisms from manure sources, and thus maintain a relative steady "background" population (Savageau, 1983). This background *E. coli* population might be further subjected to surface runoff transport when located in the top centimeters of the soil profile as surface erosion occurs. Muirhead et al. (2006) performed laboratory-scale experiments to compare surface runoff transport of *E. coli* attached to silt loam soil particles versus planktonic cells in surface runoff. They observed reductions in *E. coli* when attached to soil particles, but this reduction did not impact the overall transport. On the other hand, planktonic cells rapidly attached to small particles that remained in suspension while being transported in surface runoff. In addition, they found no significant *E. coli* transport differences between slope (e.g., 5% and 15%) and flow rates (e.g., 0.6 and 2 mL s⁻¹).

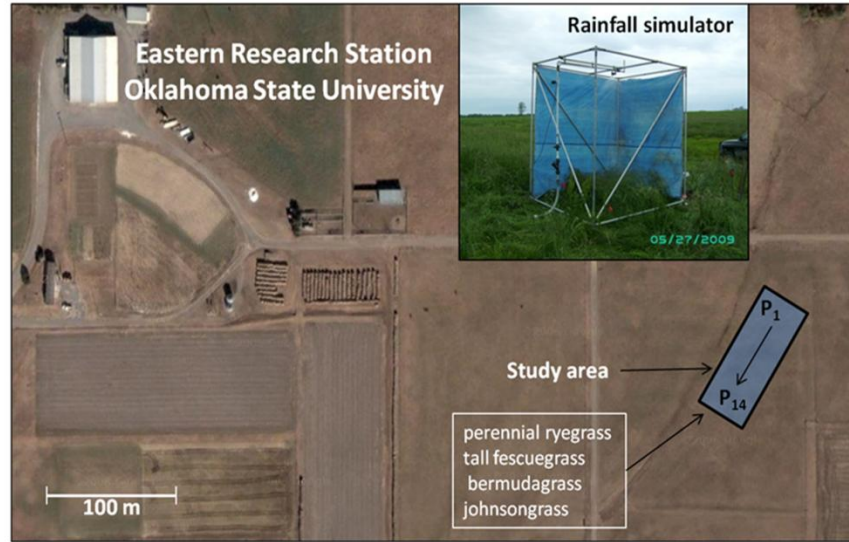
In eastern Oklahoma, much of the poultry litter produced is land-applied to pastures for forage production. Questions exist regarding the effects of time lag and rainfall intensity on the potential for *E. coli* event mean concentration (EMC) and other biological contaminants from pasture-applied poultry litter to reach receiving water bodies during surface runoff events. The objective of this study was to investigate *E. coli* concentrations transported by surface runoff after poultry litter application on a series of

pasture plots selected with similar soil, slope, and vegetation characteristics and subjected to 2-year and 5-year storm event intensities using a rainfall simulator.

3.3. MATERIAL AND METHODS

Field experiments consisting of fourteen 2 m × 2 m pastureland plots were used to evaluate *E. coli* surface runoff transport. The plots were located at the Oklahoma State University Eastern Research Station in Haskell, Oklahoma (Figure 3.1). Two of these fourteen plots were used as control plots without poultry litter application. Plots were set up by berming the soil along the perimeter of the plot and digging a trench at the drainage (i.e., downslope) end. Special attention was given during plot preparation to avoid external contamination resulting from stepping on the plot, exogenous soil particles, or altering the existing vegetation. In addition, plots were separated by a distance of at least 5 m to avoid cross-contamination. One-year-old broiler litter (moisture content = 25% and pH = 8) collected the same day from a commercial poultry house, typically cleaned out once per year, was manually surface applied at an application rate of 4,942 kg ha⁻¹ on twelve plots. Litter was collected directly from a poultry house floor following a zig-zag pattern while avoiding large clumps of litter (e.g., caked litter) and mixed before field application. Additionally, litter was applied to an area 20 cm in diameter and 1 cm in depth outside the plots to quantify *E. coli* populations in litter exposed to the same environmental conditions over time.

(a)



(b)

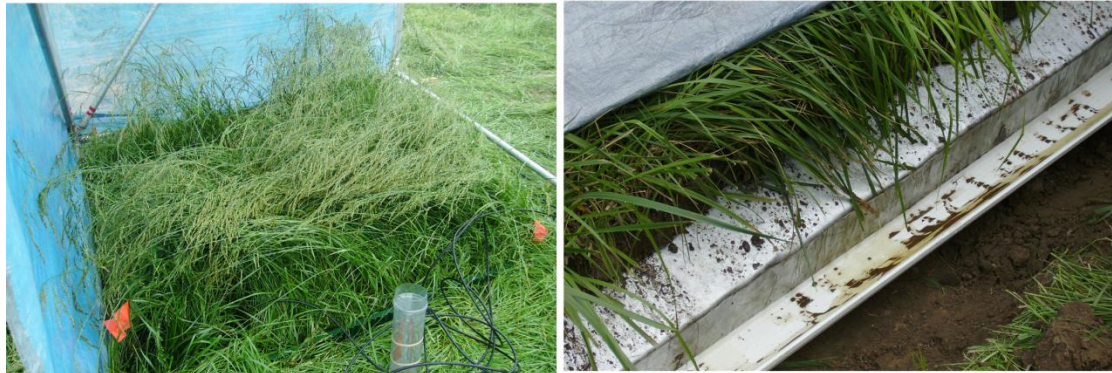


Figure 3.1. (a) Aerial image of the Oklahoma State University Eastern Research Station in Haskell, Oklahoma, including the study area location of the plots and the rainfall simulator used for the 2-year and 5-year rainfall intensities, and (b) illustration of vegetation, rain gauge, and borders of one of the plots and the outflow flume and flow collection device at the downslope end of the plot.

In each plot, an artificial rainfall event was simulated using a standard rainfall simulator (Miller, 1987) with the intensity equivalent to a 2-year or 5-year return period event and for 30 or 45 min duration (Tortorelli et al., 1999). Rainfall was applied 0 h, 24 h, or 120 h after litter application (Table 3.1) to evaluate the effect of time lag on *E. coli*

transport. During the 5 d span of the experiments, there was no natural rainfall. One control plot was tested at the beginning of the experiment (e.g., 0 h time lag in plot 1), while the second control plot was tested at the end (e.g., 120 h time lag in plot 14).

Table 3.1. Characteristics of the rainfall events, plot slope, and surface runoff for the experiments.

Note that all surface runoff times are non-dimensionalized by the duration of the rainfall event, t_d .

Plot	Time Lag (h)	Plot Slope (%)	Storm Event				Surface Runoff			EMC (MPN/100 mL)
			T (year)	Intensity, i (mm h ⁻¹)	Duration, t_d (min)	Volume (mm)	t/t_d	Mean (mm h ⁻¹)	Peak (mm h ⁻¹)	
1 ^[a]	0	3.6	2	58.4	45	43.8	0.46	35.7	58.7	7.7×10^3
2	0	5.1	2	58.4	45	43.8	0.46	29.3	51.9	2.2×10^5
3	0	4.4	2	58.4	45	43.8	0.55	31.0	66.5	1.9×10^5
4	0	3.2	5	76.2	30	38.1	0.63	19.9	44.9	5.0×10^4
5	0	4.8	5	76.2	30	38.1	0.52	41.9	93.4	1.7×10^5
6	24	4.9	2	58.4	45	43.8	0.45	36.3	66.4	2.6×10^4
7	24	5.2	2	58.4	45	43.8	0.42	36.8	56.3	7.6×10^3
8	24	7.4	5	76.2	30	38.1	0.43	55.0	85.9	1.1×10^4
9	24	5.4	5	76.2	30	38.1	0.39	53.7	86.1	7.1×10^3
10	120	3.0	5	76.2	30	38.1	0.36	40.4	56.9	1.9×10^4
11	120	2.1	2	58.4	45	43.8	0.85	34.4	45.4	6.2×10^4
12	120	3.8	2	58.4	45	43.8	NA ^[b]	NA ^[b]	NA ^[b]	5.0×10^4
13	120	3.3	2	58.4	45	43.8	0.30	44.6	64.8	4.0×10^4
14 ^[a]	120	3.9	2	58.4	45	43.8	0.50	35.7	58.7	5.8×10^3

^[a] Control plots.

^[b] Runoff data eliminated due to measurement error (flow underneath the outflow flume).

3.3.1. Experimental Area

The experimental area consisted of pastureland with a mixture of perennial ryegrass (*Lolium multiflorum* Lam.), tall fescue grass (*Festuca arundinacea*), bermuda grass (*Cynodon dactylon*), and some Johnsongrass (*Sorghum halepense* (L.) Pers.) grown for hay production (Figure 3.1.). Cattle had not been allowed access to the pasture for over one year, and poultry litter had previously been applied one year prior to the study on 16 May 2008 at an approximate application rate of 8,649 kg ha⁻¹. The topographical slopes in the experiment area varied from 0% to 8% with some isolated small depressions. Plots drained to an intermittent natural drainage channel (Figure 3.1) with

soils mainly from clayey residuum weathered from shale and silty alluvium parent material. Soils series were primarily Dennis-Verdigris complex (Dennis: 35%, Verdigris: 25%, minor components: 40%) and Parsons silt loam (Mollic Albaqualfs). A weather station located on site measured rainfall, air temperature, relative humidity, wind speed, and solar radiation (Figure 3.2).

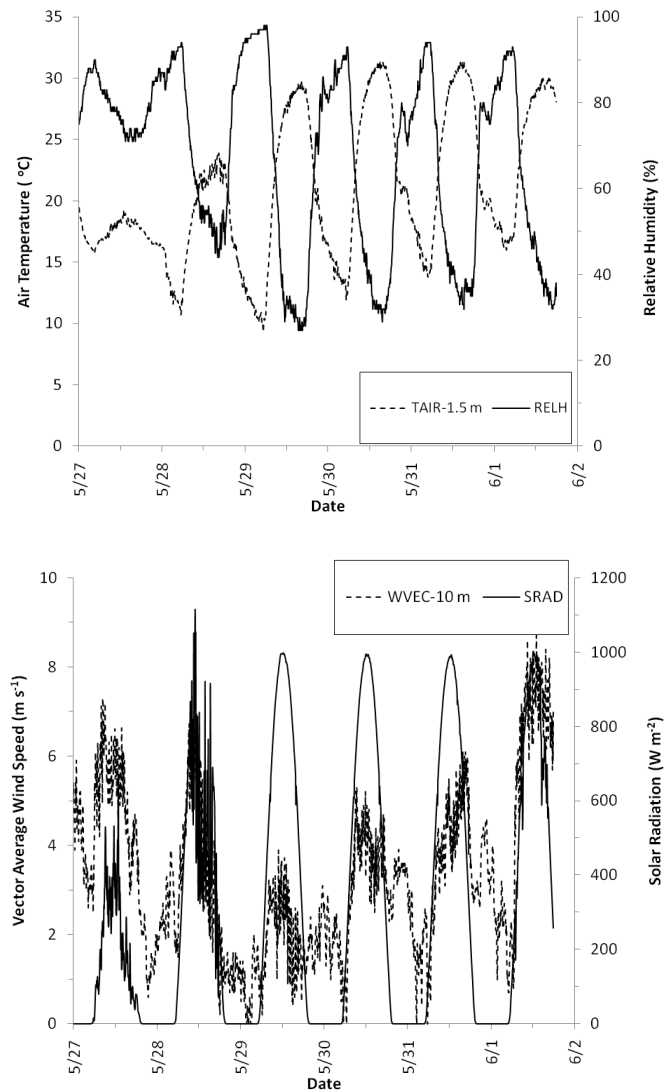


Figure 3.2. Meteorological conditions during the experimental 5 d period: (a) air temperature at 1.5 m (TAIR-1.5 m) and relative humidity (RELH), and (b) wind speed at 10 m (WVEC-10 m) and solar radiation (SRAD).

3.3.2. Rainfall Simulator

A solenoid-operated rainfall simulator (Miller, 1987) was used to simulate 2-year and 5-year storm event intensities for a 30 or 45 min duration (Figure 3.1). The rainfall intensity provided by the simulator was calibrated and controlled by an on-off cycle (2.0 s on and 1.8 s off for the 2-year event, and 2.0 s on and 0.4 s off for the 5-year event) of the solenoid valve (MKC-2, Sporlan Division, Washington, Mo.). A single nozzle (TeeJet 1/2 HH-SS50WSQ, Spraying Systems Co, Chicago, Ill.) placed in the center of the simulator frame (3.0 m high, 2.8 m long, and 2.3 m wide) was used to spray the water. A water tank that was previously disinfected and connected to a centrifugal gasoline-operated pump (Honda, WB30X) was used to provide the pressure head required by the rainfall simulator. The setup included a valve to regulate the pressure head. During simulator calibration prior to the field experiments, rainfall intensity was measured in three rainfall collectors randomly located in an equivalent plot of 2 m \times 2 m. As part of the rainfall simulator setup, a manometer located in the water distribution pipe was used to monitor the pressure head provided by the pump. A calibration curve was derived to estimate the on-off cycle at 103 kPa for the rainfall intensities.

3.3.3. Plot Instrumentation

The hydrological response in all plots was measured by collecting the overland flow using a flume at the downslope end of each plot. The flume was installed 15 cm below the surface by mechanical insertion into the manually dug trench (Figure 3.1). Runoff was measured by mass using a bucket attached to a weighing scale (GX-12K, A&D, San Jose, Cal.) recording data every 5 s. Three Hydra Pro II sensors (Stevens, Portland, Ore.) connected to a XR-10 datalogger (Campbell Scientific, Logan, Utah)

were setup during the experiments (one outside and two inside each plot) to measure salinity, soil temperature, and volumetric moisture content every 5 s. Rainfall amounts were collected using a rain gauge installed inside the plastic berm in order to verify the applied rainfall intensity and confirm that the applied water was not a source of *E. coli*. Equipment, sensors and the flume were cleaned and disinfected after each experiment.

3.3.4. *Escherichia coli* Concentration

Water samples were collected approximately every 2 min at the end of the flume during the experiments. Samples were stored on ice until *E. coli* enumeration, not more than 6 h after sampling. *E. coli* was quantified by the most probable number (MPN) technique using the Colilert reagent and semi-automated Quanti-Tray method (IDEXX, Westbrook, Maine), which provides counts from 0.0 to 2,419.6 per 100 mL (Garbrecht et al., 2009; Guzman et al., 2009). Yellow wells with fluorescence in the IDEXX panels were considered positive for *E. coli*. Triplicate litter samples taken before application and collected outside the plots at 0 h, 24 h, and 120 h were stored on ice and enumerated for *E. coli* by placing 10 g of litter in 100 mL of distilled water, shaking periodically for 20 min, and sampling the supernatant.

3.3.5. *Data Processing*

Raw data from the weighing scale were adjusted to eliminate the effects of water sampling and water disposal when the bucket hanging from the weighing scale reached capacity and had to be emptied. Hydrographs were obtained after processing and smoothing the adjusted data in each plot using a Fourier series with a number of harmonics defined by a periodogram analysis (Salas et al., 1997). The same technique was used to estimate the average hydrological response for the 2-year and 5-year storm

events. Runoff data from plot number 12 were eliminated due to measurement problems with respect to water flowing underneath the outflow flume.

E. coli event mean concentrations (EMC) were estimated for the 2-year or 5-year storm events and lag times using the following equation:

$$EMC = \frac{\sum_{i=1}^N Q_i C_i}{\sum_{i=1}^N Q_i} \quad (3.1)$$

where Q_i is the runoff discharge for the 2-year or 5-year averaged hydrological response at time i , C_i is the effluent *E. coli* concentration at time i for a specific time lag, and N is the combined number of measurements for the corresponding time lag and storm event (Garbrecht et al., 2009). Estimated EMC values were tested for normality by fitting the data to a normal distribution with 95% confidence intervals. An ANOVA unstaked test with 95% confidence limits was used to test for significant differences in the average EMCs for the various treatments.

3.4. RESULTS AND DISCUSSION

3.4.1. Hydrological Response

In all plots, runoff initiated shortly after the beginning of the simulated rainfall, peaked at the end of the storm duration, and then rapidly receded for 10 to 15 min for both the 2-year and 5-year storm events (Figure 3.3). Peak runoff was directly proportional to the storm intensity, while the time to peak runoff was inversely proportional to the storm intensity. The average peak runoff was 58.7 and 73.4 mm h⁻¹ for the 2-year and 5-year storm events, respectively (Table 3.1). The variance in peak runoff observed for the individual plots was most likely due to variability in infiltration between

the plots, microrelief, water pressure fluctuations in the rainfall simulator, wind effects, and some interflow bypassing the flume collector at the end of the plot. Moisture content sensors indicated saturation conditions at the end of the rainfall events. The average plot slope ranged between 2.1% and 7.4%; no significant difference was observed relative to slope in the plots used for the 2-year and 5-year storm intensities.

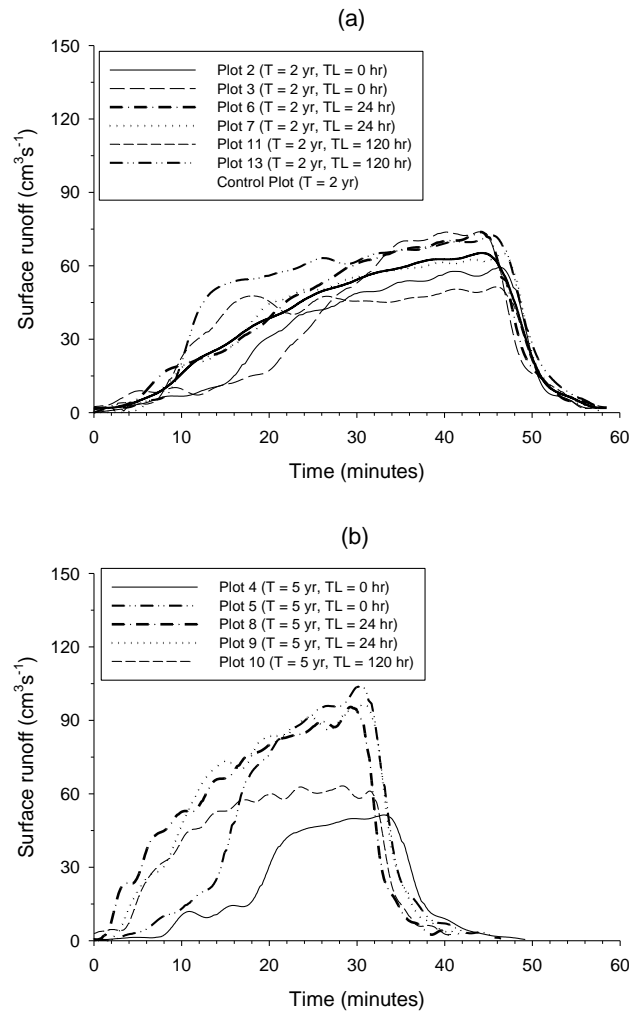


Figure 3.3. Smoothed hydrograph response from each plot for (a) $T = 2$ -year and (b) $T = 5$ -year rainfall intensity relative to the time lag (TL) between litter application and rainfall. Only 2-year storm intensities were simulated in the control plots.

3.4.2. *Escherichia coli* Event Mean Concentrations

Average *E. coli* loads applied to the plots were approximately 8.2×10^{10} MPN ha⁻¹ or 3.3×10^7 MPN. Computed *E. coli* EMCs were the combination of *E. coli* concentrations from other sources and the immediate litter application. Averaged *E. coli* EMC in table 3.2 decreased as a function of the time lag (e.g., 24 h and 120 h) when compared to the EMC for rainfall events immediately following litter application (e.g., 0 h time lag). This EMC reduction was in the range of one order of magnitude independent of the storm event intensity. In addition, EMC for each time lag followed a similar pattern for both storm event intensities (Figure 3.4).

Table 3.2. *E. coli* event mean concentration (EMC, MPN/100 mL) and ANOVA test results (95% confidence limits, CL) for significant differences in the EMC averages as a function of the time lag. P-values lower than 0.050 indicated a significant difference in the average EMCs.

	Control	0 h	24 h	120 h
Average EMC	6.8×10^3	1.6×10^5	1.3×10^4	4.3×10^4
Maximum EMC	7.7×10^3	2.2×10^5	2.6×10^4	6.2×10^4
Minimum EMC	5.8×10^3	5.0×10^4	7.1×10^3	1.9×10^4
P-Values from ANOVA Test on Average EMCs (95% CL)				
0 h	0.053	--	0.008	0.024
24 h	0.412	0.008	--	0.026
120 h	0.058	0.024	0.026	--

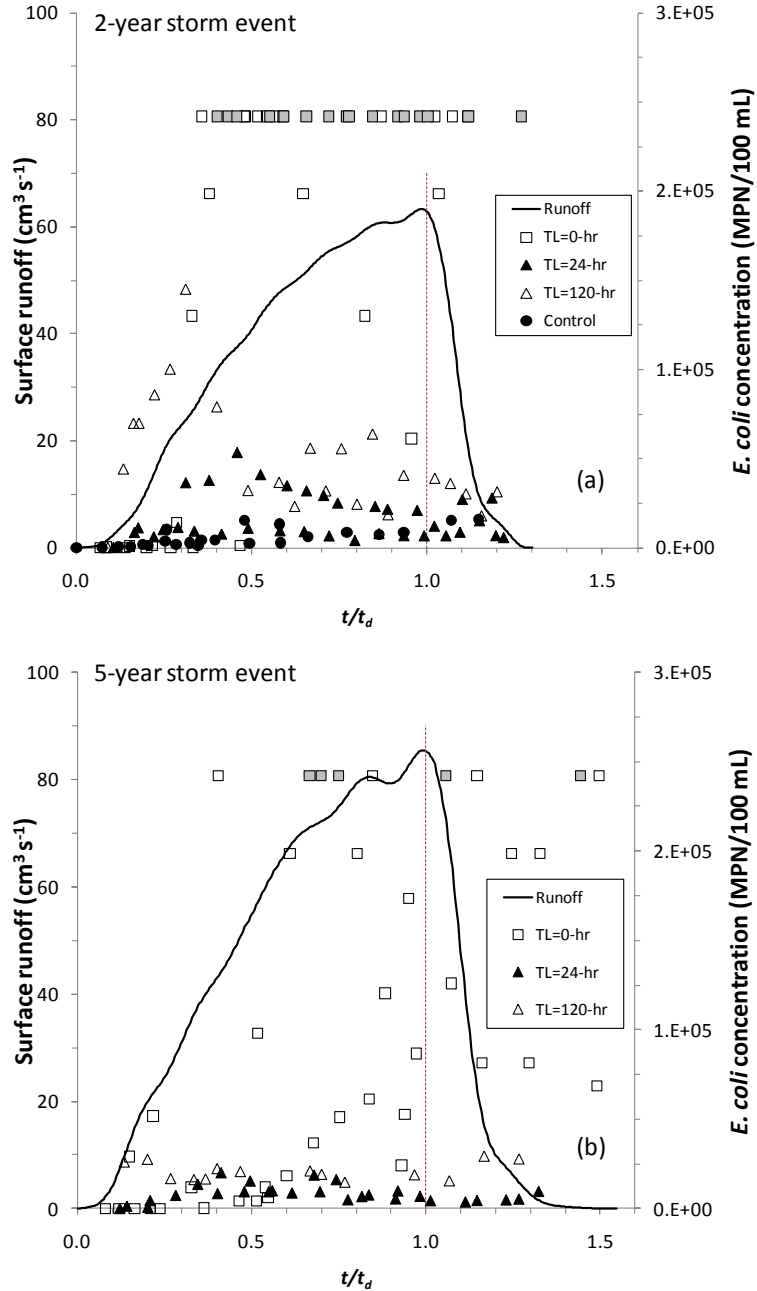


Figure 3.4. *E. coli* concentration for the 2-year and 5-year storm intensity and time lags: (a) *E. coli* concentration and average runoff from the 2-year storm intensity, and (b) *E. coli* concentration and average runoff from the 5-year storm intensity. Only 2-year storm intensities were simulated in the control plots. Filled square symbols correspond to the minimum concentration (e.g., water samples in which *E. coli* concentrations were over the range of quantification). TL = time lag (h) and t_d is the rainfall event duration time.

No significant differences were observed in average EMCs across the storm intensities (2-year and 5-year storm intensity). Therefore, data were grouped as a function of the time lag. Statistical analyses between the 0 h versus 24 h, 24 h versus 120 h, and 0 h versus 120 h time lag experiments indicated that average EMCs were significantly different. On the other hand, the average EMCs from the control and treated plots were not significantly different (Table 3.2) at 95% confidence limits. This was perhaps the result of the limited number of control experiments. However, note in table 3.2 that the average EMCs between the control plots and the 0 h versus 120 h time lag EMC can be considered significantly different at 90% confidence limits.

3.4.3. Escherichia coli Surface Runoff Concentrations

In both control plots (e.g., 0 h and 120 h time lag), *E. coli* was always detected. Concentrations were observed to vary as a function of the surface runoff volume. This observed *E. coli* concentration indicated the presence of fecal contamination from sources other than the immediate poultry litter application. The background *E. coli* initially present in the control plots were capable of sustaining *E. coli* release proportional to the surface runoff development during the duration of the rainfall event. The average *E. coli* concentration always increased with time during the rainfall events (Figure 3.4).

The source of background *E. coli* may be due to rodents, birds, and other small mammals in the area. In addition, a previous poultry litter application had occurred on the plots one year earlier. Jenkins et al. (2006) found during a series of experiments in four small watersheds located in Watkinsville, Georgia, that *E. coli* persisted in soil months after poultry litter application. They reported an initially undetectable *E. coli* concentration in soil samples and a "marginally detectable" *E. coli* concentration on the

order of 102.7 to 104.2 MPN per kg⁻¹ of soil nine to eleven months after the first litter application. However, *E. coli* runoff concentrations were on the whole minimal and were not greater than background concentrations following a runoff event seven months after litter application.

As shown in figure 3.4, background *E. coli* concentrations should not be considered negligible and significantly contributed to the total *E. coli* biomass transport. In all field conditions, surface runoff has the capability to erode, re-suspend, and transport soil particles and colloids in which *E. coli* might attach or adhere. Further investigation on the effect of long-term litter application facilitating fecal bacteria background populations in soils is needed. Some studies have demonstrated that soils treated with animal manure can result in higher soil organic carbon content (Gerzabek et al., 1997; Peacock et al., 2001), an increase in the soil microbial biomass located in the top soil (e.g., 0 to 5 cm soil depth), and significant changes in the microbial community structure (Peacock et al., 2001).

In experimental plots with litter application, *E. coli* concentrations for rainfall immediately after application increased compared to the background *E. coli* concentrations for the 2-year and 5-year storm events (Figure 3.4). For the 0 h time lag, sustained *E. coli* concentrations were observed after the peak concentration, while for the 24 h and 120 h time lag, *E. coli* concentrations peaked and then decreased. Reductions in the *E. coli* concentrations as a function of the time lag (e.g., 24 h and 120 h) indicated bacteria die-off of approximately one order of magnitude (Figure 3.4). It should be noted that in figure 3.4 the filled square symbols correspond to the minimum concentrations

(e.g., water samples in which *E. coli* concentrations were over the range of quantification for the dilution factor).

However, a slight increase in *E. coli* concentrations was observed during the 120 h time lag experiments as compared to the 24 h experiments. This increase in average *E. coli* concentrations for the 120 h time lag experiment was hypothesized to be due to *E. coli* growth in litter when in contact with the soil surface and protected from ultraviolet light by vegetation. In addition, litter samples from outside the plots indicated an initial decrease in *E. coli* concentration 24 h after application and an increase in *E. coli* concentration 120 h after application (Figure 3.5). Wang (2003) reported *E. coli* re-growth after manure excretion for three to five days, during which temperature was considered the most critical variable, followed by moisture. Poultry litter is a non-homogeneous compound formed by bedding materials and manure. Particle size in litter ranges from millimeters in particulate litter to centimeters in cake compounds with a heterogeneous *E. coli* population distribution as a function of the litter particle size. As poultry litter is applied on the field, litter with higher mass (e.g., larger aggregation around manure droppings) is deposited close to the soil surface, where it is protected from UV light exposure, experiences more stable temperatures, and may have access to available moisture. Meteorological conditions and deposition location might promote *E. coli* survival as a function of moisture variation in the litter particles. Air temperatures during the experiments were in the range of 10°C to 32°C, solar radiation peaked at approximately 1200 W m⁻², and relative humidity averaged 90% during nights and sporadically some hours during the day (Figure 3.2). These environmental conditions were not optimal (e.g., maximum multiplication rate) for *E. coli* re-growth but can buffer

E. coli populations in larger litter particles or small cake fractions deposited close to the soil surface from inactivation.

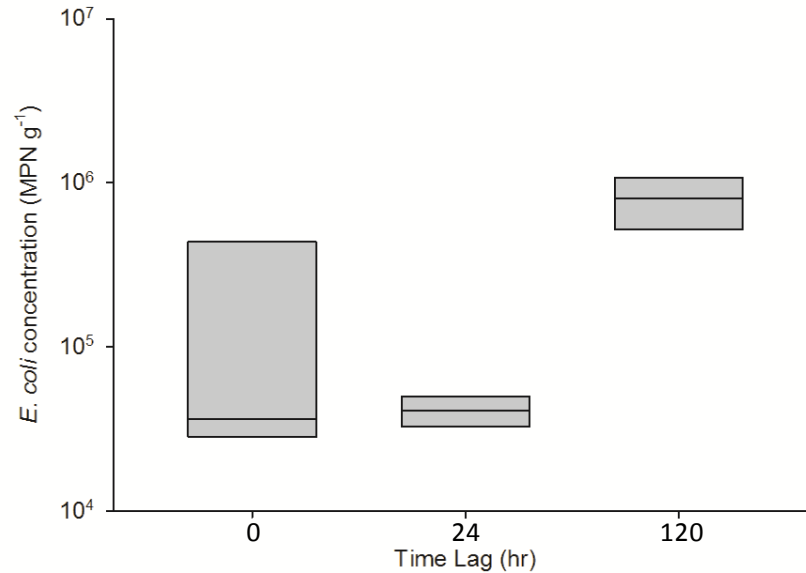


Figure 3.5. *Escherichia coli* concentration in poultry litter samples collected outside the treated plots as a function of time lag.

3.5. SUMMARY AND CONCLUSIONS

The objective of this research was to investigate *E. coli* event mean concentrations in surface runoff after poultry litter application on a series of fourteen 2 m × 2 m pasture plots subjected to 2-year and 5-year storm event intensities and for various time lags between litter application and rainfall. No significant differences were observed in average event mean concentrations relative to storm intensity. However, statistically significant differences were observed in average EMCs relative to time lag between litter application and rainfall. The relationship between time lag and litter application was not straightforward. The event mean concentrations were expected to be a maximum immediately following litter application and then decrease as a function of the time lag. However, the expected bacteria die-off rate was buffered due to hypothesized *E. coli*

growth in plots 120 h after litter application. It should be noted that the plots used for this research were only 2 m × 2 m, and this research did not address fate and transport mechanisms as runoff generated from these plots traveled to receiving water bodies.

In control plots, *E. coli* was always detected, indicating the presence and transport of fecal bacteria from sources independent from poultry litter application, with an average *E. coli* event mean concentration of 6.8×10^3 MPN/100 mL. The observed *E. coli* background concentration and its resulting contribution to the *E. coli* event mean concentration cannot be neglected as an important source of *E. coli*, especially in regard to the time lag between litter application and rainfall events. For example, the percentage contribution of the background fecal contamination was on average 4%, 52%, and 16% of the *E. coli* event mean concentration during the 0 h, 24 h, and 120 h time lag experiments, respectively. Therefore, poultry litter applications may contribute to runoff *E. coli* event mean concentrations when rainfall events occur shortly after litter application. However, other sources of fecal contamination serve as a significant component of the total *E. coli* event mean concentration, especially as the time lag between litter application and rainfall events increases. Bacteria survival and growth was hypothesized to depend on the location of deposited litter within the plot (i.e., on the surface of the grass or reaching the soil surface), suggesting that distribution of litter among various compartments within the system is needed to adequately represent available *E. coli* biomass for transport in runoff. Attempts at modeling the fate and transport of *E. coli* from surface-applied litter to pastureland should account for different deposition locations. In addition, future studies using more advanced biological analysis

techniques (i.e., DNA profiling) should be conducted to better resolve the possible sources of the control plot *E. coli* concentrations.

CHAPTER 4

Implementation and Validation of Biopore and Fecal Bacteria Fate and Transport Routines into the Root Zone Water Quality Model (RZWQM)

4.1. ABSTRACT

Surface runoff and infiltration are primary fecal bacteria transport mechanisms occurring in agricultural fields following manure application. Macropores and biopores increase water infiltration, decrease surface runoff and allow fecal bacteria and water to rapidly bypass the soil matrix during rainfall or irrigation events. This research incorporates fecal bacteria transport and biopore routines into the Root Zone Water Quality Model (RZWQM), to simulate flow and fecal bacteria transport through the soil, to subsurface drainage, and in runoff. Flow, soil fecal transport routines, and the influence of macropores and biopores on this transport were evaluated based on a series of soil column experiments (28 cm by 50 cm by 85 cm) with two contrasting soil types (e.g., loamy sand and sandy loam) in which artificial open surface connected biopores were placed at two different depths (e.g., 55 cm and 65 cm). Simulations of fecal transport in runoff were evaluated from a series of 2 m by 2 m plot experiments treated with poultry litter and subjected to two artificial rainfall storm event intensities. The new routines improved RZWQM's capability to predict rapid flow (e.g., shape of the

hydrograph, time to peak, and flow breakthrough. Simulated Nash-Sutcliffe efficiency index ranged between 0.65 and 0.81 and soil fecal transport (e.g., absolute error for the simulated event mean concentrations (EMCs) ranged between 4% and 109%) resulting from macropores, biopores, and subsurface drainage interconnectivity. Fecal transport concentrations were underestimated in some cases. The modified model captured the trend in concentrations observed during the soil column but not the plot experiments. The updated model is a simple, prediction tool capable of simulating fecal bacteria transport in runoff and to subsurface drainage with and without the presence of biopores and macropores.

4.2. INTRODUCTION

Surface runoff and water infiltration are primary fecal bacteria transport mechanisms following manure application in agricultural fields (Jamieson et al., 2002; Tyrrel and Quinton, 2003). During infiltration, the physical, chemical, and biological interactions in the soil matrix may result in fecal bacteria inactivation, transport retardation or immobilization (Fontes et al., 1991; Unc and Goss, 2003; Darnault et al., 2004). The presence of macropores (i.e., soil fractures and mesopores) and biopores (i.e., tunneling macropores from anecic earthworms) in soils may increase infiltration allowing rapid transport of solutes and microorganisms to deeper soils and/or subsurface drainage systems (Kemper et al., 1988; Shipitalo and Gibbs, 2000; Akay and Fox, 2007; Guzman et al., 2009).

A few physically-based or conceptual hydrological models at the column, plot and catchment scale have been used to simulate soil bacteria transport and preferential flow. Examples of these models are MACRO (Jarvis, 1994) and HYDRUS (Šimunek et al.,

2005; Šimunek et al., 2006). Recently, Köhne et al., (2009a,b) published a detailed review of models application for structured soils, and transport of tracers and pesticides. In most cases, bacteria transport has been simulated in a continuum porous media representation by solving the advection-diffusion equation in one, two or three-dimensions using Richard's equation and/or the Green-Ampt method. Also, soil structure has been incorporated into models assuming a uniform soil macroporosity in dual porosity or dual permeability models. However, assumptions made to simulate water flow at the pore scale in physically-based models are too restrictive in the presence of biopores that can invalidate the representative element volume concept (Jarvis, 2007).

The Root Zone Water Quality Model (RZWQM) is a one-dimensional physically-based lumped model with the capability to simulate the physical, biological, and chemical processes occurring in the vadoze zone under different scenarios and management practices. The main hydrological processes in the vadoze zone are modeled using the one-dimensional Richard's equation for soil moisture redistribution, the Green-Ampt method during infiltration, and the integrated Hooghoudt's equation (Bouwer and van Schilfgaarde, 1963) for the subsurface drain flow. Also, RZWQM has the capability to incorporate soil structure into the model by using uniform macroporosity per soil horizon (Ahuja et al., 2000). Moreover, flow and solute transport from directly connected macropores to subsurface drainage systems can be simulated using the express fraction concept (Fox et al., 2004). This model has also been considered for use by governmental agencies for simulating contaminant transport in soils; however, the model currently lacks routines for soil fecal bacteria fate and transport and rapid flow in the presence of biopores.

During the infiltration process, biopores may cause water and contaminants to bypass rapidly specific soil depths (Akay et al., 2008). This condition allows the propagation of a secondary wetting front down to the end of the biopore length, and along the biopore. A rapid rise in the water table may result from biopore flow bypassing a portion of the soil matrix increasing flow and transport at the drain as a function of the soil properties, macropores, and layer thickness between the end of the biopore and the subsurface drain (Akay and Fox, 2007; Akay et al., 2008; Guzman et al., 2009).

The objectives of this research were to (1) incorporate routines in RZWQM to simulate fecal bacteria transport through the soil matrix, macropores, and in surface runoff; and (2) to incorporate a new open surface connected (OSC) biopore routine to improve flow and transport simulations to subsurface drains. This model is the first to simulate fecal bacteria fate and transport through soils incorporating macropore and biopore flow at the plot scale.

4.3 MATERIALS AND METHODS

Routines to simulate fecal bacteria fate and transport were incorporated into RZWQM's water redistribution and infiltration subroutines. Additionally, a routine simulating OSC biopores from anecic earthworms was added to the infiltration module for rapid flow and transport to a specific soil depth (Figure 4.1). No additional routines were included to account for surface runoff or subsurface drain flow routing.

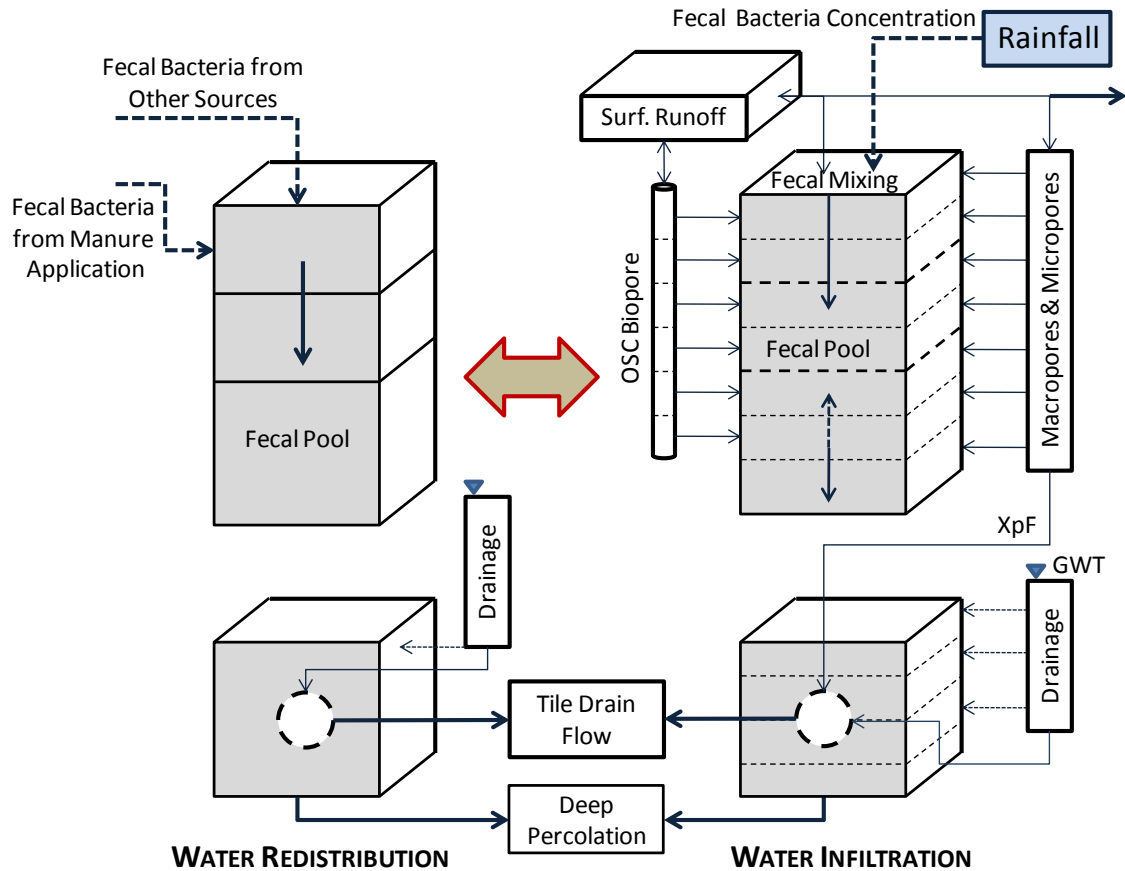


Figure 4.1. Conceptual diagram of the main RZWQM hydrological processes and the new biopore concept. Where XpF is the express fraction concept (Fox et al., 2004) and GWT is the ground water table.

4.3.1 Fecal Bacteria Fate and Transport Modeling

Soil fecal bacteria fate and transport was modeled based on the conservation of mass at the layer (e.g., infiltration) or horizon discretization (e.g., redistribution) in a unitary volume (e.g., 1 cm^3 fecal bacteria pools). Fecal bacteria transport by advection, attachment, detachment, straining, and dieoff were considered in the liquid and/or solid phase. Attachment was represented by a non-linear function (see Chapter 2) while detachment was assumed to occur linearly. Straining was linearly represented (Foppen et

al., 2005) as a fraction of the fecal bacteria mass transported in the liquid phase from an adjacent layer:

$$\left(\frac{\Delta N}{\Delta t}\right)_{LP} = \left(\frac{u}{\Delta z} C\right)_{adv} - \left(\frac{u}{\Delta z} K_{str} C\right)_{str} - \left(\frac{\rho_{bulk}}{\Delta t} q\right)_{att} - \left(\frac{N}{\Delta t} e^{-kt}\right)_{dieoff} \quad (4.1)$$

$$q = AC^b \quad (4.2)$$

$$\left(\frac{\Delta N}{\Delta t}\right)_{SP} = \left(\frac{u}{\Delta z} K_{str} C\right)_{str} + \left(\frac{\rho_{bulk}}{\Delta t} q\right)_{att} - \left(\frac{D_{det}}{\Delta t} N\right)_{det} - \left(\frac{N}{\Delta t} e^{-kt}\right)_{dieoff} \quad (4.3)$$

where C is the fecal bacteria concentration in the liquid phase (MPN mL^{-1}); u is the flow velocity at the receiving layer (cm h^{-1}); ρ_{bulk} is the soil bulk density (g cm^3); q represents the fecal bacteria attachment concentration (MPN g^{-1}); A and b are constants for the non-linear attachment function; K_{str} is the straining coefficient fraction; D_{det} is the detachment coefficient fraction; t is the time in hours; z represents the vertical direction, k is the dieoff rate (h^{-1}), and N is the fecal bacteria mass in the liquid or solid phase pools per unitary volume (MPN cm^{-3}). adv, str, att, LP, and SP indicate advection, straining, attachment, liquid phase and solid phase, respectively.

Fecal bacteria die-off was simulated by an exponential inactivation model (Chick's, 1908). During simulation, the first order die-off rate was adjusted at each time step as a function of the water temperature in the soil profile using the Arrhenious equation (Hrishikesh et al., 2007; Garzio-Hadzick et al., 2010):

$$k = A_r e^{-\left(\frac{E}{RT}\right)} \quad (4.4)$$

where A_r is a constant in the Arrhenious equation; E is the activation energy; R is the gas constant, and T is the water layer temperature. Variables affecting bacteria fate such as

moisture content, microbial competition, UV radiation, pH, and soil organic matter content were not considered in the model.

In cases in which the integrated Hooghoudt's equation contributed flow to the drain, transport of fecal bacteria was estimated as a function of the advection, detachment and straining occurring in the soil volume fraction of the layer separating two drain pipes:

$$N_{DP} = K_{HVF} DP_{SEP} (1 - K_{str}) u C \Delta t \Delta z \Delta y \quad (4.5)$$

where N_{DP} is the bacteria mass transported to the drain pipe (MPN); K_{HVF} is the effective horizontal layer volume contributing fecal bacteria; DP_{SEP} is the drain pipes spacing (cm); K_{str} is the straining coefficient; u represent the horizontal flow velocity (cm h⁻¹); C is the fecal bacteria concentration in the liquid phase and y is the layer depth (cm).

4.3.2 Biopore Flow and Transport

Biopores were described in the model by a vertical circular opening reaching a specific soil depth in contact with saturated or unsaturated soil layers (Figure 4.1).

Biopores were assumed to occur homogenously in the one-dimensional soil profile as a function of the biopore macroporosity estimated as the biopore volume per 1-cm soil layer volume. Seasonal biopore opening variation as well as tillage biopore disruption was allowed using a daily fraction biopore opening parameter (Ramirez et al., 2009). The effective biopore length was expressed as a function of the biopore tortuosity. Flow routed through biopores was proportional to the remaining surface runoff portion following soil matrix and macropore infiltration including the express fraction. Biopores propagate water into the soil matrix downward and upward at the biopore end. Layer flow propagation was estimated as the result of the minimum flow between the maximum

infiltration capacity and the saturated hydraulic conductivity or saturation water deficit for a saturated or unsaturated layer, respectively.

The maximum infiltration capacity was estimated by the Hagen-Poiseuille law (1939) or tank model for the unsaturated or saturated layer condition, respectively. The final maximum biopore infiltration flow resulted from multiplying the former value by an effective lateral infiltration constant and the daily biopore opening parameter:

$$Q = K_{BPf} K_{eff}^u \frac{\pi r^4 \Delta P}{8 \mu \tau L} \quad (4.6)$$

$$Q = K_{BPf} K_{eff}^s 2 \pi r \sqrt{2 g L} \quad (4.7)$$

where K_{BPf} is the biopore opening fraction; K_{eff}^u and K_{eff}^s are the effective lateral infiltration coefficient per soil horizon for the unsaturated and saturated condition, respectively; r is the biopore radius; ΔP is the pressure difference over the corresponding layer; μ is the water dynamic viscosity; L is the biopore soil profile depth at each layer; and τ is the tortuosity.

The volume of water propagating downward was limited by the infiltration capacity of the layer containing the end of the biopore. In cases in which the biopore end layer become saturated, a downward piston flow was allowed until the water front reached the drain pipe depth or the propagating water become exhausted in the adjacent layers. Excess of water reaching the drain pipe was added to the subsurface drain flow. For the upward water propagation, piston flow was also allowed in saturated layers. At the surface, the excess water after the downward and upward propagation process, if any, was returned to the surface runoff.

4.3.3 Sources of Fecal Bacteria

Three sources of fecal bacteria were considered in the model: (i) fecal bacteria from manure application, (ii) fecal bacteria from other sources, and (iii) fecal bacteria from rainfall events (Figure 4.1). Fecal bacteria from other sources represent bacteria mass that is deposited on the top layer of the soil from animal excretions, such as from rodents and birds. It was considered to form part of the solid phase based on user-defined monthly mean concentrations and standard deviations. Routines to allow a source of fecal bacteria as part of RZWQM's management practices were added based on daily application of injected liquid manure or broadcasted manure as a function of the application rate and fecal bacteria concentration. Following manure application, fecal bacteria was subject to attachment at the corresponding layer (equation 4.2). To allow the model to simulate laboratory soil column experiments (Guzman et al., 2010), fecal bacteria concentrations in the rainfall were allowed. This condition is very rare in field condition but served to simulate fecal bacteria transport in soil columns in which the source of fecal bacteria is applied such as a rainfall event.

4.3.4 Model Calibration and Validation

In order to evaluate the capability of the model to predict the hydrological response and fecal bacteria transport at the subsurface drain flow and surface runoff, the updated model was calibrated and evaluated to two sets of experiments. First, the model was calibrated and evaluated for subsurface drain transport with biopores using a series of five-day experiments carried out in a laboratory 28 x 50 x 85 cm soil column using artificial OSC biopores of 55 cm and 65 cm in depth in two soil types. In these experiments, the soil column was initially packed and then flushed with deionized water

(DI), 48-hr later flushed with diluted liquid swine manure, and then finally 48-hr after the manure application flushed with DI (Guzman et al., 2009). Flow and *E. coli* concentrations were measured in the subsurface drainage.

Second, the model was calibrated and evaluated for surface runoff based on a series of experiments using two artificial rainfall events, 2-yr and 5-yr return periods applied on a 2 x 2 m pastureland plots manually treated with poultry litter at the rate of 4,942 kg ha⁻¹ (Guzman et al., 2010). Surface runoff and *E. coli* concentrations were measured at the collecting flume located at the drainage end of the plots.

In all cases, the hydrological responses were evaluated by the Nash-Sutcliffe (Nash and Sutcliffe, 1970) efficiency index (NSI) and absolute error between the observed and simulated mass of subsurface drainage or runoff:

$$\eta = 1 - \frac{\sum (\hat{y}_i - y_i)^2}{\sum (\hat{y}_i - \bar{y})^2} \quad (4.8)$$

where η is the Nash-Sutcliffe efficiency index; y_i and \hat{y}_i are the observed and simulated values at time i , respectively, and \bar{y} is the mean of the observed values. Fecal bacteria transport was evaluated in two steps. First, the absolute difference between the observed and simulated fecal transport was assessed based on the event mean concentrations (EMC) from the observed and simulated fecal bacteria breakthrough curves (Garbrecht et al., 2009; Guzman et al., 2010) and loads:

$$EMC = \frac{\sum \Delta t_i Q_i C_i}{\sum \Delta t_i Q_i} \quad (4.9)$$

where t_i is the time between two measurements; Q_i is the observed or simulated runoff for the soil column or plot experiments at time i ; and C_i is the effluent *E. coli* concentration

at time i . Second, observed and simulated trends were evaluated by normalizing the observed and simulated fecal bacteria concentrations by its maximum value and then computing the NSI.

For the soil column experiments, the updated RZWQM was calibrated (e.g., soil hydraulic, macropore and biopore properties) based on the cumulative drainage runoff at the end of the manure flush. The final DI flush (e.g., 48-h after the manure flush) served to validate the corresponding model calibration. For the surface runoff plot experiments, model calibration was based on the flow from the 2-yr return period storm event and then validated based on flow from the 5-yr return period storm event. Also, the calibrated 2-yr storm event was used to estimate the equivalent *E. coli* rainfall concentration proportional to the *E. coli* background concentration observed during the experiments (Guzman et al., 2010). This fecal background concentration was used during the model validation.

Attachment and detachment parameters affecting transport were obtained from soil sorption experiments after mixing 6 g of soil and diluted swine manure in a series of batch experiments (see Chapter 2). The straining coefficient for the loamy sand was obtained from Garbrecht et al., (2009) experiments while for the other soils it was assumed. Die-off rates and the effective horizontal soil layer contribution fraction were assumed in all cases.

4.4 RESULTS AND DISCUSSION

4.4.1 Hydrological Response

Tables 4.1 to 4.3 summarize the calibrated parameters controlling the hydrological response for both the soil column and field experiments. Tables 4.4 and 4.5 summarize the experimental setup and goodness-of-fitness indices assessing the model

performance. Graphical representations of the model performance are shown in Figures 4.2 and 4.3 for the subsurface drain flow and surface runoff, respectively.

The biopore routine notably improved the subsurface flow simulation at the drain during the soil column experiments. The hydrograph shape, tile drain flow, breakthrough time and time to peak were in general properly represented (Figure 4.2). Also, the new routines characterized the rapid increase in flow at the drain pipe typically observed in presence of biopores. On the other hand, simulations without biopores could not properly represent the shape and peak of the hydrograph even though macropores were included in the simulations.

For the plot experiments, RZWQM underestimated the hydrological response. Note that as a one-dimensional model RZWQM does not have surface runoff routing capabilities. However, the model represented the total surface runoff volume accurately in all cases but not the shape of the hydrograph (Figure 4.3). This condition indicates that RZWQM may properly represent runoff at the daily but not the subdaily time scale. As the rainfall event intensity increased, deviation in the simulated runoff proportionally increased (Figure 4.3b). On the other hand, lower rainfall intensities resulted in higher infiltration volume decreasing the available surface runoff subject to routing (Figure 4.3a). As an example, the total observed losses during the 2-yr and 5-yr storm event were 42.0% and 27.8%, respectively (see Table 4.5).

Table 4.1 Soil macropores and biopore properties for the soil column and plot experiments after calibration. Note that SC is the soil column, MP is macropore radius, FDEP is the fraction of dead end pores, ELWT is the effective lateral wetting thickness, and K_{eff} is the effective biopore infiltration constant.

Exp.	Soil Type	Biopore		MP	Macroporosity		FDEP	ELWT	K_{eff}	
		Depth cm	radius cm	Radius cm	Biopore $cm^3 cm^{-3}$	MP $cm^3 cm^{-3}$			Unsat.	Sat.
SC	Loamy sand	55	0.4	0.04	3.59E-04	6.30E-04	0.500	1.0	5.5E-03	3.5E-02
SC	Loamy sand	65	0.4	0.04	3.59E-04	1.15E-04	0.460	1.0	9.5E-05	5.6E-03
SC	Sandy loam	55	0.4	0.04	3.59E-04	4.30E-05	0.465	1.0	1.0E-02	9.3E-04
Plot	Silt loam	-	-	0.04	-	3.00E-06	0.460	1.0	9.5E-05	5.6E-03
Plot	Silt loam	-	-	0.04	-	3.00E-06	0.460	1.0	9.5E-05	5.6E-03

Table 4.2 Soil hydraulic properties for the soil column and plot experiments after calibration. Note that h_b is the bubbling pressure, λ is the pore size distribution index, N is the exponent for the $k(h)$ curve, K_{sat} is the saturated hydraulic conductivity, θ_r is the residual water content, θ_s is the saturation water content, and K_{sat-d} is the lateral saturated hydraulic conductivity to the drain.

Soil Type	Experiment	h_b cm	λ	N	K_{sat} $cm h^{-1}$	θ_r	θ_s	K_{sat-d} $cm h^{-1}$
Loamy sand	OSC-55	7.905	0.484	3.422	11.110	0.035	0.396	0.710
Loamy sand	OSC-65	10.090	0.474	3.422	3.900	0.035	0.396	2.450
Sandy loam	OSC-55	12.740	0.322	2.966	2.580	0.041	0.472	0.995
Silt loam	Plot	7.537	0.361	2.633	0.424	0.015	0.472	15.00

Table 4.3 Soil textural properties for the soil column and plot experiments after calibration, where BD is the soil bulk density and ϕ is the soil porosity.

Soil Type	BD g cm ⁻³	ϕ	Sand Fraction	Silt	Clay
Loamy sand	1.6	0.396	0.85	0.1	0.05
Sandy loam	1.4	0.472	0.65	0.25	0.10
Silt loam	1.4	0.472	0.2	0.65	0.15

In all cases, RZWQM poorly represented the recession part of the hydrographs at the end of the rainfall event. However, the depletion part was properly represented in the soil column experiments (Figure 4.2 and 4.3). This phenomenon occurred at the time the model shifted from infiltration to water redistribution computations in the column experiments and impacted the mass curves in Figure 4.2 right after the end of the rainfall event. It was explained due to a rapid drop in the simulated water table and quick change in moisture conditions no properly simulated by the Richard's equation during water redistribution. Note in Table 4.4 the high average infiltration rates for the loamy sand (e.g., 3.0 cm³ s⁻¹ for the OSC-65 and 13.8 cm³ s⁻¹ for the OSC-55 experiments) driving a rapid rise in the water table during infiltration.

Additionally, high deviations in the simulated flow occurred during high infiltration rates (Figures 4.2a, 4.2b and 4.2d) right after the breakthrough. This condition may indicate the presence of direct macropore connectivity occurring between the end of the biopore and the subsurface drain pipe contributing rapid flow. The express fraction can help better represent this process after some modifications, which should be considered in future research. On the other hand, the lack of surface runoff routing capabilities in RZWQM explained the lack of the recession part of the hydrograph in the plot experiments (Figures 4.3).

Also, the fact that RZWQM cannot simulate other surface runoff mechanisms such as the presence of water storage in surface depressions, interception, interflow, surface roughness and spatial variability in the slope, explains the shape of the simulated hydrograph in the sub-daily basis simulations. Note that the simulated runoff in RZWQM corresponded to the excess water resulting from the rainfall event and infiltration at specific time step in a 1 cm² area.

Table 4.4 Subsurface drainage soil column calibration and validation results, where MC_{obs} and MC_{sim} are the mass curve values for the observed and simulated drainage runoff; NSI is the Nash-Sutcliffe efficiency index; MC_{err} is the mass curve error; f_{avg} is the average infiltration rate; REC is the rainfall *E. coli* concentration; Man is the manure flush; and DI is the distilled water flush.

		Flush		Rainfall	MC _{obs}	MC _{sim}	NSI	MC _{err}	f_{avg}	REC
		Time		cm ³	cm ³	cm ³		%	cm ³ s ⁻¹	MPN mL ⁻¹
OSC-55 Loamy sand	Man	Start	9:25		0	0		-		
		End†	9:45	13,830	1,774	1,779	0.01	0.3%	11.51	153.6
		End‡	23:07		15,234	14,614		4.1%		
	DI	Start	9:45		0	0		-		
		End†	9:59	13,920	1,557	2,001	0.65	28.5%	16.05	0
		End‡	18:24		12,438	11,043		11.2%		
OSC-65 Loamy sand	Man	Start	10:40		0	0		-		
		End†	12:29	14,190	7,645	7,326	0.76	4.2%	2.15	115.2
		End‡	22:05		13,203	13,270		0.5%		
	DI	Start	9:35		0	0		-		
		End†	10:39	14,470	6,349	6,070	0.75	4.4%	3.76	0
		End‡	23:05		12,440	12,539		0.8%		
OSC-55 Sandy loam	Man	Start	11:59		0	0		-		
		End†	14:07	14,085	6,666	7,600	0.81	14.0%	1.82	83.6
		End‡	23:22		10,964	10,366		5.5%		

† Final time for the rainfall event. ‡ Final time for the mass transport assessment.

Table 4.5 Surface runoff plot experiments calibration and validation results, where MC_{obs} and MC_{sim} are the mass curve for observed and simulated surface runoff, NSI is the Nash-Sutcliffe efficiency index, MC_{err} is the mass curve error, $Losses_{avg}$ is the average infiltration, interception and evaporation volume, and PREC is the proportional rainfall *E. coli* concentration.

Exp.	Time		Rainfall Cm	MC _{obs} cm ³	MC _{sim} cm ³	NSI	MC _{err} %	Losses _{avg} cm	PREC MPN mL ⁻¹
2-year storm event	Start	15:24		0	0		-		
	End†	16:09	4.38	90,949	90,955	0.81	0.0%	1.84	1,660
	End‡	16:19		101,453	95,444		5.9%		
5-year storm event	Start	19:27		0	0		-		
	End†	19:57	3.81	85,460	84,471	0.05	1.2%	1.06	1,660
	End‡	20:13		110,053	110,136		0.1%		

† Final time for the rainfall event. ‡ Final time for undetectable surface runoff.

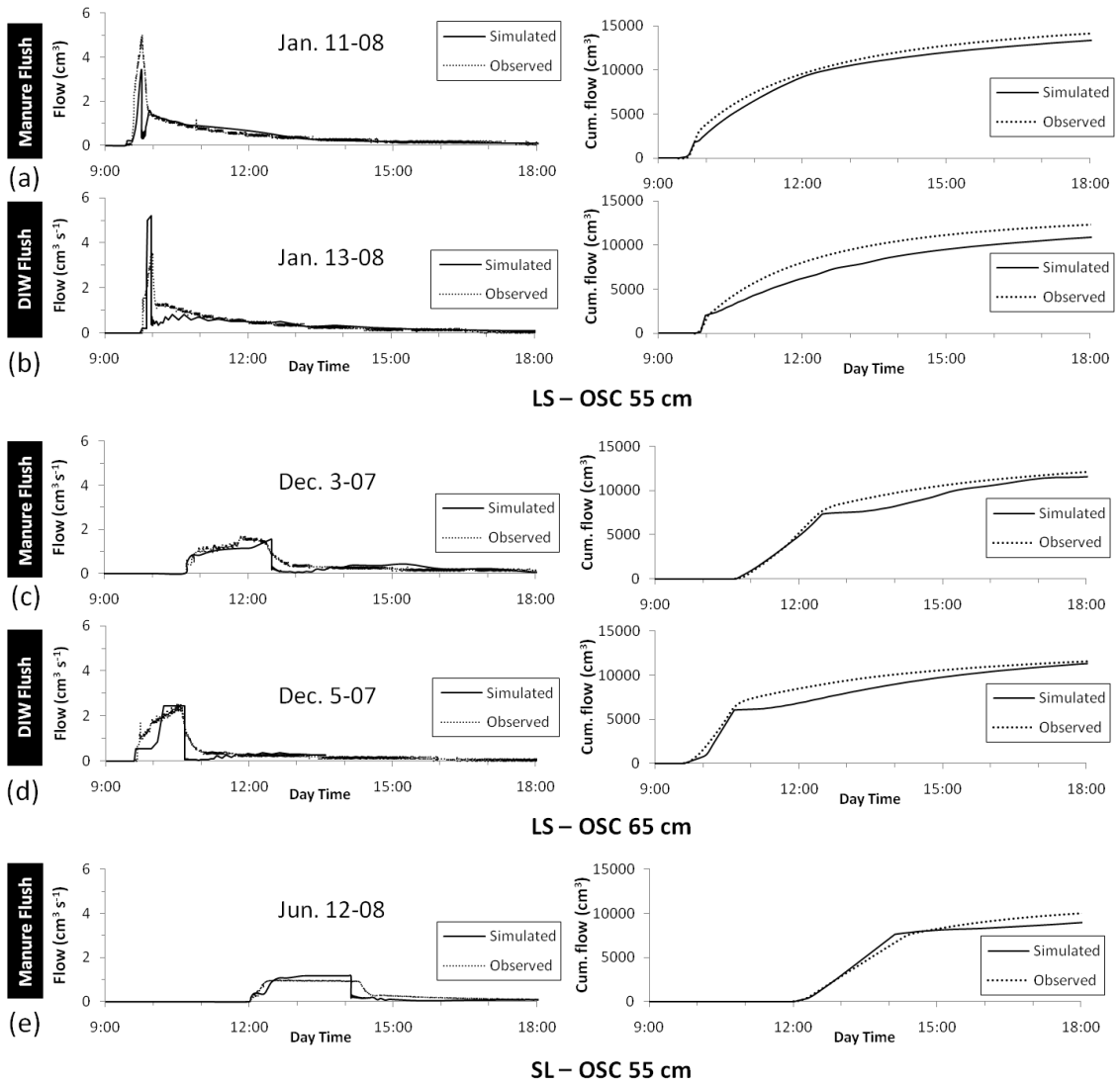


Figure 4.2 Subsurface drain flow and mass curves for the soil column experiments.

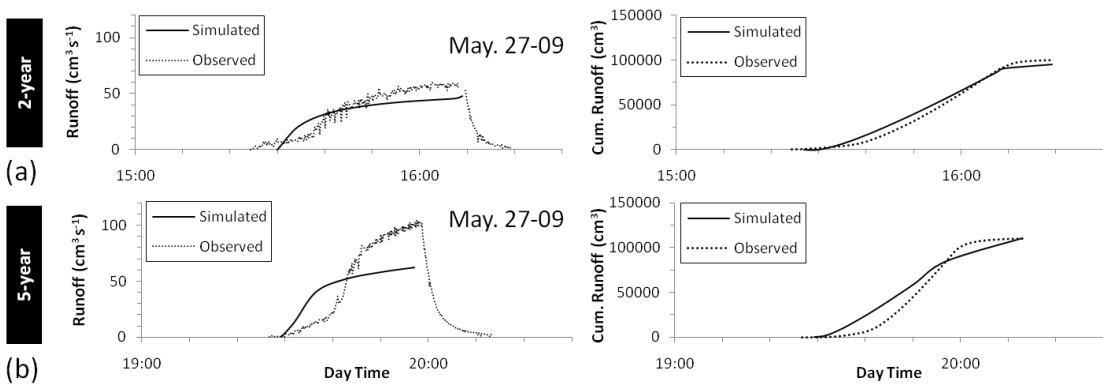


Figure 4.3 Surface runoff and mass curve for the plot experiments.

4.4.2. Transport of Fecal Bacteria

Table 4.6 summarizes the fecal transport parameters used during the simulations. The new transport routines and biopore concept notably improved the simulation of fecal bacteria transport at the subsurface drain in the soil column experiments. For example, simulated EMCs using the biopore concept were predicted with an absolute error in the range of 4% to 109% when compared to the observed EMC (Table 4.7 and 4.8). Note that during the column experiments a few samples were available after the rainfall event (Figure 4.4). Also, *E. coli* concentrations showed high variability during the 5-yr storm event (Figure 4.5). Without the biopore routine, simulated EMC for the column experiments were zero during the manure flush but represented a maximum of 2.2% of the observed EMC for the DI flush in the LS OSC-65 experiment (Table 4.7). Fecal bacteria concentration trends were properly simulated for the LS-OSC-65 and SL-OSC-65 column experiments (Figure 4.4 and Table 4.7). However, for the LS-OSC-55 experiment, the model poorly represented the fecal concentration trends perhaps due to piping flow previously discussed. Additionally, when the model shifted from infiltration to redistribution, concentrations were poorly represented during the recession part of the hydrograph.

Table 4.6 Transport parameters for the soil column and plot experiment simulations, where K_{str} is the straining coefficient, D_{tchm} is the detachment coefficient, LP is the liquid phase, SP is the solid phase, and Top is the soil top layer.

Soil Type	Attachment		K_{str} Fraction	D_{tchm} Fraction	Die-off rate (d^{-1})		
	A	B			LP	SP	Top
Loamy sand	0.38	1.01	0.01	0.24	0.05	0.03	0.1
Sandy loam	213.4	0.324	0.05	0.20	0.05	0.03	0.1
Silt loam	342.5	0.315	0.01	0.20	0.05	0.03	0.1

Table 4.7 Fecal transport event mean concentrations (EMC) for the soil column experiments, where NEMC is the normalized event mean concentration (EMC_{sim}/EMC_{obs}), NBP refers to the simulations with no biopore routine included, and REC is the rainfall *E. coli* concentration.

Exp.	Flush		EMC_{obs} MPN mL ⁻¹	EMC_{sim} MPN mL ⁻¹	Abs. Error	Trend NSI	$EMC_{sim-NBP}$ MPN mL ⁻¹	REC MPN mL ⁻¹
LS OSC-55	Man	Rainfall	6.5	13.6	109.2%	-0.41	0.0	153.6
		Total	21.7	6.9	68.2%			
	DI	Rainfall	25.1	11.8	53.0%	-0.90	0.0	0.0
		Total	18.1	17.3	4.4%			
LS OSC-65	Man	Rainfall	15.3	12	21.6%	0.79	0.0	115.2
		Total	16.2	7.6	53.1%			
	DI	Rainfall	14.1	26.5	87.9%	0.97	0.3	0.0
		Total	13.7	17.6	28.5%			
SL OSC-55	Man	Rainfall	0.6	0.8	27.0%	0.73	0.0	83.6
		Total	1.4	0.7	50.4%			

During the depletion part of the hydrograph, the model underestimated the observed fecal concentrations even though flow simulations were properly represented. This condition was perhaps the result of underestimated fecal transport at the above adjacent layers contributing most of the drainage flow in the model. Further calibration of the transport parameters may improve simulations as a function of a specific objective function for subdaily simulations.

For the plot experiments, concentrations were underestimated in most cases as well as loads (Figure 4.5 and Table 4.8). However, when using the upper observed poultry litter concentration (Guzman et al., 2010), simulated EMC accounted for 48% and 43% of the observed EMC during the 2-yr and 5-yr storm events, respectively. Note that poultry litter has high fecal concentration variability when dispersed in water as it is mainly composed of aged droppings in bedding materials heterogeneously distributed. Trends in the fecal transport concentrations were poorly represented as indicated by the

negative NSI in Table 4.8. These results indicated that the RZWQM surface mixing model can represent fecal bacteria concentrations in runoff and future research is needed to incorporate routing processes in RZWQM and fecal bacteria release from manure application.

Table 4.8 Fecal transport event mean concentrations (EMC) for the plot experiments, where REC is the rainfall *E. coli* concentration.

Exp.	EMC _{obs} MPN mL ⁻¹	EMC _{sim} (MPN mL ⁻¹)			Absolute error			Trend NSI	REC (MPN mL ⁻¹)		
		avg	min	max	avg	min	max		avg	min	Max
2-year	1,838	415	62	1,088	77.4%	96.6%	40.8%	-0.79	1,660	246	4,317
5-year	1,784	446	67	1,169	75.0%	96.3%	34.5%	-0.25			

4.5 SUMMARY AND CONCLUSIONS

The implementation of routines to simulate fecal bacteria transport in the vadoze zone, as well as flow and transport through biopores, improved the capability of RZWQM. For model evaluations based on subsurface drainage experiment, the new routines improved the simulation of the hydrograph shape, time to peak, and flow breakthrough when biopores were present. Also, fecal transport concentrations were properly represented in some cases, but not total load. The modified RZWQM poorly represented flow during the recession part of the hydrograph, while the depletion was properly described. This condition strongly impacted fecal transport simulations as well as the goodness-of-fitness indices. Moreover in some cases, the new routines underestimated the rapid increase in flow observed in the subsurface drain immediately after the flow breakthrough perhaps due to biopore/subsurface drain/macropore interconnectivity.

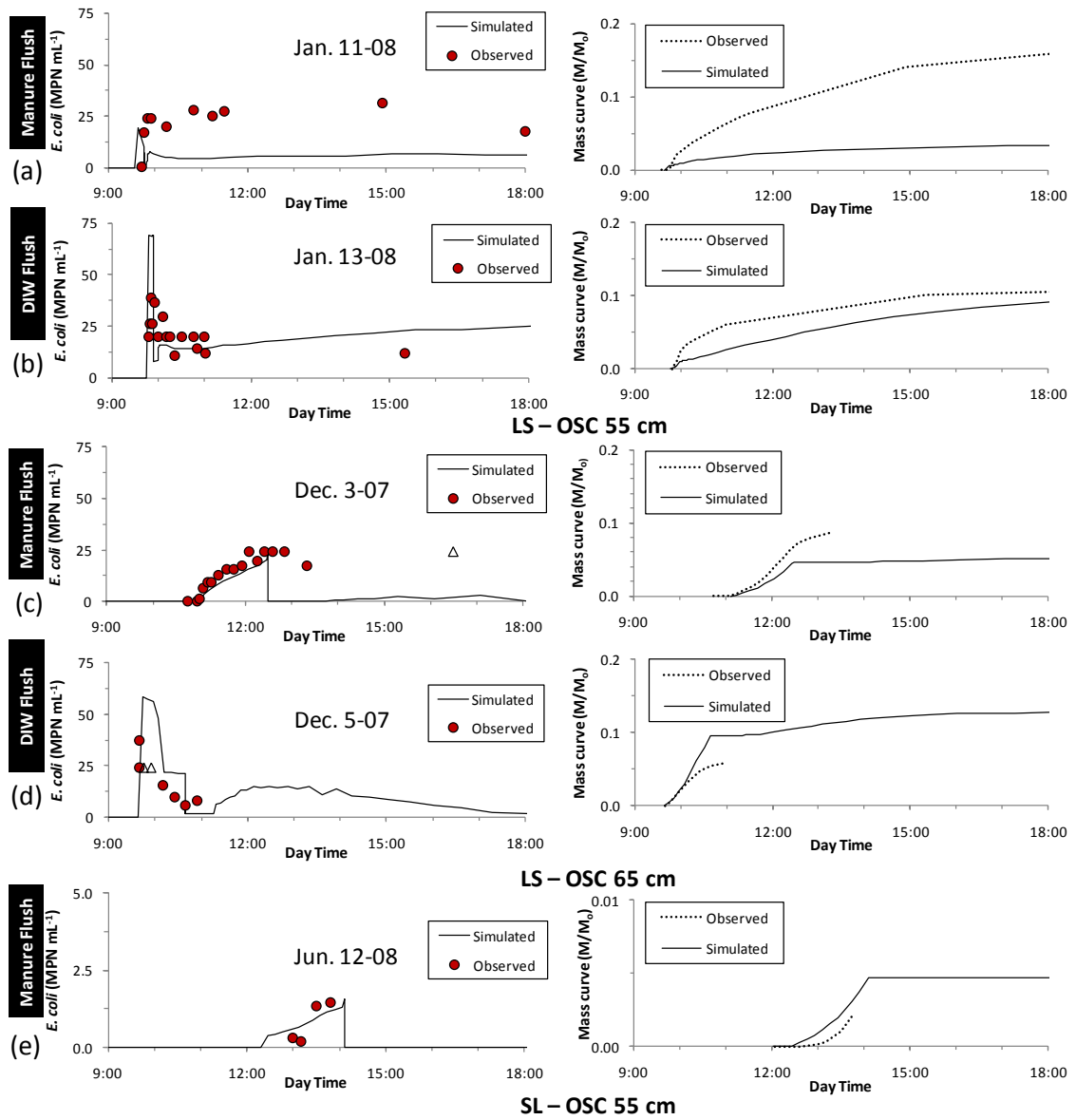


Figure 4.4 Observed and simulated fecal bacteria concentrations and mass curves for the soil column experiments. Triangle legends represent observed concentrations over the detection range.

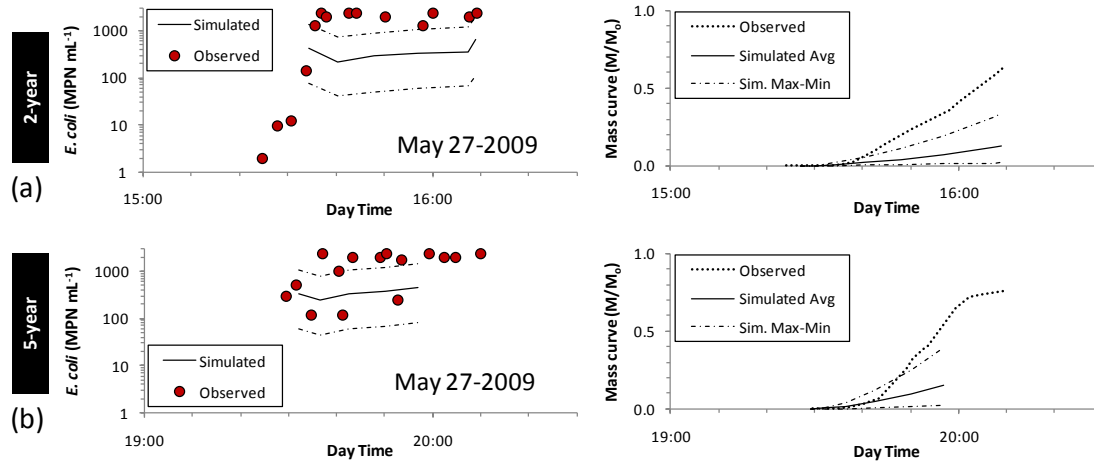


Figure 4.5 Observed and simulated fecal bacteria concentrations and mass curves for the plot experiments.

Evaluation of the model based on surface runoff experiments with artificial rainfall indicated that RZWQM can properly represent the total runoff volume but not the shape of the hydrograph, as RZWQM does not include surface runoff routing processes. Fecal bacteria concentrations in surface runoff were underestimated by the model and the observed trends in concentrations were not properly represented. Implementation of routing processes for surface runoff and subsurface drain flow may help improve RZWQM's capabilities for predicting flow and soil fecal transport.

CHAPTER 5

Summary and Conclusions of Dissertation

Fecal bacteria fate and transport in soils treated with manure effluent are driven by multiple interrelated physical, chemical and biological processes. In most cases, the soil matrix can retard, immobilize and/or inactivate fecal bacteria being transported. However, facilitated flow and fecal bacteria transport through macropores and biopores allow fecal bacteria to bypass a portion of the soil matrix and reach deeper soils and subsurface drainage systems. Manure effluent constituents can potentially change the soil bulk solution pH and favor ionic exchange resulting in varying soil-bacteria or soil bacteria-substrate sorption mechanisms. Fecal bacteria die-off rates vary as a function of lag time between manure application and the occurrence of rainfall or irrigation events, and environmental variables. The new routines implemented in RZWQM allow fecal bacteria fate and transport simulation in the soil matrix, runoff, soil profile, and drainage system. Also, the implemented biopore concept allows RZWQM to simulate non-equilibrium flow conditions.

5.1 SPECIFIC CONCLUSIONS

In the first chapter, the importance of surface connected and disconnected (buried) biopores on *Escherichia coli* transport was investigated when biopores were located near subsurface drains. The results were:

- *Escherichia coli* transport to the drain was observed with either open surface connected or buried biopores.
- *Escherichia coli* transport to the drain in the surface connected biopores was a function of the soil type and the layer thickness between the end of the biopore and drain.
- Buried biopores contributed flow and *E. coli* to the drain in the less sorptive soil (loamy sand) and the sorptive soil (sandy loam) containing a wide (i.e., with mesopores) pore space distribution prevalent due to the moist soil packing technique.
- Biopores provide a mechanism for rapidly transporting *E. coli* into subsurface drains during flow events.

In the second chapter, soil sorption/attachment of *Escherichia coli* and the influence of swine manure constituents were investigated using a series of artificial and natural soils treated with manure effluents at varying dilution ratios (i.e., swine manure effluent concentration). The results were:

- Fecal bacteria in swine effluents consisted primarily of sessile (i.e., attached) bacteria (90%) compared to free cells in suspension (10%).
- Removal of sessile *E. coli* from solution by sorption/attachment and/or flocculation/precipitation appeared to be controlled by processes occurring in the substrate (i.e., surfaces to which the bacteria attached).
- For soils up to 30% clay content and 3.0% total carbon content, nonlinear equations characterized the sorption of *E. coli* from multi-constituent manure effluent in the artificial and natural soils with the equation parameters predicted

by the amorphous aluminum and iron content, percent clay, and percent organic carbon.

- Dispersion resulting from alkalinity buildup due to adding effluent to the soils decreased observed sorption of *E. coli*, especially at higher effluent ratios.

In the third chapter, transport of *E. coli* in runoff was investigated on fourteen 2 m by 2 m pastureland plots treated with poultry litter and subjected to artificial rainfall intensities equivalent to 2-yr and 5-yr storm events after poultry litter application, and after 24 and 120 hr. The results were:

- No significant differences were observed in *E. coli* average event mean concentrations (EMCs) relative to storm intensity.
- Statistically significant differences were observed in average *E. coli* EMCs relative to time lag between litter application and rainfall.
- A nonlinear relationship was observed between average *E. coli* EMC and time lag, with the EMC decreasing between 0 h and 24 h and then increasing at 120 h.
- *Escherichia coli* were always detected in the control plots, indicating the presence and transport of fecal bacteria from sources independent of the immediate poultry litter application and serving as a significant component of the total *E. coli* EMC, especially as the time lag between litter application and rainfall events increases.

Finally, in the fourth chapter routines were incorporated in the Root Zone Water Quality Model (RZWQM) to simulate fecal bacteria transport through the soil, subsurface drain and runoff. Also, a biopore concept was developed to model the rapid flow and transport of fecal bacteria bypassing a portion of the soil matrix. The results were:

- The new routines improved RZWQM's capability to predict rapid flow and soil fecal bacteria transport in the soil matrix, macropores, biopores, and subsurface drains.
- For model evaluations based on subsurface drainage experiment, the new routines improved the simulation of the hydrograph shape, time to peak, and flow breakthrough when biopores were present. Also, fecal concentrations were properly represented in some cases but not fecal loads.
- The modified RZWQM poorly represented flow during the recession part of the hydrograph, while the depletion was properly described for the soil column experiments.
- Fecal concentrations were underestimated in some cases but the modified model captured the observed concentration trend in the drain for the column experiments but not in runoff for the plot experiments.
- The updated model is a simple, prediction tool capable of simulating fecal bacteria transport in runoff and to subsurface drainage with and without the presence of biopores and macropores.

5.2 FUTURE RESEARCH

A more comprehensive approach should be adopted in future soil fecal bacteria fate and transport research to avoid over simplification of the physical, chemical and biological variables and their relationship. Also, the use of mono-strain cultured bacteria suspended in inert solutions typically used in homogeneous porous media and granular soils should be limited as fecal bacteria from manure effluents are mainly in sessile form

and agricultural lands primarily develop on soils possessing varying soil minerals and organic matter and are subjected to macropore/biopore development.

Investigations on colloidal-facilitated fecal bacteria fate and transport should be conducted at both field and laboratory scales due to the preference of fecal bacteria to be surface bonded. Also, soil colloidal interaction in the presence of solute concentrations should be investigated as changes in the colloids carrying fecal bacteria can increase fecal bacteria detection. In addition, acquisition of long term fecal bacteria fate and transport data in runoff and in the soil profile is needed to advance the understanding of fate and transport mechanisms of fecal bacteria in soils and improve modeling capabilities at the field scale.

Finally, further research is needed to incorporate surface and subsurface runoff routing capabilities, simulate fecal bacteria release from manure amendments, incorporate open surface disconnected biopore routines, improve the express fraction concept, and perhaps incorporate a dual permeability model for the water redistribution subroutine in RZWQM.

REFERENCES

- Akay, O., and G.A. Fox. 2007. Experimental investigation of direct connectivity between macropores and subsurface drains during infiltration. *Soil Sci. Soc. Am. J.* 71:1600–1606.
- Akay, O., G.A. Fox, and J. Simunek. 2008. Numerical simulation of flow dynamics during macropore-subsurface drain interaction using HYDRUS. *Vadose Zone J.* 7:909–918.
- Ahuja, L.R., K.E. Johnson, and G.C. Heathman. 1995. Macropore transport of a surface-applied bromide tracer: Model evaluation and refinement. *Soil Sci. Soc. Am. J.* 59:1234–1241.
- Ahuja, L.R., K.E. Johnson, and K.W. Rojas. 2000. Water and chemical transport in soil matrix and macropores. In L.R. Ahuja et al. (ed.) *Root zone water quality model: Modelling management effects on water quality and crop production*. Water Resources Publ., Highlands Ranch, CO.
- Amoozegar, A., and G.V. Wilson. 1999. Methods for measuring hydraulic conductivity and drainable porosity. p. 1149–1205. In R.W. Skaggs and J. van Schilfgaarde (ed.) *Agricultural drainage*. Agron. Monogr. 38. ASA, CSSA, and SSSA, Madison, WI.
- Ball Coelho, B.R., R.C. Roy, E. Topp, and D.R. Lapen. 2007. Tile water quality following liquid swine manure application into standing corn. *J. Environ. Qual.* 36: 580–587.
- Brown, P.A., S.A. Gill, and S.J. Allen. 2000. Metal removal from wastewater using peat. *Water Res.* 34: 3907–3916.
- Bossman, D. 2005. Saving American agriculture and building the rural economy by solving the manure problem. In *Proc. Development of Alternative Technologies for the Processing and Use of Animal Waste*, 9-11. Raleigh, N.C.: North Carolina State University, Animal Waste Management Center.
- Bouwer, H., and J. van Schilfgaarde. 1963. Simplified method of predicting the fall of water table in drained land. *Trans. ASAE* 6:288–291.
- Chick, H. 1908. An investigation of the law of disinfection. *Journal of Hygiene* 8: 92–158.
- Choudhary, M., L.D. Bailey, and C.A. Grant. 1996. Review of the use of swine manure in crop production: Effects on yield and composition and on soil and water quality. *Waste Manage. Res.* 14: 581–595.
- Chu-Agor, M.L., G.A. Fox, R.M. Cancienne, and G.V. Wilson. 2008. Seepage caused tension failures and erosion undercutting of hillslopes. *J. Hydrol.* 359:247–259.

- Dane, J.H., and J.W. Hopmans. 2002. Water retention and storage. p. 671–717. In J.H. Dane and G.C. Topp (ed.) *Methods of soil analysis: Part 4. Physical methods*. ASA and SSSA, Madison, WI.
- Darnault, C.J.G., T.S. Steenhuis, P. Garnier, Y.-J. Kim, M.B. Jenkins, W.C. Ghiorse, P.C. Baveye, and J.-Y. Parlange. 2004. Preferential flow and transport of *Cryptosporidium parvum* oocysts through the vadose zone: Experiments and modeling. *Vadose Zone J.* 3:262–270.
- de Rezende, C. L., E. T. Mallinson, N. L. Tablante, R. Morales, and A. Park. 2001. Effect of dry litter and airflow in reducing *Salmonella* and *Escherichia coli* populations in the broiler production environment. *J. Applied Poultry Research* 10: 245-251.
- Dorner, S.M., W.B. Anderson, R.M. Slawson, N. Kouwen, and P.M. Huck. 2006. Hydrologic modeling of pathogen fate and transport. *Environ. Sci. Technol.* 40:4746–4753.
- Dunne, W.M. 2002. Bacterial adhesion: Seen any good biofilms lately? *Clin. Microbiol. Rev.* 15: 155–166.
- Fontes, D.E., A.L. Mills, G.M. Hornberger, and J.S. Herman. 1991. Physical and chemical factors influencing transport of microorganisms through porous media. *Appl. Environ. Microbiol.* 57:2473–2481.
- Foppen, J.W.A., A. Mporokoso, and J.F. Schijven. 2005. Determining straining of *Escherichia coli* from breakthrough curves. *J. Contam. Hydrol.* 76:191–210.
- Foppen, J. W. A., and J. F. Schijven. 2006. Evaluation of data from the literature on the transport and survival of *Escherichia coli* and thermotolerant coliforms in aquifers under saturated conditions. *Water Res.* 40:401-426.
- Fox, G.A., R.W. Malone, G.J. Sabbagh, and K. Rojas. 2004. Interrelationship of macropores and subsurface drainage for conservative tracer and pesticide transport. *J. Environ. Qual.* 33:2281–2289.
- Fox, G.A., G.J. Sabbagh, R.W. Malone, and K. Rojas. 2007. Modeling parent and metabolite fate and transport in subsurface drained fields with directly connected macropores. *J. Am. Water Resour. Assoc.* 43:1359–1372.
- Garbrecht, K., G.A. Fox, J.A. Guzman, and D. Alexander. 2009. *E. coli* transport through soil columns: Implications for bioretention cell removal efficiency. *Trans. ASABE* 52: 481–486.
- Gantzer, C., L. Gillerman, M. Kuznetsov, and G. Oron. 2001. Adsorption and survival of faecal coliforms, somatic coliphages and F-specific RNA phages in soil irrigated with wastewater. *Water Sci. Technol.* 43: 117–124.
- Gee, G.W., and D. Or. 2002. The solid phase in methods of soil analysis: Part 4. Physical Methods. Soil Science Society of America, Inc. Madison, WI, pp 278-283.
- Georgacakis, D., D.M. Sievers, and E.L. Iannotti. 1982. Buffer stability in manure digesters. *Agricultural Wastes* 4:427–441.

- Gerzabek, M. H., F. Pichlmayer, H. Kirchmann, and G. Haberhauer. 1997. The response of soil organic matter to manure amendments in a long-term experiment at Ultuna, Sweden. *European J. Soil Sci.* 48:273-282.
- Gronewold, A.D., and R.L. Wolpert. 2008. Modeling the relationship between most probable number (MPN) and colony-forming unit (CFU) estimates of fecal Coliform concentration. *Water Res.* 42:3327-3334.
- Guan, T.Y., and R.A. Holley. 2003. Pathogen survival in swine manure environments and transmission of human enteric illness: A review. *J. Environ. Qual.* 32:383-392.
- Gupta, R.K., D.K. Bhumbra, and I.P. Abrol. 1984. Effect of sodicity, pH, organic matter, and calcium carbonate on the dispersion behavior of soils. *Soil Sci.* 137:245-251.
- Guzman, J.A., G.A. Fox, R. Malone, and R. Kanwar. 2009. *Escherichia coli* transport from surface applied manure to subsurface drains through artificial biopores. *J. Environ. Qual.* 38:2412-2421.
- Guzman, J.A., G.A. Fox, and J.B. Payne. 2010. Surface runoff transport of *Escherichia coli* after poultry litter application on pastureland. *Trans. ASABE* 53: 779-786.
- Hagen-Poiseuille (1939)
- Hill, J., O. Kalkanci, J.L. McMurtry, and H. Koser. 2007. Hydrodynamic surface interactions enable *Escherichia coli* to seek efficient routes to swim upstream. *Phys. Rev. Lett.* 98:068101.
- Hrishikesh A., D.L. Barnes, S. Schiewer, and D.M. White. 2007. Total Coliform survival characteristics in frozen soils. *J. Environ Eng. – ASCE* 133:12 1098-1105.
- Huang, P.-M., M.-K. Wang, and C.-Y. Chiu. 2005. Soil mineral-organic matter-microbe interactions: Impacts on biogeochemical processes and biodiversity in soils. *Pedobiologia* 49:609-635.
- Hubert, F., V. Hallaire, P. Sardini, L. Caner, and D. Heddadj. 2007. Pore morphology changes under tillage and no-tillage practices. *Geoderma* 142:226-236.
- Husted, S., L.S. Jensen, and S.S. Jørgensen. 1991. Reducing ammonia loss from cattle slurry by the use of acidifying additives: The role of the buffer system. *J. Sci. Food Agric.* 57:335-349.
- Huysman, F., and W. Verstraete. 1993. Water facilitated transport of bacteria in unsaturated soil columns: Influence of inoculation and irrigation methods. *Soil Biol. Biochem.* 25:91-97.
- Jamieson, R.C., R.J. Gordon, K.E. Sharples, G.W. Stratton, and A. Madani. 2002. Movement and persistence of fecal bacteria in agricultural soils and subsurface drainage water: A review. *Canadian Biosystems Engineering.* 44: 1.1-1.9.
- Jarvis, N. J., 1994. The MACRO model (Version 3.1): Technical description and sample simulations . Reports and Dissertations, 19, Department of Soil Sciences, Swedish University of Agricultural Sciences , Uppsala, 51 pp.

- Jarvis, N. J., 2007. A review of non-equilibrium water flow and solute transport in soil macropores: principles, controlling factors and consequences for water quality. *Eur. J. Soil Sci.* 58: 523–546.
- Jenkins, M. B., D. M. Endale, H. H. Schomberg, and R. R. Sharpe. 2006. Fecal bacteria and sex hormones in soil and runoff from cropped watersheds amended with poultry litter. *Sci. Total Environ.* 358:164-177.
- Jenkins, M. B., C. C. Truman, G. Siragusa, E. Line, J. S. Bailey, J. Frye, D. M. Endale, D. H. Franklin, H. H. Schomberg, D.S. Fisher, and R.R. Sharpe. 2008. Rainfall and tillage effects on transport of fecal bacteria and sex hormones 17 β -estradiol and testosterone from broiler litter applications to a Georgia Piedmont Ultisol. *Sci. Total Environ.* 403:154-163.
- Jiang, G., M.J. Noonan, G.D. Buchan, and N. Smith. 2007. Transport of *Escherichia coli* through variably saturated sand columns and modeling approaches. *J. Contam. Hydrol.* 93:2–20.
- Kemper, W.D., P. Jolley, and R.C. Rosenau. 1988. Soil management to prevent earthworms from riddling irrigation ditch banks. *Irrig. Sci* 9: 79-87.
- Kelley, T. R., O. Pancorbo, W. Merka, S. Thompson, M. Carbrera, and H. Barnhart. 1994. Fate of selected bacterial pathogens and indicators in fractionated poultry litter during storage. *J. Appl. Poultry Res.* 3(3):279-288.
- Kim, H.N., and S.L. Walker. 2009. *Escherichia coli* transport in porous media: Influence of cell strain, solution chemistry, and temperature. *Colloid Surfaces B: Biointerfaces* 71:160–167.
- Köhne, J.M., S. Köhne and J. Šimůnek. 2009a. A review of model applications for structured soils: a) Water flow and tracer transport. *J. Contam. Hydrol.* 104: 4-35.
- Köhne, J.M., S. Köhne and J. Šimůnek. 2009b. A review of model applications for structured soils: b) Pesticide transport. *J. Contam. Hydrol.* 104: 36-60.
- Kouznetsov, M.Y., Y.A. Pachepsky, L. Gillerman, C.J. Gantzer, and G. Oron. 2004. Microbial transport in soil caused by surface and subsurface drip irrigation with treated wastewater. *Int. Agrophysics* 18:239–247.
- Kunze, G.W. 1965. Pretreatment for mineralogical analysis. p. 568-577. In C.A. Black et al. (ed.) *Methods of soil analysis. Part 1.* Agron. Monogr. 9. ASA, Madison, WI.
- Leung, K., and E. Topp. 2001. Bacterial community dynamics in liquid swine manure during storage: Molecular analysis using DGGE/PCR of 16S rDNA. *FEMS Microbiol. Ecol.* 38:169–177.
- Ling, T.Y., E.C. Achberger, C.M. Drapcho, and R.L. Bengtson. 2002. Quantifying adsorption of indicator bacteria in a soil-water system. *Trans. ASAE* 45:669–674.
- Lobry de Bruyn, L.A., and A.J. Conacher. 1994. The effect of ant biopores on water infiltration in soils in undisturbed bushland and in farmland in a semi-arid environment. *Pedobiologia* 38:193–207.

- Lovanh, N., J. Warren, and K. Sistani. 2010. Determination of ammonia and greenhouse gas emissions from land application of swine slurry: A comparison of three application methods. *Bioresource Tech.* 101:1662–1667.
- Mankin, K.R., L. Wang, S.L. Hutchinson, and G.L. Marchin. 2007. *Escherichia coli* sorption to sand and silt loam soil. *Trans. ASABE* 50:1159–1165.
- McGechan, M.B., and A.J.A. Vinten. 2003. Simulation of transport through soil of *E. coli* derived from livestock slurry using the MACRO model. *Soil Use Manage.* 19:321–330.
- McKeague, J.A., and J.H. Day. 1966. Dithionite and oxalate extractable Fe and Al as aids in differentiating various classes of soils. *Can. Soil Sci.* 46:13–22.
- McLaughlin, M.R., J.P. Brooks, and A. Adeli. 2009. Characterization of selected nutrients and bacteria from anaerobic swine manure lagoons on sow, nursery, and finisher farms in the Mid-South USA. *J. Environ. Qual.* 38:2422–2430.
- McMahon, M.J., and A.D. Christy. 2000. Root growth, calcite precipitation, and gas and water movement in fractures and macropores: A review with field observations. *Ohio J. Sci.* 100:88–93.
- Mawdsley, J.L., A.E. Brooks, and R.J. Merry. 1996a. Movement of the protozoan pathogen *Cryptosporidium parvum* through three contrasting soil types. *Biol. Fertil. Soils* 21:30–36.
- Mawdsley, J.L., A.E. Brooks, R.J. Merry, and B.F. Pain. 1996b. Use of a novel soil tilting table apparatus to demonstrate the horizontal and vertical movement of the protozoan pathogen *Cryptosporidium parvum* in soil. *Biol. Fertil. Soils* 21:215–220.
- Miller, W. P. 1987. A solenoid-operated, variable-intensity rainfall simulator. *SSSA J.* 51: 832-834.
- Muirhead, R. W., R. P. Collins, and P. J. Bremer. 2006. Interaction of *Escherichia coli* and soil particles in runoff. *Applied Environ. Microbiol.* 72:3406-3411.
- Nash, J.E., and J.V., Sutcliffe. 1970. River flow forecasting through conceptual models. Part I: A discussion of principles. *J. Hydrol.*, 10: 282-290.
- Odes, H.S., R. Muallem, R. Reimer, S. Ioffe, W. Beil, M. Schwenk, and K.-F. Sewing. 1995. Effect of somatostatin-14 on duodenal mucosal bicarbonate secretion in guinea pigs. *Digest Dis Sci.* 40:678–684.
- Pachepsky, Y.A., A.M. Sadeghi, S.A. Bradford, D.R. Shelton, A.K. Gruber, and T.H. Dao. 2006. Transport and fate of manure-borne pathogens: Modeling perspective. *Agric. Water Mgmt.* 86:81–92.
- Paul, J.W., and E.G. Beauchamp. 1989. Relationship between volatile fatty acid, total ammonia, and pH in manure slurries. *Biological Wastes* 29:313–318.
- Peacock, A. D., M. D. Mullen, D. B. Ringelberg, D. D. Tyler, D. B. Hedrick, P. M. Gale, and D. C. White. 2001. Soil microbial community responses to dairy manure or ammonium nitrate applications. *Soil Biology and Biochem.* 33:1011-1019.

- Ramirez, N.E., P. Wang, J. Lejeune, M.J. Shipitalo, L.A. Ward, S. Sreevatsan, and W.A. Dick. 2009. Effect of tillage and rainfall on transport of manure-applied *Cryptosporidium parvum* oocysts through soil. *J. Environ. Qual.* 38: 2394-2401.
- Reddy, K.R., R. Khalee, and M.R. Overcash. 1981. Behavior and transport of microbial pathogens and indicator organisms in soil treated with organic wastes. *J. Environ. Qual.* 10:255-266.
- Redman, J.A., S.L. Walker, and M. Elimelech. 2004. Bacteria adhesion and transport in porous media: Role of the secondary energy minimum. *Environ. Sci. Technol.* 38:1777-1785.
- Safley, L.M., J.C. Barker, and P.W. Westerman. 1992. Loss of nitrogen during sprinkler irrigation of swine lagoon liquid. *Bioresource Tech.* 40:7-15.
- Saini, R., L.J. Halverson, and J.C. Lorimor. 2003. Rainfall timing and frequency influence on leaching of *Escherichia coli* RS2G through soil following manure application. *J. Environ. Qual.* 32:1865-1872.
- Salas, J. D., J. W. Delleur, V. Yevjevich, and W. L. Lane. 1997. [Chapter 3. Statistical principles and techniques for time series modeling]. In *Applied Modeling of Hydrologic Time Series*, 74-86. Highlands Ranch, Colo.: Water Resources Publications.
- Santos, F. B. O., X. Li, J. B. Payne, and B. W. Sheldon. 2005. Estimation of *Salmonella* populations from commercial North Carolina turkey farms. *J. Applied Poultry Research* 14(4):700-708.
- Savageau, M. A. 1983. *Escherichia coli* habitats, cell types, and molecular mechanisms of gene control. *American Naturalist* 122(6):732-744.
- Shipitalo, M.J., and F. Gibbs. 2000. Potential of earthworm burrows to transmit injected animal wastes to tile drains. *Soil Sci. Soc. Am. J.* 64:2103-2109.
- Šimunek, J., M. Th. van Genuchten, and M. Šejna. 2005. The HYDRUS-1D software package for simulating the one-dimensional movement of water, heat, and multiple solutes in variably-saturated media. Version 3.0, HYDRUS Software 115 Series 1, Department of Environmental Sciences, University of California Riverside, Riverside, CA, 270 pp.
- Šimunek, J., M. Th. van Genuchten, and M. Šejna. 2006. The HYDRUS software package for simulating two- and three-dimensional movement of water, heat, and multiple solutes in variably-saturated media, Technical Manual, Version 1.0, PC Progress, Prague, Czech Republic, pp. 241.
- Sistani, K. R., C. H. Bolster, T. R. Way, H. A. Tobert, D. H. Pote, and D. B. Watts. 2009. Influence of poultry litter application methods on the longevity of nutrient and *E. coli* in runoff from tall fescue pasture. *Water, Air, and Soil Pollution* 206:3-12.
- Smith, M.S., G.W. Thomas, R.E. White, and D. Ritonga. 1985. Transport of *Escherichia coli* through intact and disturbed soil columns. *J. Environ. Qual.* 14:87-91.

- Sørensen, S.J., T. Schyberg, and R. Rønn. 1999. Predation by protozoa on *Escherichia coli* K12 in soil and transfer of resistance plasmid RP4 to indigenous bacteria in soil. *Appl. Soil Ecol.* 11:79–90.
- SSSA. 2008. Glossary of soil science terms. SSSA, Madison, WI.
- Stoddard, C.S., M.S. Coyne, and J.H. Grove. 1998. Fecal bacteria survival and infiltration through a shallow agricultural soil: Timing and tillage effects. *J. Environ. Qual.* 27:1516–1523.
- Sutera, S.P., and M.H. Mehrjardi. 1975. Deformation and fragmentation of human red blood cells in turbulent shear flow. *Biophys J.* 15:1–10.
- Tarchitzky, J., and Y. Chen. 2002. Rheology of sodium-montmorillonite suspensions: Effects of humic substances and pH. *Soil Sci. Soc. Am. J.* 66:406–412.
- ter Laak, T.L. 2005. Sorption to Soil of Hydrophobic and Ionic Organic Compounds: Measurement and Modeling. Ph.D. Dissertation, Utrecht University, Utrecht, Netherlands.
- Torkzaban, S., S.S. Tazehkand, S.L. Walker, and S.A. Bradford. 2008. Transport and fate of bacteria in porous media: Coupled effects of chemical conditions and pore space geometry. *Water Resour. Res.* 44, W04403, doi:10.1029/2007WR006541.
- Tortorelli, R. L., A. Rea, and W. H. Asquith. 1999. Depth-duration frequency of precipitation for Oklahoma. USGS Water-Resources Investigations Report 99-4232. Reston, Va.: U.S. Geological Survey.
- Tyrrel, S.F., and J.N. Quinton. 2003. Overland flow transport of pathogens from agricultural land receiving faecal wastes *J. Appl. Microbiol.* 94: 87-93.
- Unc, A., M.J., Goss. 2003. Movement of faecal bacteria through the vadose zone. *Water Air Soil Poll.* 149: 327–337.
- U.S. EPA. 1986. Ambient water quality criteria for bacteria: 1986. EPA 440/5-84-002. Washington, D.C.: U.S. Environmental Protection Agency.
- U.S. EPA. 2004. Final rule: Water quality standards for coastal and Great Lakes recreation waters. EPA Title 40, Part 131. Washington, D.C.: U.S. Environmental Protection Agency.
- van Genuchten, M.Th. 1980. A closed-form equation for predicting the hydraulic conductivity of unsaturated soils. *Soil Sci. Soc. Am. J.* 44:892–898.
- Villholth, K.G., K.H. Jensen, and J. Fredericia. 1998. Flow and transport processes in a macroporous subsurface-drained glacial till soil. I: Field investigations. *J. Hydrol.* 207:98–120.
- Wang, L. 2003. Fecal bacteria survival in cow manure and *Escherichia coli* release and transport through porous media. PhD diss. Manhattan, Kans.: Kansas State University, Department of Biological and Agricultural Engineering.
- Yamaguchi, T., T. Takei, Y. Yazawa, M.T.F. Wong, R.J. Gilkes, and R.S. Swift. 2004. Effect of humic acid, sodium, and calcium addition on the formation of water-stable aggregates in Western Australia wheatbelt soils. *Australian J. Soil Res.* 42:435–439.

Zhuang, J., and G.R. Yu. 2002. Effects of surface coatings on electrochemical properties and contaminant sorption of clay minerals. *Chemosphere* 49:619–628.

VITA

Jorge A. Guzmán

Candidate for the Degree of

Doctor of Philosophy

Dissertation: SOIL PATHOGEN FATE AND TRANSPORT: BIOPORES
FACILITATING *ESCHERICHIA COLI* TRANSPORT

Major Field: Biosystems Engineering

Biographical:

Personal Data:

Phone: (405)762-6425

e-mail: jguzman.priv@gmail.com

Education:

Completed the requirements for the degree of Doctor of Philosophy in Biosystems Engineering at Oklahoma State University, Stillwater, Oklahoma in December, 2010.

Completed the requirements for the degree of Master of Science in Hydrology and Water Resources at UNESCO-IHE, Delft, The Netherlands in February, 2003.

Completed the requirements for the degree of Master in Computer Science at Universidad Industrial de Santander, Bucaramanga, Colombia, 1994.

Completed the requirements for the degree of Bachelor of Science in Civil Engineering at Universidad Industrial de Santander, Bucaramanga, Colombia, 1989.

Professional Memberships: American Society of Agricultural and Biological Engineers (ASABE)

Name: Jorge A. GUZMAN

Date of Degree: December, 2010

Institution: Oklahoma State University

Location: Stillwater, Oklahoma

Title of Study: SOIL PATHOGEN FATE AND TRANSPORT: BIOPORES
FACILITATING *ESCHERICHIA COLI* TRANSPORT

Pages in Study: 102

Candidate for the Degree of Ph.D.

Major Field: Biosystems and Agricultural Engineering

Scope and Method of Study: Laboratory and field experiments, and computational model.

Findings and Conclusions:

Following manure application, rapid transport of fecal bacteria in runoff and infiltration may result in fecal bacteria contamination of deeper soils and adjacent water bodies. Fecal microorganisms are a group of virus, bacteria and protozoa commonly not pathogenic. Investigations for fecal soil and water contamination, and fate and transport are typically conducted using indicator organisms such as *Escherichia coli* and *Enterococcus faecalis*. Fecal bacteria fate and transport in soils treated with manure effluent are driven by multiple interrelated physical, chemical and biological processes. This research investigated the significance of biopores in facilitating fecal bacteria transport to deeper soils and subsurface drainage systems and incorporated fecal bacteria fate and transport routines and a biopore concept in the Root Zone Water Quality Model (RZWQM). In most cases, the soil matrix can retard, immobilize and/or inactivate fecal bacteria being transported. However, facilitated flow and fecal bacteria transport through macropores and biopores allow fecal bacteria to rapidly bypass a portion of the soil matrix and reach deeper soils and subsurface drainage systems as a function of the soil type and the presence of macropores from soil structure or cracks. Also, manure effluent constituents can potentially change the soil bulk solution pH and favor ionic exchange resulting in varying soil-bacteria or soil bacteria-substrate sorption mechanisms. Fecal bacteria die-off rates vary as a function of lag time between manure application and the occurrence of rainfall or irrigation events, and environmental variables. New routines implemented into RZWQM allow fecal bacteria fate and transport simulation in the soil matrix, runoff, soil profile, and drainage system. Moreover, the implemented biopore concept allows RZWQM to simulate non-equilibrium flow conditions. In combination with the macropore model available in RZWQM, the implemented biopore concept improved flow and fecal bacteria transport simulations at the drain pipe, in runoff and through the soil profile and therefore may be useful when assessing fecal bacteria contamination of soil and water and helping to address mitigation and regulatory strategies.

ADVISER'S APPROVAL: Garey A. FOX